

CR 114575



PSU AERSP 73-1

# **AEROACOUSTIC RESEARCH IN WIND TUNNELS: A STATUS REPORT**

by

James Bender

and

R.E.A. Arndt

Prepared for

United States Army Air Mobility Research and  
Development Laboratory — Ames Directorate  
Under Contract NAS2-6312

Department of Aerospace Engineering  
The Pennsylvania State University  
University Park, Pa.

REPRODUCED BY  
NATIONAL TECHNICAL  
INFORMATION SERVICE  
U.S. DEPARTMENT OF COMMERCE  
SPRINGFIELD, VA. 22161

February, 1973

(NASA-CR-114575) AEROACOUSTIC RESEARCH IN  
WIND TUNNELS: A STATUS REPORT  
(Pennsylvania State Univ.) 163 p HC  
CSCL 14B  
G3/11  
Unclas  
67405  
N73-20277



**PSU AERSP 73-1**

# **AEROACOUSTIC RESEARCH IN WIND TUNNELS: A STATUS REPORT**

by

James Bender

and

R.E.A. Arndt

Prepared for

United States Army Air Mobility Research and  
Development Laboratory – Ames Directorate  
Under Contract NAS2-6312

Department of Aerospace Engineering  
The Pennsylvania State University  
University Park, Pa.

February, 1973

1. a

N O T I C E

THIS DOCUMENT HAS BEEN REPRODUCED FROM THE BEST COPY FURNISHED US BY THE SPONSORING AGENCY. ALTHOUGH IT IS RECOGNIZED THAT CERTAIN PORTIONS ARE ILLEGIBLE, IT IS BEING RELEASED IN THE INTEREST OF MAKING AVAILABLE AS MUCH INFORMATION AS POSSIBLE.

TABLE OF CONTENTS

	<u>Page</u>
Abstract . . . . .	iii
I. Introduction . . . . .	1
II. Present Status of Experimental Aeroacoustic Research . . . . .	5
Aeroacoustic Facilities Visited during this Study . . . . .	5
NSRDC Anechoic Wind Tunnel. . . . .	5
United Aircraft Research Laboratories Acoustic Wind Tunnel. . . . .	9
MIT Acoustics and Vibration Laboratory Anechoic Wind Tunnel. . . . .	13
MIT Department of Aeronautics and Astronautics Wind Tunnel. . . . .	15
BB & N Anechoic Wind Tunnel . . . . .	17
The University of Maryland 7- x 10-Foot Wind Tunnel . . . . .	18
Experimental Investigation of the Acoustical Properties of Wind Tunnels . . . . .	18
III. Background Information . . . . .	23
Overall Acoustic Response. . . . .	23
Background Noise and Turbulence Problems . . . . .	30
Correction Procedure . . . . .	32
Generalized Scaling Laws . . . . .	39
IV. Experimental Program . . . . .	45
Summary of Previous Experimental Work. . . . .	45
The Penn State Experimental Program. . . . .	47
Experimental Method. . . . .	48
Source Selection and Calibration. . . . .	48
Background Noise. . . . .	50
Reverberation and Steady State Response . . . . .	53
Results and Discussion . . . . .	58
Background Noise. . . . .	58
Steady State Response . . . . .	59
Impulsive Response. . . . .	60

TABLE OF CONTENTS (CON.)

	<u>Page</u>
V. Conclusions. . . . .	63
Recommendations for Tunnel Modification. .	63
Corrections to Specific Problems . . . . .	73
Experimental Procedures. . . . .	75
Data Correction. . . . .	76
Limitations on Experimental Research . . .	76
Suggestions for Further Work . . . . .	77
Summary. . . . .	79
References . . . . .	80
Bibliography . . . . .	83
Tables . . . . .	85
Figures. . . . .	90
Appendix A. Investigation of Panel Damping on Reverberant Buildup. . . . .	146
Appendix B. Design Procedure. . . . .	152
Table B-1. . . . .	155
Appendix C. . . . .	158

ABSTRACT

The increasing attention given to aerodynamically generated noise brings into focus the need for quality experimental research in this area. To meet this need several specialized anechoic wind tunnels have been constructed. In many cases, however, budgetary constraints and the like make it desirable to use conventional wind tunnels for this work. Three basic problems are inherent in conventional facilities, high background noise, strong frequency dependent reverberation effects and unique instrumentation problems. This report critically evaluates the known acoustic characteristics of several conventional wind tunnels and presents new data obtained in a smaller 4- x 5-foot wind tunnel which is convertible from a closed jet to an open jet mode. The data from these tunnels serve as a guideline for proposed modifications to a 7- x 10-foot wind tunnel. Consideration is given to acoustic treatment in several different portions of the wind tunnel. Model scaling, data reduction techniques and instrumentation requirements are reviewed. It is concluded that meaningful acoustic data can be obtained in conventional wind tunnels but only under specific conditions. The overall technique will require a careful balance of acoustic treatment, selection of proper model scaling and specialized experimental techniques and data reduction schemes.

## I. INTRODUCTION

The subject of aerodynamically generated noise is becoming increasingly important from both a military and civilian point of view. It is expected that the full utilization of helicopters and other V/STOL vehicles will depend on the ability to operate at acceptable noise levels. One feature of the overall problem is the radiation of noise from rotors, propellers, fans and other rotating devices.

Recent advances have been made in the theoretical analysis of this problem but there is still a great need for meaningful experimental data. This fact is underscored when one notes that current rotor noise theory requires detailed aerodynamic data as input. In order to obtain meaningful experimental data in this area, careful attention must be paid to modelling the aerodynamics of a given problem under controlled conditions in an environment which is suitable for acoustic measurements. This implies that experimental research of this type is an order of magnitude more difficult than standard aerodynamic tests since not only is dynamic similitude necessary but the resulting acoustic signal must be received undistorted and reasonably free of background noise.

In order to obtain experimental measurements of all types of aerodynamically-generated noise under controlled conditions the acoustician or aerodynamicist is resorting more and more to the use of wind tunnels. Powered models or air jets have been installed in the test section of both open and closed throat wind tunnels and noise

measurements taken with microphones mounted both internally and externally to the tunnel. Most of these investigators will probably admit that such measurements are questionable; certainly on an absolute basis and possibly even on a relative basis. The reasons for the uncertainty in the measurements arise from several causes. First, one is faced with the background noise level which is present to varying degrees in wind tunnels. This arises from various mechanical sources associated with the wind tunnel fan and its power source; it also results from noise generated aerodynamically by flow separation from various parts of the circuit or from secondary or periodic flows produced by the turning vanes; it is also produced by turbulent fluctuations in the shear layer along the interior walls of the tunnel or; in the case of an open jet, in the boundary between the jet and the surrounding air.

Another problem arises from the reverberation produced by the confining and reflecting tunnel walls. Any noise signal produced by the object under study will propagate to the various tunnel components and will be reflected and scattered which results in a distorted signal at the receiver.

One other problem with obtaining reliable noise measurements in a wind tunnel concerns the scaling of the noise measurements obtained with the model in order to predict the levels which would be produced by the full sized machine. Assuming certain scaling parameters to be constant, one can make predictions, for example, of how the noise of a given geometric rotor design will vary with the rotor size. However,



if the model of this rotor is fairly small then one must be concerned with Reynolds number effects, which could appreciably alter the noise characteristics of the rotor (for example, that noise produced by vortex shedding). A summary of some of the problem areas is given in Table I.

The objective of this study is to critically evaluate the state of the art in experimental aeroacoustic research and to provide baseline data applicable to rotor noise studies currently underway. Three clearly different avenues of approach are open to investigation; design and build a completely new facility featuring specially designed acoustic treatment for low background noise levels and incorporating an anechoic test section, modifying an existing wind tunnel or the use of a conventional wind tunnel in its present configuration.

The approach taken during this study consisted of two phases: a review of the "state of the art" and some initial experimentation and design computations to determine the feasibility of making noise measurements in a conventional 7- x 10-foot subsonic wind tunnel with suitable acoustic treatment. Various aeroacoustic facilities were visited to determine their operational characteristics and to provide baseline data for a design study. A survey of available theory was made to determine if an adequate theoretical foundation was available for design computations. It was concluded that supplementary experimental data was required. Such data were obtained in a 4- x 5-foot wind tunnel of plywood construction which is convertible from a closed jet section to an open jet with anechoic chamber configuration. This tunnel is presently in the development stage and thus complete

operational characteristics are not available. However, this configuration allowed determination of the effect of changes in test section configuration on reverberation and background noise in addition, temporary treatment at the tunnel elbows allowed the collection of data on the effects of treatment in these areas on reverberation characteristics. This work was supplemented by a review of experimental methods and correlation techniques which may aid in overcoming the acoustic disadvantages of a wind tunnel. Emphasis was placed on dovetailing the findings of this study with the current USAAMRDL rotor noise effort.

## II. PRESENT STATUS OF EXPERIMENTAL AEROACOUSTIC RESEARCH

### Aeroacoustic Facilities Visited During this Study

Five different aeroacoustic facilities have been visited and evaluated. The variation in facility design objectives provide a broad cross section of current thought in acoustic testing, ranging from a multi-million dollar anechoic wind tunnel designed for some particular types of experiments to the modification of an existing wind tunnel for rotor noise studies. Some of the pertinent details and operating characteristics are summarized in Table II. A detailed description of various facilities is given below:

NSRDC Anechoic Wind Tunnel. - To date, the NSRDC wind tunnel represents the most elaborate attempt to develop a facility for flow noise experimentation. A plan view of this wind tunnel is shown in Figure 1. The unique features are provisions for both a partially treated closed jet and open jet test section and special mufflers at the inlet and outlet of the fan. Both test sections are eight feet square. The open jet test section is enclosed by an anechoic chamber which is provided with two foot deep wedges designed to provide good sound absorption down to 150 Hz. A maximum design speed in the test section of 200 fps has been exceeded because the aerodynamic efficiency of the tunnel is better than expected.

The tunnel is fabricated out of concrete to eliminate vibrational problems associated with steel panels. Its foundation is isolated from the bedrock to eliminate structure borne noise from other wind tunnels, etc., which are located at NSRDC. Acoustic isolation joints are provided throughout the tunnel. In addition to the anechoic chamber and mufflers, acoustic treatment is used on the walls in selected areas and the convex

sides of the turning vanes are treated with acoustic dampening material to prevent "singing". Special consideration was made in the fan design to optimize diameter, rotational speed and blade strut configuration for minimal noise output. Other than the special features incorporated for noise studies, the tunnel circuit is of fairly standard design as shown in Figure 1.

The cross-section is generally rectangular with corner fillets. These have been provided to remove undesirable secondary flows which are present in the corners of square cross-section channels.

One problem that the authors have determined will occur in this facility is due to the constraints put on measurement locations by the relatively small size of the anechoic chamber and length of the open jet. This chamber is only  $2.8 \times 2.8 \times 2.3$ , wavelengths at 150 Hz. Noise measurements are constrained by staying at least one wavelength away from the source and one-quarter wavelength away from the wedges of the anechoic chamber. To prevent scattering effects, measurement positions should be selected that avoid the regions adjacent to the collector and the nozzle. The distance between the collector and the nozzle set an upper limit on the maximum included angle for measurement of directivity patterns. In the NSRDC tunnel  $72^\circ$  out of a possible  $180^\circ$  can be measured. The anechoic chamber is designed for absorption down to 150 Hz. At this frequency additional constraints of being  $1/4$  wavelengths away from treated surfaces results in even further limitations on the directivity measurements. If a source of finite size is used there is no position in the anechoic chamber where accurate measurements can be made at 150 Hz. In fact, assuming a reasonable size model, accurate data probably cannot be collected below 350 Hz to 400 Hz without violating one or more of the usual constraints. Therefore, low

frequency measurements are limited by the geometry of the test section rather than the acoustic treatment. In this case a wedge designed for a higher cut-off frequency would have allowed greater utilization of the given space.

A similar problem can possibly occur in the closed test section of this facility which is untreated. There is, however, five feet of acoustic treatment at the nozzle of the open test section. This treatment is provided to attenuate the noise that is entering the open test section. The remainder of the closed test section upstream of the open jet nozzle is fabricated out of concrete. The fact that the walls are untreated severely limits the frequency over which measurements can be made. The cited constraints are typical limits to low frequency noise measurements in all the tunnels studied. However, they are not discussed here because these problems will be critical in the NSRDC tunnel because of the relatively small size of the anechoic chamber. The incorporation of a closed test section probably limited to some extent the size of the anechoic chamber. Whether this resulted in a balanced design is questionable.

Careful attention was given to the design of the mufflers from both an aerodynamic and acoustic point of view. The mufflers consist of two sinuous baffles in the middle of the muffler and one along each concrete wall. The baffles have perforated zinc-coated steel sheet facing with 20 percent open area that is backed with acoustic absorptive material. These were designed for the attenuation of fan noise, particularly in the low frequency range. The profile of the muffler walls was selected to minimize wake and turbulence generation which could compromise the quality of flow in the test section.

A 1/8 scale wind tunnel model was used to verify the aerodynamic design. The most significant problem area which showed up in the model tests was a bad flow separation at the collector cowl in the open jet test section. A redesign of the cowl cured this problem. The collector was redesigned to reduce the size of the secondary vortex so that interactions between it and the nozzle were greatly reduced.

Overall, the NSRDC wind tunnel is fairly well designed and incorporates latest design philosophy. However, there is some evidence of cost constraints which compromised the usefulness of the facility. In particular, the anechoic test section is relatively small. Its geometric constraints do not allow accurate measurements at the cut-off frequency. There is also some evidence that the cross sectional area in the muffler region is relatively small creating higher than desirable flow velocities in this region and the possibility of flow noise.

United Aircraft Research Laboratories Acoustic Wind Tunnel. - This facility, although not as elaborate as the NSRDC tunnel, is also designed specifically for aerodynamic noise studies. As shown in Figure 2, it has an open jet test section located within a 16 ft. high by 18 ft. x 22 ft. anechoic chamber, lined with 12 inch acoustic wedges, capable of sustaining differential pressures up to one-third of an atmosphere. The geometry and area of the test section can be adapted to a variety of requirements by use of alternate final nozzle contraction sections and jet collector pieces. Operating with an open jet length of 4.5 ft. and a test section area of 5 sq. ft., the tunnel is capable of a maximum test section velocity of 650 ft/sec (Mach number 0.61). This condition produces a maximum Reynolds number of approximately  $4.0 \times 10^6$  per foot. The maximum test area is 10 sq. ft. with a corresponding maximum testing velocity of 300 ft/sec.

A large low-velocity inlet of square cross section has been provided. A honeycomb section is located immediately downstream of the bellmouth of this inlet to suppress large eddies. Honeycomb cell size is one-eighth inch, giving an effective length to diameter ratio of 144 in each cell. Up to seven removable turbulence screens can be inserted in the flow path downstream of the honeycomb, with minimum turbulence achieved by use of screens having a pressure drop coefficient of  $1.6 q$ . After contraction through an area ratio of 16:1, minimum turbulence levels of 0.05% can be achieved in the test section. Higher turbulence levels, for tests requiring controlled turbulence levels, are achieved by the installation of turbulence rods in the airstream.

The anechoic chamber housing the tunnel test section permits measurements in the far field of sound generated in the test section. All surfaces

of this chamber are lined with commercial acoustic fiberglass wedges having a large normal absorption coefficient for medium and high-frequency incident sound ( $\alpha = .99$ ). The low frequency free-field cutoff condition, determined by wedge geometry, is set at 250 Hz for this chamber. The wedges were formed by fiberglass blankets of varying length.

The air supply system consists of a 1500 hp induction motor driving a single stage, backward curved vane, centrifugal fan. The fan speed is 1800 rpm with flow rate controlled by variable vanes located in the fan exit. Low ambient noise levels in the anechoic chamber are achieved by use of a muffling section between the fan and the diffuser. The muffling section consists of two acoustically lined corners located between two additional parallel baffle sections. Resulting fan attenuation varies from a minimum of 30 db (low frequency) to a maximum of 60 db over the frequency range of 25 to 10,000 Hz. A three-stage diffuser is located upstream from the muffling section. Diffusion through a total area ratio of 5.6 is achieved by the use of a cylindrical settling section between two conical diffusing stages.

Provision has been made for supporting a variety of models within the airstream. When isolated airfoils or cascades are to be tested, a test section with two hard closed walls (to support the model) and two open sides (to allow the noise to radiate out) is provided. Power is available for driving propeller and compressor models immersed in the airstream. An instrumentation and control room, adjacent to the anechoic chamber, houses required recording and analysis equipment.

One operational problem did crop up in the initial use of this facility which is of interest. A strong edge tone was encountered whose magnitude is a function of the distance between the nozzle and the collector cowl. The strong dependence on this length parameter is easily



understood, if one considers the feedback mechanism involved with a disturbance originally generated at the nozzle lip being convected downstream in time to impinge on the collector cowl and generate a new disturbance which propagates back in phase with another disturbance being generated at the nozzle. Obviously the phasing of this feedback loop can be adjusted by changing the length at a constant velocity. A "fix" in the case was found through the use of serrations at the nozzle lip very similar to the leading edge devices being tried for the reduction of rotor noise. The exact nature of the problem is depicted in a recent paper by Patterson, et al. (1)\*. Figure 3 is reproduced from this paper and illustrates the tab arrangement investigated. Also plotted in this figure is the effect of the tabs on the background noise spectrum. Without the tabs the inter-collector resonance can be seen in the frequency range from 30 Hz to 1000 Hz. With 20 tabs around the nozzle lip this effect is considerably reduced. However, above 3000 Hz these tabs generate noise and increase the overall background noise by approximately 3 dB. Another type of "fix" for the inter-collector resonance problem could be an arrangement for varying the open jet test section length. Plotted in Figure 4, reproduced from Patterson, et al. (1), is the effect of test section length on tunnel background spectra. It is seen here that the background noise decreases with decreasing test section length, which improves the signal to noise ratio. However, a minimum test section length exists for a given experiment below which interference

---

\* Numbers in parentheses refer to reference numbers.

with directivity patterns occurs. This effect precludes the use of varying test section length to reduce inter-collector resonance.

Another problem typical of an open jet test section is the deflection of the jet by a lifting system model. This deflection will cause higher velocity portions of the shear layer to impinge on the collector. This will be an important noise source as shown by Patterson, et al. (1) in Figure 5. For a four degree deflection, which is a moderate deflection when considering testing of V/STOL lifting systems, a 10 dB increase in background is observed. It was concluded that the effect is minimized by using a large area jet collector. However Heyson (2) suggests deflections of up to  $30^{\circ}$  are possible with model helicopter rotors. This large a deflection could not be minimized even with a reasonably large area collector and is considered, by the authors, an inherent problem associated with open jet test sections. Another problem associated with the jet deflection is the fact that there will be a recirculation in the test section that could be ingested through the model rotor causing the model noise to increase considerably. This would create an inaccurate prediction of full-scale rotor noise.

A further problem incurred with an open jet is shear layer refraction. The findings at UARL indicate that shear layer refraction effects are important in interpreting open jet acoustic data. Work is being done at UARL on an analytical method to provide corrections to the measured data. Since the refraction is a function of the type and orientation of the source, a correction for most practical experimental sources will be difficult. More will be said about this problem in the following section.

A disadvantage of the open return configuration of the UARL wind tunnel is that outside background noise could cause problems. Background

noise of the surrounding area, such as trucks and aircraft, has a direct airborne path to the test section, since it is open to the atmosphere. This type of background noise is intermittent and uncontrollable. The study at UARL reports that the atmospheric conditions have a negligible or correctable effect on the aerodynamic properties of the tunnel, but no consideration is given to the background noise from sources other than the wind tunnel.

MIT Acoustics and Vibration Laboratory Anechoic Wind Tunnel. - This facility is rather moderate in both size and cost when compared with the two previously cited tunnels. However, it does represent a benchmark in experimental noise research since it appears to be the first wind tunnel designed specifically for this application in this country. An elevation view of the wind tunnel is shown in Figure 6. In a manner similar to the UARL tunnel, an open circuit design is used. Flow enters a 67 inch square settling chamber having a honeycomb fabricated from soda straws and several sets of screens. The honeycomb serves as a flow straightener and as a muffler. A nozzle of 20:1 contraction ratio is used to provide a 15 inch x 15 inch jet of low turbulence air in the test section which is maintained at below atmospheric pressure. Provision is made for both open or closed jet operation. In the open jet configuration the flow is collected by a cowl and is diffused in a combination muffler-diffuser wherein it enters the inlet section of a 20 hp blower. The muffler is a cruciform wedge placed in the circular diffuser duct. This blower and associated drive motor is mounted on a concrete block which is isolated from the building foundation. A turbulence level of less than 0.1% is achieved in the jet. The test section is enclosed by a concrete block room which serves as either an anechoic chamber or reverberant room.

This convertible arrangement is achieved by simply removing the acoustic treatment from the hard walls.

The diffuser-muffler in this wind tunnel was designed to attenuate blower noise before it reaches the test section. The overall interior dimensions and flow resistance of the fiberglass lining are set to produce quarter wavelength effects over the range of the blade passing frequency, 150 Hz to 300 Hz. The transmission loss of the muffler and diffuser, as reported by Hanson (3), is shown in Figure 7. The maximum transmission loss occurs at 320 Hz, this corresponds to an attenuation of nearly 4 dB per foot of duct. This muffler has good attenuation characteristics through moderately high frequencies. However, high frequency noise could still be heard in the test section. This was eliminated when the downstream honeycomb was installed. This effect was attributed to the high frequency attenuation characteristics of the soda straws.

A problem that came up in the background studies of this tunnel was an unacceptable high background noise level with the reverberant chamber in the frequency range from 200 Hz to 1000 Hz. This was attributed to excited wall panels (600 Hz) and the excitation of the first cross resonant mode of the duct (560 Hz). This problem was alleviated by sand loading the involved wall panels. This approach increases mass and damping without changing the stiffness. The background noise levels in the reverberant chamber with the closed test section are plotted in Figure 8, from Hanson (3). The dashed curve is the background noise levels with the original ducts. The solid curves are background noise levels measured after the walls had been sand loaded.

This facility also encountered a collector resonance similar to that in the UARL wind tunnel. In this case, the resonance was eliminated by changing the shape of the collector.

The open return configuration of this facility, like the UARL tunnel, allows a direct airborne path for extraneous background noise. Although this wind tunnel is entirely indoors, background noise from other laboratory equipment may cause problems. Depending on the type of equipment, this background noise can be controlled by conducting experiments when it is not operating.

The objections to an open jet test section have been discussed previously. The other mode of operation for this tunnel is a closed, hardwall, test section. This configuration is suitable only for measurement of radiated sound power.

The convertible feature of anechoic/reverberant chamber in this wind tunnel allows more flexibility in noise measurements than in a tunnel with an anechoic chamber only. Sound power measurements can be carried out in the reverberant mode, while directivity patterns can be measured in the anechoic chamber.

MIT Department of Aeronautics and Astronautics Wind Tunnel. - This facility is of interest to this study because it represents a modification of an existing wind tunnel. A lot of valuable information is connected with the reconstruction of this facility since a step by step evaluation of various types of acoustic treatment is available.

The wind tunnel is depicted schematically in Figure 9. It is of wood construction and originally a closed jet, closed return design. A section of the test section has been removed to allow for a 4 1/2 x

7 1/2-foot octagonal free jet. The flow is collected by a porous cowl which has worked out quite well. Acoustic treatment in the form of fiberglass wedges has been placed at the two vertical walls at each end of the wind tunnel. This treatment has been very effective in reducing fan noise. The turning vanes have also been acoustically treated, apparently with little or no reduction in the aerodynamic efficiency. This treatment was a fiberglass blanket on the pressure surface of the turning vane.

An anechoic chamber is provided which is rather unique since its interior surface consists of a porous metal backed with acoustic treatment. The original intent was to add acoustic wedges to the walls to achieve a more or less standard acoustic treatment. However, the porous wall served to both provide adequate attenuation of sound to the exterior surroundings and to provide adequate absorption above 600 Hz. Thus no additional acoustic treatment has been provided at this time.

The effect of these acoustic treatments on background noise, reported by Bauer and Widnall (4) is shown in Figure 10. The original background spectrum is plotted along with background spectra with the various treatments in place. After the wedges were installed the background noise increased in the low frequency band and decreased at higher frequencies. When the hard test section walls were removed the background noise was reduced since the acoustic energy is no longer confined to the test section. A further reduction was obtained when the turning vane treatment was installed. When the microphone was moved out of the open jet, the background noise was again reduced. In this case the microphone self noise has been eliminated by moving the microphone out of the flow. The lowest background level was obtained after the anechoic chamber was in place.

This spectrum is nearly flat above 1000 Hz. Care must be taken in interpreting quantitative effects of the treatments due to these background levels, since the test section velocity and microphone position vary in each case.

A further indication of the effects of acoustic treatment is the transmission loss between the return section and the test section. This is shown in Figure 11, taken from Bauer and Widnall (4). The test procedure is also sketched in the same figure. The transmission loss is the difference in sound pressure level between point A (return section) and point B (test section). In this case the transmission loss is along a number of paths. There are two airborne paths and the structural path. Because of the complex internal geometry of the tunnel, these transmission losses only give a qualitative idea of the effect of the modifications.

One objection that can be raised concerning the acoustic treatment of this tunnel is the use of acoustic wedges in the flow. The acoustic wedges have a maximum depth of 18 inches. These are placed in the tunnel in locations where the cross section dimensions are 8 feet. This blockage causes a drop in maximum test section velocity from 140 feet per second, before the wedges are installed, to 120 feet per second after installation. Bauer and Widnall (4) suggest the wedge is chosen to attenuate acoustic energy above 250 Hz. A 2 to 4 inch thick fiberglass blanket having a sound absorption coefficient of approximately 0.9 at 250 Hz would attenuate this acoustic energy without the blockage penalty.

BB & N Anechoic Wind Tunnel. - Another rather modest anechoic wind tunnel is available in the Cambridge laboratory of Bolt, Beranek and

Newman. The facility is illustrated in Figure 12. This tunnel operates in the suction mode (i.e., the pressure in the test section is less than atmospheric). Air enters the room through a 15:1 contraction ratio nozzle at speeds varying from 20 to 120 fps. Two nozzles are available; a 16 inch square cross section or an 18 inch diameter round cross section. The chamber is of plywood construction and is generally operated in a semi-reverberant mode. Cotton batting is sometimes used for sound absorption. Because of the rather flimsy construction the acoustic characteristics of this facility are questionable. No data are available to the authors which would allow quantitative evaluation.

The University of Maryland 7- x 10-Foot Wind Tunnel. - This facility was not visited during this study but is of interest because it is a conventional closed return, low speed wind tunnel which is used for propeller noise studies. A minimal amount of temporary acoustic treatment is provided in the test section in the form of standard acoustic tile. According to a private communication with personnel at the Naval Ship Research and Development Center, successful noise studies have been achieved in the frequency range above 500 Hz.

#### Experimental Investigation of the Acoustical Properties of Wind Tunnels

In addition to the specially designed facilities mentioned in the previous section, several detailed investigations have been initiated to determine the acoustic properties of other available facilities. The large scale, 40- by 80-foot wind tunnel at the NASA-Ames Research Center, shown in Figure 13, has received considerable attention. Hartman and Soderman (5) and Hickey, Soderman and Kelly (6) found that the acoustic properties were comparable to the classical semi-reverberant



room. They suggested a calibration curve for the facility. This calibration is obtained by considering the difference between sound pressure level at a given distance from an omni-directional source with the sound pressure level at the same distance from the source in the free field. These results were obtained experimentally with a white noise source. No attempt was made to consider tunnel response in frequency bands or with pure tones.

Cox (7 and 8) made a detailed analysis of the background noise in this facility. He concluded that a rotor noise investigation would be possible. A full scale rotor, with standard and tapered tip blades, was utilized in a research program on rotor noise radiation at high tip Mach number. The reverberation correction of Hartman and Soderman was applied to the data obtained which then agreed with flyover data to within 2 dB. Arrdt and Bergman (9) utilized these data to confirm a theoretical analysis of noise radiation due to drag divergence and thickness effects at high advance ratio and tip Mach number.

The work of Hartman and Soderman was extended by Bies (10). The approach taken was to develop and test data acquisition and data reduction procedures which would be compatible with the goals of a given test program. No attempt was made to modify the tunnel for reduction of background noise. The sources that could be studied were restricted to those that were sufficiently above the background levels measured. This study developed a procedure for obtaining forward and backward radiated sound power levels and total radiated sound power measurements from upstream and downstream sound pressure level measurements. By considering portions of the tunnel upstream and downstream as reverberant volumes and measuring sound pressure

levels in these regions, data reduction techniques were devised to give radiated sound power. The tunnel was calibrated with an omnidirectional source to develop these data reduction techniques. This procedure would give answers to whether most of the noise radiation propagated forward or aft of the flight vehicle. Radiated power measurements with calibrated sources proved to be reasonably accurate. A porous pipe microphone was developed during the study which proved to have better performance in a flow than the standard Brüel and Kjaer 1/2-inch nose cone wind screen when oriented in the direction of the flow. The general results of the sound propagation study in the Ames 40- by 80-foot wind tunnel appear to be applicable to any large closed test section, air return wind tunnel.

Further work along these lines of Hartman and Soderman and Bies were described by Arndt and Boxwell (11) in an unpublished report. Their work was concerned with the acoustic characteristics of the USA AMRDL 7- x 10-foot wind tunnel. Of particular interest was the determination of reverberant response in frequency bands. This work indicated that the reverberation was strongly dependent on frequency and a reverberation correction based on overall response to a white noise signal would be totally inadequate. Since this work is of direct interest to this study, it is reviewed in detail in the experimental section of this report.

An acoustical evaluation of the NASA Langley 30- x 60-foot wind tunnel was made by Vér, Malme and Meyer (12). The approach here is again to find experimental procedures and data reduction techniques to make acoustical measurements. No attempt is made to reduce the ambient noise of the tunnel. The background noise present is con-

sidered one of the limitations of the tunnel to sources that can be tested in the tunnel. The authors suggested that for a direct sound measurement with an accuracy of 1 dB the signal to noise ratio should exceed 6 dB and the measurement distance should not exceed half the hall radius. The hall radius is defined as the distance where the sound pressure of the direct field equals the space average sound pressure of the reverberant field. The investigation of this facility included a study of background noise, wind tunnel response and the decay characteristics. A limitation, in determining sound power output, was use of only an omni-directional source, since the test section was found not to be diffuse. A generally valid relation between the space averaged sound pressure level in the test section and the sound power output of an unknown source could not be found. The study in this facility was similar to the preliminary investigations in the AMEDL 7 x 10-foot wind tunnel and the Penn State's Aerospace Engineering Department wind tunnel. The Langley study indicated that a quantitative evaluation of the effectiveness of a sound absorbing wall treatment in a small-scale model was needed. By gradually adding sound absorbing treatment to various hard interior surfaces the optimal location and the minimum amount of sound absorbing material required to yield a desired result can be determined.

Two reports by Schultz (13 and 14), describe an acoustic study of the German Laboratory for Air and Space Travel (DVL) Subsonic Wind Tunnel. This wind tunnel is similar to the Aerospace Department tunnel, except the fan is located just upstream from the first corner beyond the test section. The approach taken in this program was to first evaluate

the acoustic properties and limitations to noise studies of the DVL wind tunnel, then apply modifications to the tunnel to reduce these limitations, i.e., sound absorbing material to reduce ambient noise and finally to test the performance and acoustical properties of the wind tunnel after modifications. This was carried out in two parts. The first part of the study was the preliminary evaluation and suggested modifications. The second part of the study evaluated the effects of the modifications on the wind tunnel properties and included initial noise measurements in the DVL wind tunnel. The modifications proposed in this study were concerned primarily with background noise from the fan. It was originally suggested that an open jet be employed. The reason for this was that the fan noise would spread in spherical waves from the nozzle and collecting cone and decay rapidly, thus causing a lower sound pressure level in the test section than if a closed jet configuration was used. However, in later studies it became evident that jet noise was a problem, after fan noise had been eliminated through treatment. It was finally suggested that a porous or slotted closed jet section with the walls adjoining deep, sound damped spaces might give the best results. Other suggestions proposed were to apply sound damping material at the bends upstream and downstream from the fan and also to the walls between these bends. For the walls of the collecting cone, sound dampening plates were suggested. It was also recommended that a narrow, central sound dampener be placed lengthwise to the flow in the diffuser. This study concluded by suggesting the need for a microphone that, at speeds up to 180 feet per second, would not have a serious self-noise problem.

### III. BACKGROUND INFORMATION

#### Overall Acoustic Response

Making acoustic measurements in a wind tunnel requires design and modification guidelines and data correction procedures. Before these guidelines and procedures are formalized it would be helpful to theoretically predict the acoustic response of the wind tunnel. Knowing the way in which a particular tunnel responds to noise in various frequency bands determines what happens to the source noise signature with regard to directivity and spectral content. However, a complete analytical description of the acoustic response of a wind tunnel does not exist. However, it may be possible to consider the tunnel in several component parts which are idealized to match known acoustic properties. The interrelation of these component parts may then be determined through a statistical energy approach as suggested by Smith and Lyon (15). This technique is probably limited, however, to acoustic power. By considering the energy densities and volumes,  $V_i$ , of the components and by determining the coupling coefficients, the power balance equations can be written. These equations say that the power introduced into volume  $V_i$  equals the power dissipated in the remaining volumes  $V_j$  plus the power transmitted from volume  $V_i$  to volumes  $V_j$ , plus the power from volume  $V_i$  dissipated in the connecting ducts, minus the power transmitted from the volumes  $V_j$  to  $V_i$ . Thus a knowledge of the response of each component is required. A knowledge of the power flow between the components and the response of each component allows the determination of the response of the tunnel.

As an indication of what the idealized acoustic response of various components might be, the nozzle may be considered as a special class of horn. The wave equation for a plane wave travelling through a variable cross section duct is given by

$$\frac{\partial^2 \phi}{\partial t^2} = a_o^2 \left[ \frac{\partial^2 \phi}{\partial x^2} + \frac{1}{A} \frac{\partial A}{\partial x} \frac{\partial \phi}{\partial x} \right] \quad (1)$$

where

$$p = \rho \frac{\partial \phi}{\partial t} \quad (2)$$

and  $\phi$  is the velocity potential. In the general case of a nozzle, equation (1) would have to be evaluated numerically. A classic solution to equation (1) exists for an exponential horn, where the area variation is given by

$$A = A_o e^{mx} \quad (3)$$

This results in the following equation

$$\frac{\partial^2 \phi}{\partial t^2} = a_o^2 \left[ \frac{\partial^2 \phi}{\partial x^2} + m \frac{\partial \phi}{\partial x} \right] \quad (4)$$

The solution to equation (4) is of the form

$$\phi = e^{-\alpha x} [Ae^{i[\omega t - \beta x]} + Be^{i[\omega t + \beta x]}] \quad (5)$$

where

$$\alpha = \frac{m}{2} \quad (6)$$

$$\beta = \sqrt{\zeta^2 - m^2/4} \quad (7)$$

$$\zeta = \frac{\omega}{a_o} \quad (8)$$

In this particular case, the speed of propagation is given by

$$a' = \frac{a_0}{\beta} = \frac{a_0}{\sqrt{1 - m^2/4\zeta^2}} \quad (9)$$

The acoustic pressure is obtained from equation (5) through the relation

$$p = \rho \frac{\partial \phi}{\partial t} \quad (10)$$

When the wave number  $\zeta$  is equal to  $m/2$  we have a situation where the propagation speed is infinite and no propagation takes place. This corresponds to a cut-off frequency of

$$f_c = \frac{ma_0}{4\pi} \quad (11)$$

below which acoustic radiation is nil.

Another important component is the tunnel test section. It is desirable to mathematically model the test section in order to assess the value of various acoustic treatments. The following is a theoretical analysis, developed by Mangiarotty, Marsh and Feder (16), to predict the attenuation of sound in ducts with varying cross sections. This method also develops a duct lining optimization on the basis of maximum reduction depending on the shape of the input spectrum.

Assuming the sound pressure in the duct is low enough, the linear wave equation is valid,

$$\frac{1}{a_0^2} \frac{\partial^2 p}{\partial t^2} - \frac{\partial^2 p}{\partial x^2} - \frac{\partial^2 p}{\partial y^2} - \frac{\partial^2 p}{\partial z^2} = 0$$

Separating variables and assuming harmonic waves traveling in the positive z-direction along the duct,

$$p(x, y, z) = X(x) Y(y) Z(z) T(t)$$

where,

$$X(x) = C_x \cos k_x x + S_x \sin k_x x$$

$$Y(y) = C_y \cos k_y y + S_y \sin k_y y$$

$$Z(z) = \exp(-ik_z z)$$

$$T(t) = \exp(i\omega t)$$

where,  $k^2 = k_x^2 + k_y^2 + k_z^2$ ,  $k$  is the complex wave number of a wave propagating in free air. From a superposition of these solutions, a general solution is,

$$p = \sum_{i=1}^{\infty} a_i X_i Y_i Z_i T_i$$

The constants  $a_i$  are chosen to accurately describe a particular sound pressure distribution at the sound source end of the duct.

Now writing the derivatives of the wave equation in terms of the separated functions,

$$\frac{\partial^2 p}{\partial x^2} = \frac{\partial^2 X}{\partial x^2} YZT$$

$$\frac{\partial^2 p}{\partial z^2} = \frac{\partial^2 Z}{\partial z^2} XYT$$

$$\frac{\partial^2 p}{\partial y^2} = \frac{\partial^2 Y}{\partial y^2} XZT$$

$$\frac{\partial^2 p}{\partial t^2} = \frac{\partial^2 T}{\partial t^2} XYZ$$



This leads to,

$$\frac{1}{a^2} \frac{1}{T} \frac{\partial^2 T}{\partial t^2} - \frac{1}{X} \frac{\partial^2 X}{\partial x^2} - \frac{1}{Y} \frac{\partial^2 Y}{\partial y^2} - \frac{1}{Z} \frac{\partial^2 Z}{\partial z^2} = 0$$

This can be further broken down into a number of ordinary differential equations by means of separation constraints.

A solution that represents a wave propagating in the axial direction, restricted to one frequency component is,

$$Z(z) = \exp(-ik_z z)$$

where  $k_z$  is the axial wave number

The boundary conditions are

$$x = a, \sin k_x a = 0, k_x = m\pi/a \quad (m = 0, 1, 2, 3, \dots)$$

$$y = b, \sin k_y b = 0, k_y = n\pi/b \quad (n = 0, 1, 2, 3, \dots)$$

Each solution represents a mode of propagation in a duct with width  $a$  and height  $b$ . To solve a particular problem, a combination of modes of modal order numbers  $m$  and  $n$  must be taken with different phase and amplitude and matched to the sound pressure distribution at the source end of the duct. By introducing the boundary conditions of acoustic admittances  $L(0, a)$  and  $L(0, b)$  of linings in a duct of dimensions  $a$  and  $b$ , the sound attenuation of a broadband-resistive-resonator lining can be calculated. Letting  $k_z = \alpha + i\beta$ , then,

$$Z(z) = \exp(-i\alpha z) \exp(\beta z)$$

This is the attenuation of sound pressure per unit length of duct in the axial direction. In decibels, the attenuation between  $z_1$  and  $z_2$  is,

$$D(z_2 - z_1) = 20 \log \left| \frac{p(z_1)}{p(z_2)} \right| = - 8.68 \beta (z_2 - z_1)$$

then,

$$D = 8.68 \beta$$

is the attenuation per unit length.

The wave number  $k_z$ , and also the phase constant  $\beta$  is obtained through the wave number relation,

$$k_z = \pm (k^2 - k_x^2 - k_y^2)^{1/2}$$

To obtain the attenuation in the duct under the influence of flow, the effects of turbulence, boundary layers and other aerodynamic effects can be taken into account by experimentally deriving the lining characteristics under actual flow conditions. Eversman (17) describes an analytical model similar to this, but this analysis begins with the non-linear wave equation, i.e., convective term included, and derives the effect of Mach Number on the attenuation,

$$\frac{k_z}{k} = \frac{1}{1 - M^2} \{- M \pm [1 - (1 - M^2) (\frac{k_y}{k})^2]^{1/2}\}$$

where  $M$  is the Mach Number of the flow in the duct.

Following the mathematical model described above, a design procedure has been devised by Beranek (18) for the design of acoustic treatment for a duct. This procedure is applicable to the plane wave mode of

sound propagation neglecting end reflections for either a homogeneous absorber or a resistive resonator type treatment. If the duct height,  $h$ , the duct length,  $L$ , and the design frequency,  $f_o$ , of which maximum attenuation is desired are specified, then the treatment depth,  $d$ , porous layer thickness,  $t$ , honeycomb size,  $\delta$ , normalized flow resistance  $R_f/\rho a_o$ , impedance,  $Z/\rho a_o$ , flow resistivity,  $R$ , and the theoretical attenuation,  $D_h$ , for a length of duct equal to the height,  $h$ , or total attenuation,  $D_h \times L/h$ , can be predicted. Figures 14 and 15 contain the calculation results for the AMRDL 7- x 10-foot wind tunnel. The treatment for the floor and ceiling have been designed for maximum attenuation at 400 Hz and the treatment on the walls has been designed for maximum attenuation at 250 Hz. The design parameters for this treatment are shown in Figure 14 and the theoretical attenuation for each treatment and the total attenuation is shown in Figure 15. The attenuation assumes a treatment length equal to the duct height,  $h$ . This analysis incorporated the concept of one treatment on the floor and ceiling and a different treatment on the walls. The attenuation curves shown in Figure 15 cover a rather narrow band width while the range of frequencies that require attenuation in a typical test is rather wide. The attenuation predicted is very high. Results from the Aerospace wind tunnel indicate that the predicted results may be overly optimistic. This is due to the fact that other modes in addition to plane waves play a major role. The assumption of end reflections is also invalid. End reflections will be important as long as treatment is not provided to attenuate these reflections.

In addition, experiments indicate that sound waves, which are not reflected, can propagate around the tunnel circuit back to the test section. End treatment alleviated this problem. Further details of this design procedure are given in Appendix B.

#### Background Noise and Turbulence Problems

Turbulence induced noise can occur along the flow passages and around the turning vanes of a wind tunnel. Along flow passages noise can be generated by turbulence a number of different ways. When the boundary layer along the wind tunnel walls is turbulent the wall panels can be excited. The fluctuations within the turbulent boundary layer, which would be broadband in nature, can cause the panels to generate sound at the resonance frequency of the structure. The turbulence in the boundary layer can itself generate noise. When the turbulent layer is subjected to an adverse pressure gradient, separation will occur, causing large turbulent regions. The eddies in these turbulent regions will also generate noise in the same manner as the eddies formed in an open jet. These generating mechanisms can also occur at the turning vanes, where turbulent boundary layers and separation may also occur. In addition there is the possibility of edge tones occurring and causing the turning vanes to "sing." Considering the possibility of turbulent effects in designing a tunnel, care should be taken to eliminate boundary layer separation. Additional structural integrity will raise resonance frequencies and eliminate panel excited noise.

At first glance the use of an open jet, anechoic test section appears to be the best method for obtaining acoustic measurements. However, there are certain problems with this configuration which should not be overlooked. One factor is the additional background noise inherent with the natural mixing process of the jet. In addition an edge tone type of feedback mechanism can exist between disturbances at the nozzle lip and disturbances introduced at the collector cowl. Under certain conditions a strong edge tone can result. This problem can generally be corrected by changes in cowl design and varying the relative length of the jet. It should also be recognized that the open jet will induce secondary currents in "stagnant" portions of the anechoic chamber where microphones are placed for the collection of acoustic data. If care is not taken, the induced secondary currents will result in additional microphone self-noise. Other factors to be considered in the use of open jets include the refraction of the source signal as it passes through the mixing zone of the jet. This refraction effect will result in a distorted directivity pattern. For example an omnidirectional noise source placed within a jet can appear highly directional.

As an example of how strong this refraction effect can be, experimental data were gathered from the literature and cross plotted to show this effect in Figure 16. An omni-directional source placed along the axis of a jet has its directivity pattern shifted by refraction to resemble a "heart-shape". The largest refraction effect is in the  $0^{\circ}$  position, i.e., on the jet axis. At this position a large dip occurs. This is called the refraction trough. Figure 17 reproduced from Atvars et al. (19), shows these refraction troughs for various Mach numbers. Figure 16 shows the sound pressure level reduction in the refraction trough plotted against jet Mach number. A linear increase

in SPL reduction above a jet Mach number of 0.1 is found for each frequency. The data plotted here were obtained in a 3/4 inch jet, therefore, the frequency and non-dimensional frequency parameter,  $fd/a_0$ , are shown. For a typical rotor noise experiment in the Aerospace wind tunnel or the AMRDL tunnel, the frequency parameter will be approximately equal to 1.0, i.e., the wave length of emitted sound is approximately equal to a typical test section dimension. This should correspond to a large refraction effect that must be considered in a typical experiment.

The above example is for a point source alone. Refraction is a function of the type of source. A refraction correction for a simple source would not be valid for a dipole or quadrupole source. Also the refraction by an open jet is dependent on the orientation of the dipole or quadrupole axes. Since model sources in the test section would be a superposition of various elementary sources any refraction correction would be a function of the model. The data in Figure 16 would be valid only for a monopole source in an open jet. However, this curve does show that refraction can be an important effect.

Another way in which a jet can distort the source signal is by scattering of sound by the turbulence in the open jet. The scattering can influence the directivity pattern of the source signal. Scattering has an attenuation effect on the incident sound.

#### Correction Procedure

Unless an ideal wind tunnel exists after it has been built or modified to accommodate noise measurements, a great deal of experimental and theoretical work remains in order to calibrate the facility. The result of such a calibration would be a number of corrections to be made to the data. These corrections would be necessary for a number of reasons. In an open jet test section there will be refraction and scattering due to the mean velocity gradient

and turbulence in the shear layer. Additional background noise is generated by an open jet which may interfere with measurements of rotor vortex noise.

A further correction will be required for reverberation. This type of correction will be needed in anything less than an anechoic wind tunnel, which includes most of the wind tunnels built to date. A reverberation correction would not only be a function of frequency, but it would also be a function of the model being used. An early attempt at such a correction procedure is shown in Figure 18. This correction was developed for the NASA Ames 40-x 80-foot wind tunnel, and is based on the semi-reverberant equation

$$\text{SPL} = \text{PWL} + 10 \log \left( \frac{1}{4\pi r^2} + \frac{4}{R} \right) - 0.5$$

where  $r$  is the distance in feet, SPL is sound pressure level in dB (ref  $2 \times 10^{-4}$  dynes/cm<sup>2</sup>), PWL is the power level (ref  $10^{-13}$  watts) and  $R$  is the room constant in square feet. The room constant is defined as

$$R = \frac{S\bar{\alpha}}{1 - \bar{\alpha}}$$

where  $S$  is the surface area of the "room" and  $\bar{\alpha}$  is the absorption coefficient.

The idea behind such a calibration curve is that at a given distance,  $r$ , from the source the difference between the free field and semi-reverberant response can be simply subtracted from the data. Such simple corrections have in limited cases agreed with

fly-over data. However, the correction is based on the overall response to a broadband signal. Such a response curve masks the highly reverberant response at lower frequencies as illustrated by the response curves obtained in the AMRDL 7- x 10-foot wind tunnel. A similar reverberant response study will be required after any tunnel modifications are completed.

Other noise measuring techniques have been investigated. Correlation techniques may prove valuable in application to wind tunnel noise measurement and correction procedures. One correlation technique developed by Arai (20) can be used to measure the acoustic power of an individual source in the presence of other sound sources. The principle of this technique is developed here. The acoustic power,  $W$ , radiated from a source is

$$W = \int I \, dS; \quad I = \overline{pv}$$

where  $I$  is the power per unit area,  $S$  the surface area,  $p$  the near field sound pressure and  $v$  the normal surface velocity component. The quantity  $\overline{pv}$  is given by,

$$\overline{pv} = \sqrt{\overline{p^2}} \sqrt{\overline{v^2}} R$$

where  $\sqrt{\overline{p^2}}$  and  $\sqrt{\overline{v^2}}$  are the rms values of pressure and velocity, respectively, and  $R$  is the correlation coefficient between pressure and velocity. The intensity,  $I$ , can also be expressed by

$$I = \sigma I_o \quad I_o = \rho_o a_o \overline{v^2}$$



where  $\sigma$  is the normalized radiation resistance,  $\rho_0$  the density of air and  $a_0$  the velocity of sound in air. From this it can be shown that

$$W = s W_0 \quad W_0 = \int I_0 dS$$

where  $s$  is the weighted mean of  $\sigma$ . If the source is made up of a number of elements,  $W$  is expressed as  $W_i$ , the power of the  $i$ -th source. Comparing  $W_i$  the most intense radiators can be localized and the power of an individual source excited simultaneously can be determined. The measuring equipment is a microphone in the near field of the source to measure pressure and a piezoelectric accelerometer placed on the source to measure acceleration. This is recorded on a 2-channel tape recorder to be analyzed. An integrating circuit converts acceleration to velocity. This correlation technique for measuring radiated power and localizing the most intense radiators is possible in any case of noise from vibrating surfaces, even in the presence of ambient noise, if this is uncorrelated. This method is shown valid by Arai (20), except in the lower frequency range, below 250 Hz.

Another correlation technique has been developed by Cook (21) for sound level prediction in the confines of a room and from multiple coherent sources. This method can be used to predict the sound level received at a receiver point in a room due to a noise source situated at another point. This prediction is based on the unit impulse response of the room at the receiver point due to an input at the source point. It also takes into account all the room confinements, i.e., walls, floors, ceilings and their acoustic properties such as reflection, absorption and diffraction. This

correlation technique also predicts the sound power at a receiver point due to partially coherent noise sources at any number of points. This does not depend on any of the source points or receiver points being in the confines of a room.

The mathematical basis for this correlation technique will be presented here. Figure 19 illustrates a room with a source at point A and a receiver at point R with various paths between the two points. When a time varying signal originating at the source is recorded at R, the effects of the room have changed the original signal due to lagging arrivals of multiple reflections. If white noise is input, the recording is the unit impulse response of the room confines for a source at A received at R. This can be shown by referring to Figure 20 and defining:

*	convolution operator
$N_w(t)$	white noise signal
$h_s(t)$	unit impulse response of speaker system
$h_{RA}(t)$	unit impulse response of the room confines due to a source at A and a receiver at R
$r(t)$	signal recorded at R

taking the cross correlation of  $N_w(t)$  and  $r(t)$ ,  $C_{n,r}(\tau)$

$$C_{n,r}(\tau) = \sigma_n^2 h_s(\tau) * h_{R,A}(\tau) \quad (12)$$

where  $\sigma_n^2$  is the power of the signal  $N_w(t)$ . By passing  $N_w(t)$  into the speaker system and recording the output in anechoic conditions,  $h_s(t)$  can be determined experimentally. Convoluting both sides of equation

(12) with the inverse of  $h_s(t)$ , say  $[h_s(t)]^{-1}$ ,

$$[h_s(t)]^{-1} * C_{n,r}(\tau) = \sigma_n^2 h_s(\tau) * [h_s(\tau)]^{-1} * h_{RA}(\tau)$$

or

$$h_{RA}(\tau) = \frac{[h_s(\tau)]^{-1} * C_{n,r}(\tau)}{\sigma_n^2}.$$

If any sound signal,  $z(t)$ , is input into the sound system at A, the received signal at R is

$$r(t) = z(t) * h_{RA}(t)$$

In terms of correlations, which is best suited to many noise control problems, this is

$$C_r(\tau) = C_z(\tau) * C_h(\tau)$$

where  $C_h$  is the autocorrelation of  $h_{RA}(t)$

To treat two partially coherent sources  $a(t)$  and  $b(t)$  at points A and B, received at R as  $r(t)$ , the approach is again to generate the autocorrelation of  $r(t)$ ,  $C_r(\tau)$ . If A is at a greater distance from R than B is, the lag in time from A to reach R is  $\rho$ , disregarding the initial common time lag, then

$$r(t) = a(t - \rho) + b(t).$$

It can be shown, by taking the autocorrelation of both sides that

$$C_r(\tau) = C_a(\tau) + C_b(\tau) + C_{ab}(\tau + \rho) + C_{ba}(\tau - \rho)$$

where  $C_{ab}(\tau)$  is the cross correlation of  $a(t)$  with  $b(t)$ . The power in  $r(t)$  is given by  $C_r(\tau)$  at  $\tau = 0$ . The power due to the combined

$a(t)$  and  $b(t)$  is

$$C_r(0) = C_a(0) + C_b(0) + 2 C_{a,b}(\rho) \quad (13)$$

The term  $2 C_{a,b}(\rho)$  is the affect on the received power at R due to partial coherence between  $a(t)$  and  $b(t)$ .

As an example to the use of equation (13) some simple cases will be illustrated, letting A and B be equidistant from R, i.e.,  $\rho = 0$ .

Example (1)      If  $a(t)$  and  $b(t)$  are noncoherent and if the powers are equal, then  $C_a(0) = C_b(0)$  and  $C_{a,b}(\tau) = 0$ . Therefore, equation (13) becomes,

$$C_r(0) = C_a(0) + C_b(0)$$

Thus the powers of  $a(t)$  and  $b(t)$  are added upon reaching R. This gives a 3 dB increase over  $a(t)$  or  $b(t)$  alone

Example (2)      If  $a(t)$  and  $b(t)$  are fully coherent and if the powers are again equal  $C_a(0) = C_b(0)$  then  $a(t) = b(t)$  and the correlations are equal  $C_{a,b}(\tau) = C_a(\tau) = C_b(\tau)$ .

Therefore, equation (13) becomes,

$$C_r(0) = 4 C_a(0) = 4 C_b(0)$$

Thus the power reaching R is increased by 6 dB

Equation (13) can be used to predict the power received at R between these extremes. It takes into account partial coherence and time lag due to A or B being at a greater distance from R.

①

Equation (13) can be generalized to  $n$  sources,  $a_1(t)$ ,  $a_2(t)$  . . .  $a_n(t)$  at points  $A_1$ ,  $A_2$ , . . .  $A_n$ . This generalization is

$$C_r(\tau) = - \sum_{i,j} C_{a_i, a_j} (\tau - \rho_{i,j})$$

where  $\rho_{i,j}$  is the time lag between the signal from  $a_i(t)$  and  $a_j(t)$ .

#### Generalized Scaling Laws

In order to achieve the goal of collecting pertinent aeroacoustic data, it is necessary to briefly review the similitude laws pertaining to this problem. Typically there will be several limitations on the size of a model rotor due to both aerodynamic and acoustic considerations. From an aerodynamic point of view, the size of a rotor must be relatively small compared to the wind tunnel dimensions because of wall effects. On the other hand, complete simulation of viscous flow phenomena dictates that the rotor should be as large as possible. From an acoustic point of view there are three factors to be considered. First, we would like to position our microphones close to the model in order to be in the direct field of acoustic radiation. On the other hand, our microphones must be positioned at least one wavelength away from the source if we wish to make far field measurements. Thirdly, the model scale should be selected such that the frequency range of interest is within the capability of existing instrumentation.

The important scaling parameters are the Mach number based on tip speed,  $M_t = \omega R_o / a_o$ , the free stream Mach number  $V_s / a_o$ , advance ratio,  $\mu = \frac{M_s}{M_t} = \frac{V}{\omega R_o}$ , Reynolds number,  $\omega R_o c / \nu$ , and Lock number,  $2\pi \rho c R_o^4 / I$ .

The Mach number criterion is probably the most important from an acoustic point of view after satisfying the usual constraints of being in the far field and the direct field at the same time. The Mach number criterion is satisfied by operating with  $\omega R_o$  the same in model and prototype and at the same advance ratio in model and prototype. Hence, the tunnel velocity should be the same as the full scale forward velocity and the rotor speed should increase with a decrease in rotor size. Since the Reynold's number is given by  $\omega R_o c/\nu$ , the equality of Reynold's number in model and prototype cannot be achieved unless a pressurized tunnel is used. For many noise mechanisms this may not be a problem. Serious consideration should be given to this problem for vortex noise measurements.

The scaling of noise can best be estimated from the simple Gutin expression

$$p_n' = \frac{bn\omega}{2\sqrt{2} \pi r a_o} \left( T \cos \delta - \frac{Q}{M_e R_e} \right) J_{nb} (bn M_e \sin \delta)$$

Now the thrust and torque are given by:

$$T \sim \rho_o \omega^2 R_o^4$$

$$Q \sim \rho_o \omega^2 R_o^5$$

so that

$$p_n' \sim bn \frac{\rho}{a_o} \omega^3 R_o^3 \frac{R_o}{\tau} \left( \cos \delta - \frac{KR_o}{M_e R_e} \right) J_{nb} (bn M_e \sin \delta)$$

In a proper test  $\omega R_o$  and  $M_e$  are constant, hence the rms pressure is proportional only to  $R_o/r$ . A similar conclusion is reached for thickness and drag divergence effects. However, Reynold's number effects should

more strongly affect the vortex noise. There is no complete solution to the problem of simultaneously satisfying Mach and Reynolds number other than operation in a pressurized tunnel. Some research should be directed toward the question of whether blades, on a rotor for example, can be artificially roughened to break up a strong tone due to a strongly coherent wake structure at certain Reynolds numbers. This type of problem is not new, but little consideration has been given to the added complexity of aeroacoustic modelling.

The directivity of the sound is another important factor which could be used conceivably to answer questions concerning the mechanism of blade slap. Consider the equations for rotational, vortex and thickness noise as written by Arndt (22)

(Rotational)

$$p_n' \sim b_n \rho_o a_o^2 M_t^3 \frac{R_o}{r} \left[ \cos \delta + \frac{\pi}{M_t} \left( \frac{R_o}{R_e} \right)^2 \right] J_{nb} \left( b_n \frac{R_o}{R_e} M_t \sin \delta \right) \quad (14)$$

(Overall Vortex)

$$p' \sim \rho_o a_o^2 M_t^3 (Rn)^{-0.2} \sqrt{\sigma} \frac{R_o}{R_e} \cos \delta$$

(Thickness)

$$p_n' \sim \rho_o a_o^2 M_t^2 \sigma^2 \frac{R_o}{R} \int_0^1 \left( \frac{t}{c} J_{nb} \left( nb \frac{R_o}{R_e} M_t \sin \delta \right) d \left( \frac{R}{R_o} \right) \right) \quad (15)$$

where  $K = Q/TR_o$ , a number of order 0.1.

For the vortex noise we only have an empirical relation for the overall sound level. For convenience consider the first mode in equations (14) and (15) and assume that the argument of Bessel function is small enough to use the approximation:

$$J_{bn} \left( bn \frac{R_e}{R_o} M_t \sin \delta \right) \approx \frac{[bn(R_e/R_o)M_t \sin \delta]^{bn}}{2^{bn} bn!}$$

For a two bladed rotor of constant thickness in the first mode the equations may be written in the form:

(Rotational)

$$p_1' \sim \rho_o a_o^2 M_t^5 \frac{R_o}{R} \left[ \cos \delta + \frac{K'}{M_t} \right] \sin^2 \delta \quad (16)$$

(Vortex)

$$p' \sim \rho_o a_o^2 M_t^3 (Rn)^{-0.2} \sqrt{\sigma} \frac{R_o}{R} \cos \delta$$

(Thickness)

$$p_1' \sim \rho_o a_o^2 M_t^4 \sigma^2 \frac{R_o}{R} \sin^2 \delta$$

where factors of  $R_e/R_o$  have been absorbed in the proportionality constants. The first term in the bracket of equation (16) represents noise due to thrust and the second term represents inplane ("drag") forces. The directionality and dependence on Mach number is different for each source. For example, noise due to vortex intersection should go like  $\cos \delta \sin^2 \delta$  whereas shockwave formation should go like  $\sin^2 \delta$ . Vortex noise goes like  $\cos \delta$  and thickness noise like  $\sin^2 \delta$ . Also note that the relative importance of various noise sources depends on the Mach number. Thus, various noise sources could be detected by varying microphone location and Mach number.



Lowson and Ollerhead (31) suggest that noise sources in helicopter rotors due to flapping and the like are small compared to the other noise generation mechanisms cited. If the dynamic response of the blades were to be modelled to simulate flapping noise from a helicopter the Lock number criterion would have to be considered. The moment of inertia may be assumed proportional to the density of the blade material and the blade proportions:

$$I \sim \rho_b t c R_o^3$$

The Lock number may be rewritten in the form:

$$L = 2\pi \frac{\rho}{\rho_b} \frac{R_o}{t}$$

or equivalently,

$$L = \frac{\rho}{\rho_b} \frac{1}{(t/c)\sigma}$$

where  $t/c$  is thickness ratio and  $\sigma$  is the solidity ratio. Thus, if a scale model blade were used, the Lock number would be the same in model and prototype. Obviously, some construction problems would be encountered in satisfying the Lock number criterion, but this effect should be small.

A summary of the various scaling parameters is given in Table III. Model scale is dictated by several considerations as previously described. Wind tunnel velocity is generally the same as the prototype forward velocity. Rotor speed will vary inversely with the scale of the model. This frequency will also scale inversely with model size.

The favorable effects of reduced scale are increased hall radius (direct field large compared to tunnel dimensions), ease of satisfying far field measurement criteria, measurements in frequency range where background noise and reverberation effects are minimized, and minimization of wall effects. On the negative side of the ledger, reduced size

creates Reynolds number scaling problems, places higher harmonics in a frequency range beyond the useful range of some instrumentation and creates additional errors due to air absorption.

Thus model scale must be carefully selected to maximize the usefulness of experimental data collected.

#### IV. EXPERIMENTAL PROGRAM

##### Summary of Previous Experimental Work

The pertinent experimental work carried out to date has been performed in two wind tunnel facilities, the USA AMRDL 7- x 10-foot wind tunnel and the Penn State Aerospace Engineering Wind Tunnel which will be referred to as the Aero Wind Tunnel for the rest of the report. In general, the experimental program consists of a background noise survey and determination of the wind tunnel response to impulsive and steady state sound. Arndt and Boxwell (11) give the details of the experimental work done at the AMRDL facility. This work is summarized here for completeness and for comparison to the data from the present study. Figure 21 is a planform view of the AMRDL wind tunnel.

The first phase of the experimental work at AMRDL was a free field study of the sources to be used in the wind tunnel. Balloons were used as an impulsive source, to determine if the site used for free field studies approximated anechoic conditions. An omnidirectional loudspeaker was then calibrated at the test site to determine its power output and frequency content. This study provided a baseline for comparison of the acoustic response of the wind tunnel.

The wind tunnel response to impulsive sound was determined by bursting balloons in the test section and measuring the decay in sound level. There were nine source locations in the test section. Four microphone locations were used, varying from upstream to downstream

of the test section. The variables of this experiment were microphone location, source location and test section flow velocities of zero and 43 knots. Figure 22 contains measured reverberation times as a function of frequency and microphone location. It was concluded from this portion of the study that for noise sources located in the test section, reverberation, absorption, and sound level decay are strong functions of frequency. The immediate area of the test section showed acoustical properties of a semi-reverberant sound field. The absorption characteristics of the tunnel indicated a need for acoustic treatment in the 125 Hz to 4000 Hz range. A high primary decay mode appeared in the test section but not in the diffuser indicating the importance of test section acoustical treatment.

An omni-directional loudspeaker was utilized as a steady state source positioned at three test section locations with various microphone locations. From this portion of the experimental program comparisons were made with free field conditions in terms of directivity, decay and correlation. Figure 23 is a typical directivity pattern that was obtained. Note that the directivity becomes more diffuse at the 90° and 270° positions corresponding to the points closest to the tunnel walls. Figure 24 shows a comparison between broadband steady state overall levels as measured in the free field and wind tunnel with a 6 dB per doubling of distance superimposed. These results indicate an increase in the overall sound level of tunnel data over free field sound levels. The rate of decay is less than 6 dB per doubling of distance typical of a semi-reverberant environment. Figure 25 presents a comparison between measured sound level in the tunnel and

equivalent free field conditions. These data are plotted as a function of frequency for a distance of 10 feet from the source. Figure 26 contains these data and also data for a distance of twenty feet from the source, plotted with the measured free field sound level as a reference. A narrow band analysis of the data was carried out to determine the difference between measured tunnel and free field broadband sound levels. Correlation techniques were used to obtain a comparison between free field and wind tunnel sound propagation properties. This showed a lack of correlation, independent of microphone separation or distance from the source. It was concluded from the steady state portion of the experiments that in the octave bands between 125 Hz. to 1000 Hz there was a large amplification of the noise signal referenced to the same signal measured in the free field. In addition there was a loss of sound propagation directivity and correlation. This was attributed to the diffuse field existing in the test section.

#### The Penn State Experimental Program

The Aero Wind Tunnel, which is currently undergoing modification to an anechoic facility, was used as a test bed for obtaining comparative design data. This facility can operate in the hard wall, closed jet configuration or in the open jet mode with an anechoic test section. Thus the extremes in test section configuration can be evaluated. In addition, the plywood construction facilities temporary placement of acoustic treatment at various positions to evaluate the effects of treating other portions of the wind tunnel. A plan view of

this facility is presented in Figure 27. The test program consisted of source calibration in an anechoic chamber and reverberant room, determination of the steady state and impulsive response of the wind tunnel in four configurations and a background noise study.

#### Experimental Method

Source Selection and Calibration. - The source selected was a duodecahedron, a regular twelve-sided polyhedron with 3 1/2 inch speakers mounted in each face. The duodecahedron has a mean diameter of 12 inches and is constructed of plywood. This source was calibrated in the Penn State Noise Control Laboratory. Directivity patterns were determined in an anechoic chamber. Calibration was accomplished with both random noise in 1/3 octave bands from 63 Hz to 16,000 Hz center frequencies and at 9 pure tones in the same frequency range. Patterns about each of the three principal axes were obtained and compared. A B & K Sine Random Generator, Type 1024, was used to drive the speakers throughout the calibration test program. A B & K 1/2" Condensor Microphone, Type 4133, mounted on a turntable with a 6 ft. boom was used in the collection of all acoustic data. A standard B & K power supply and B & K Microphone Amplifier, Type 2604, was coupled to the microphone. The output signal was filtered by a B & K Band Pass Filter Set, Type 1612. The resulting data were recorded on a B & K Level Recorder, Type 2305. A B & K piston phone was used for calibration of the equipment. This equipment was also utilized during the wind tunnel tests.

The directivity patterns indicated that the source is omni-directional up to the 2000 Hz 1/3 octave band. Above this frequency the source no longer behaves as a point source. This can be attributed to the coning effect of each speaker at high frequencies which prevents coalescence of each individual speaker signal into an omni-directional source. Integration of the directivity patterns allowed calculation of the overall sound power level and the power level in each 1/3 octave band. This power level curve is shown in Figure 28. These data were used as a free field baseline for comparison to the data obtained in the wind tunnel.

Additional calibration procedures were carried out in a reverberant room. The source was hung off center in the 4960 cubic foot room. Three microphone locations were utilized to measure the sound pressure level in 1/3 octave bands from 63 Hz to 16,000 Hz center frequencies. Random noise (20 - 20,000 Hz) was used as input at the same voltage used in the anechoic chamber. The output signal was then amplified, filtered in 1/3 octave bands and transcribed on a level recorder. The three sound pressure levels measured in each 1/3 octave band varied only slightly above 250 Hz, showing a true diffuse field. However, a satisfactory diffuse field did not exist below 250 Hz. From these data the overall power level and the power level in each 1/3 octave band were calculated. The results are plotted in Figure 28 along with the power levels computed from anechoic chamber data. The general features of the spectra of radiated power are the same but there is approximately a 3.5 dB

discrepancy. This could be related to the differences in acoustic impedances seen by the source in the two ideal environments. The overall power levels obtained were 89.5 dB in the anechoic chamber and 93 dB in the reverberant room. This calibrated source was then used to carry out experiments in the wind tunnel.

Background Noise Measurements. - The background noise associated with the wind tunnel and surrounding environment was a primary concern to making noise measurements in the wind tunnel. The background noise associated with the laboratory environment with a static wind tunnel was found to be satisfactorily low except for the intermittent operation of a few isolated pieces of equipment. These included a vacuum pump used to operate a low density hypersonic wind tunnel, a compressor used to operate a blow-down supersonic wind tunnel in the laboratory and also to operate a two inch open jet in the anechoic chamber, some machine shop equipment and a large transformer located in the building. When this machinery was operating there was a high enough background sound pressure level in the wind tunnel test section to interfere with experiments. This background noise was low frequency in nature, usually below the 160 Hz 1/3 octave band. The background noise presented no real problem because of its low frequency nature and where low frequency measurements were to be taken, they were taken when these sources were off.

Additional background noise data were obtained in the test section during wind tunnel operation. These data were collected with



two different test section configurations, a closed test section and an open test section with an anechoic chamber around it. One microphone location was in the center of the test section, oriented into the flow for each configuration. The microphone, when used to measure flow background, had a nose cone on it. A second microphone location was six inches below a 24 inch diameter hole in the floor of the closed test section. A second microphone location with the open jet was outside the jet flow but inside the anechoic chamber. This location corresponded to the center of a large eddy structure induced by the jet flow which was determined by probing with a rod with a tuft attached at the end. The three microphone locations are shown in Figure 29 as microphone locations 21, 22, and 23. Flow velocities in the test section ranged from zero to 100 mph, the maximum attainable. Figures 30 and 31 display the background spectra with flow at microphone position 22 with the closed test section and anechoic chamber, respectively. These curves are plotted as sound pressure level versus  $1/3$  octave band center frequency. The general features of these curves are similar and show approximately a 3 dB drop for each 10 mph increment reduction in flow velocity. The 10 and 20 mile per hour spectra for the closed test section are higher than expected from the trend shown otherwise. This was caused by a "scraping" sound from the motor, gear box or fan which could have been due to a bad bearing although it did not occur at other velocities or the same velocities with the anechoic chamber. Comparison of spectra obtained with the closed test section and the anechoic test section indicated a 3 to 5 dB drop in sound pressure level with the anechoic chamber. This is illustrated in Figure 32.

During this portion of the experiments, the fan rotational speed and flow rate were measured. The fan in the Aero Wind Tunnel consists of an 8 bladed axial fan with backward curved blades, 13 radial stators downstream and 6 radial supports upstream. Figure 33 is a plot of test section velocity versus fan speed. An almost linear relationship exists between those two parameters as expected.

It was believed that most of the noise associated with these background spectra was fan noise. As an indication of this, the overall sound pressure level was plotted versus the logarithm of test section flow velocity. This is shown in Figure 34 plotted as overall sound pressure level against  $\log U_o$ . Above 40 miles per hour a sixth power dependence on velocity exists as expected. Therefore above 40 miles per hour fan noise dominates. Below this figure a velocity cubed dependence is found.

Since the general shape of the flow noise spectra were found to be similar for all tunnel speeds investigated, with the overall level having a sixth power dependence on tunnel speed above 40 miles per hour, an attempt was made to normalize these data as suggested by Vér, Malme and Meyer (12):

$$SPL_N (1/3 \text{ OCT}) = SPL (1/3 \text{ OCT}, U_{\text{mph}}) - 60 \log_{10} (U_{\text{mph}})$$

where  $SPL_N (1/3 \text{ OCT})$  is the normalized third octave sound pressure level,  $SPL (1/3 \text{ OCT}, U_{\text{mph}})$  is the third octave background sound pressure level in dB (ref.  $2 \times 10^{-4}$  dynes/cm<sup>2</sup>) measured for tunnel speed  $U_o$  in miles per hour. The results are plotted in Figures 35

15

and 36 with an indication of the range and average values of the normalized ambient sound pressure levels as a function of the third octave band center frequency. Figure 35 contains the data obtained in the closed test section configuration and Figure 36 contains the data for the anechoic test section. Both sets of data were obtained from microphone position 22. The scatter in the data is illustrated by the two solid lines. In spite of a change in speed by a factor of two and one half, the relative frequency content of the signal remains unchanged and proportional to  $U^6$ . For comparison, the range of the fan fundamental frequency as a function of speed is plotted in the figures. A corresponding shift in the spectrum shape is not evident implying that there is a strong interaction between the fan noise and the tunnel reverberation characteristics. A complete answer to this problem can only be obtained through the collection of data over a wider speed range (which is not possible) and through narrow band analysis. Thus it is apparent that the spectrum at any speed within the range of measurements may be predicted from the relation

$$\text{SPL (1/3 OCT, } U_{\text{mph}}) = \text{SPL}_N \text{ (1/3 OCT)} + 60 \log_{10} (U_{\text{mph}})$$

Reverberation and Steady State Response. - The next portion of the experimental program was concerned with the determination of the wind tunnel response to a source in the test section without flow. The source was the calibrated duodecahedron described previously. The wind tunnel configuration for this portion of the experiment is

shown in Figure 29. This figure contains the twenty microphone locations, the location of the source, the location of acoustic treatment, and the test section configurations. Experiments were carried out with the wind tunnel in four different configurations; a closed test section without any type of treatment, an open jet test section with an anechoic chamber around it, the closed test section with acoustic treatment on the end walls of the test section leg of the tunnel and the anechoic configuration with end treatment. The end treatment used was two inch thick Owens/Corning Fiberglass, Type 705. The sound absorption characteristics of this material are presented in Figure 37. Approximately 240 square feet of this treatment was applied to the end walls at the locations shown in Figure 29. No treatment was used on the floor or ceiling. The treatment was installed in a temporary manner, since the prime interest was on the effects of treatment on the reverberation characteristics which could be obtained with the tunnel in its static condition.

The setup for these experiments utilized the same equipment used during the calibration of the source. A sine-random generator was used to drive the source at the same input voltage of 0.95 volts used in the calibration with random noise. All acoustic data were collected with a 1/2" microphone connected to a microphone amplifier, band-pass filter set and level recorder. Reverberation data were obtained by alternately switching the sound source off and on and recording the resulting acoustic signal.

Microphone locations 9 through 20 formed a 55 inch diameter circle around the source. These microphone positions were  $30^\circ$  apart and were used to obtain directivity patterns. Sound pressure levels were measured in 1/3 octave bands at each location. Figures 38 and 39 display the typical directivity patterns obtained at 1/3 octave band center frequencies of 500 Hz and 1000 Hz, respectively. The  $0^\circ$  radial corresponds to the tunnel center line towards the diffuser and  $180^\circ$ , the nozzle. The dashed portions of the closed test section data indicate the microphone was only 22 inches instead of 27.5 inches from the source. This was due to wall interference at the  $90^\circ$  and  $270^\circ$  positions. Each figure contains five directivity patterns, corresponding to the free field, the closed test section, the closed test section with end wall treatment, the anechoic chamber and the anechoic chamber with end wall treatment. The closed test section data, with and without end treatment, distorts the directivity patterns in the upstream and downstream directions. This is especially prevalent in the data presented in Figure 38. The highest sound pressure levels are obtained in these two configurations. The anechoic chamber polar plots also show some distortion but not as much as with the closed test section. A close approximation to free field conditions was obtained with the anechoic chamber with end treatment. As shown in Figure 38 there is, however, some distortion of an opposite nature resulting in sound levels lower than equivalent free field data in the  $120^\circ$  and  $150^\circ$  positions.

At microphone positions 1 through 8 both sound pressure levels and reverberation times were measured. Figures 40 and 41 display sound pressure level spectra obtained at microphone locations 2 and 3. The dashed portions of these graphs indicate background levels. The data indicate that the highest levels result in the configuration with the closed test section with no treatment. Adding treatment to this configuration results in a 2 to 3 dB reduction of sound pressure level. The addition of the anechoic chamber without end treatment allows an additional 5 to 6 dB reduction. The lowest sound pressure levels and apparently minimum signal distortion is obtained with the anechoic chamber with end treatment, where an overall attenuation of 10 to 15 dB is realized over the closed test section configuration. The best attenuation is in the range between 250 Hz and 2000 Hz, corresponding to the highest sound absorption coefficients of the end treatment.

A comparison of sound pressure level spectra at microphone locations 1 and 8 with data from the AMRDL 7- x 10-foot wind tunnel is presented in Figures 42 and 43. The AMRDL data are the same data as plotted in Figure 26 for a distance of 10 feet. Figures 42 and 43 are plotted in a non-dimensional form. The abscissa contains the non-dimensional parameter,  $f_c d/a_o$ , where  $d$  is the largest cross-sectional dimension of the test section,  $f_c$ , is the octave band center frequency and,  $a_o$ , is the speed of sound. The value used for  $a_o$  was 1127 feet per second. The ordinate is plotted as sound pressure level referenced to free field. All these data were taken with flat spectral content input from the source and the microphones in all cases were 10 feet from the source. The dashed portion of these curves indicates predominately background noise levels. The peaks of these curves are over the same range but the AMRDL peaks at much larger values. Apparently the reverberation effect is enhanced by the steel plate construction.

Figure 44 is a display of primary and secondary modes of reverberation time for microphone locations 5 and 6 at preferred octave band center frequencies. Reverberation times could not be found below 250 Hz because of external background interference. This external source was the compressor that was mentioned previously. The primary modes apparently are not frequency dependent and change only when end treatment is added. Without end treatment the values of reverberation time are about 2.8 seconds, when end treatment is added this value drops to about 2.2 seconds. The reverberation time does not appear to depend on the actual test section configuration. The secondary modes

of reverberant times show erratic frequency dependence. The addition of end treatment apparently attenuates many of the secondary modes found without end treatment.

### Results and Discussion

Background Noise. - The collection of background noise data lead to the conclusion that the fan noise dominates as a background source. The sixth power of velocity dependence shown in Figure 34 reflects this fact. However, below 40 miles per hour a velocity cubed dependence exists. This probably results from the fact that the fan is operating at a lower speed than it was designed for. The blade twist is no longer correct at the lower speed and the blade is probably stalled in regions close to the hub. This causes a broad wake and produces noise. Fan pitch control could overcome this problem. However, the fan is the dominate source of tunnel background noise in the test section. Any noise reduction modification to the tunnel should be concerned with this fact.

A surprising fact can be seen in the measurements, displayed in Figure 34. Both the data from the closed test section and with the anechoic chamber are nearly the same level while 1/3 octave band data show a 3 dB to 5 dB difference. This is especially prevalent above 40 miles per hour. Also both sets of data follow the velocity cubed and sixth power slopes rather well. This implies a strong reverberant response by the wind tunnel to the fan noise. This fact is also shown by the normalized data in Figures 35 and 36, since these normalized curves show similarity to response curves of Figures 40 and 41. The fact that the response curves are the same general shape as the normalized



fan background spectra and the fact that these sets of curves both show maxima in the same frequency range also implies a strong wind tunnel reverberant response to the fan noise.

Steady State Response. - The effect of the various treatments used was assessed from the steady state response data. The directivity patterns obtained indicated that the closed test section without end treatment results in a highly distorted acoustic signal. Adding end treatment attenuated some of the reverberant response but the directivity pattern was still distorted. The anechoic chamber provided a large drop in signal distortion over that realized with the closed test section configurations. Directivity patterns in the anechoic chamber showed a strong similarity to the expected free field patterns. End treatment coupled with the anechoic test section gave the best overall results. The deviation from the expected free field noise pattern was within 3 dB. Measurements of spectra also indicated that the least signal distortion was obtained with the open jet configuration and end treatment as expected.

The reverberant response of the two wind tunnels when suitably normalized with respect to a characteristic length and acoustic velocity has a similar frequency dependence. The steel panel construction of the AMRDL wind tunnel produces considerable enhancement of the reverberation effect. These data also indicate qualitative comparison can be made with different wind tunnels of approximately the same configuration.

Impulsive Response. - The effect of end treatment was apparent in reverberation data. The primary mode reverberation times were reduced by about 20 percent with the addition of end treatment. At the same time, secondary modes, especially at higher frequencies were completely eliminated.

One feature noted in the closed test section without end treatment, was a leveling off or even a slight increase of the signal during decay, followed by a return to the same decay rate. This is shown in Figure 45. In checking, it was found that the interval between these "bumps" in the decay was 0.08 to 0.12 seconds. The time for sound to travel around one circuit of the tunnel is 0.105 seconds based on centerline distance. Therefore, these "bumps" were probably due to the decaying signals completing one circuit around the tunnel. This occurrence was suppressed with the anechoic chamber and was completely eliminated when end treatment was added with either test section configuration.

From the measured reverberant times,  $T_r$ , absorption coefficients could be calculated from the Sabine formula,

$$\bar{\alpha} = \frac{.049 V}{S T_r}$$

Using the cited data and the wind tunnel volume,  $V$ , of 5000 cubic feet and surface area,  $S$ , of 2950 square feet, an average absorption coefficient,  $\bar{\alpha}$ , of 0.24 without treatment and 0.29 with end treatment was computed. For comparison the steady state sound pressure was used

to predict the absorption in the form,

$$\bar{\alpha} = \frac{4 W_0 a_0}{p_o^2 S}$$

This results in a prediction of  $\bar{\alpha} = 0.086$  about one-third of the value found using the Sabine formula. This type of disagreement implies that the application of simple reverberation theory to a complex geometry, such as a wind tunnel, is not sufficient.

An attempt was made to predict the sound power of the source using the steady state data taken in the wind tunnel and the previously cited relation for a semi-reverberant chamber:

$$p^2 = \rho_o a_o W \left[ \frac{1}{4\pi r^2} + \frac{4}{\bar{\alpha} S} \right]$$

Rearranging and taking 10 log at both sides, results in

$$PWL = SPL + 10 \log \frac{W_0 \rho_o a_o}{p_o^2} \left[ \frac{1}{4\pi r^2} + \frac{4}{\bar{\alpha} S} \right]$$

where

PWL = power level of the source (ref.  $10^{-12}$  watts)

SPL = sound pressure level (ref.  $2 \times 10^{-4}$  dynes/cm<sup>2</sup>)

r = distance from source where SPL was measured

$W_0$  = reference power,  $10^{-12}$  watts

$p_o^2$  = reference pressure,  $2 \times 10^{-4}$  dynes/cm<sup>2</sup>

$\bar{\alpha}$  = the absorption coefficient calculated from  
reverberant times

S = wind tunnel surface area

The power levels obtained are shown in Figure 46 along with an average of the calibrated power levels in Figure 28.

Two cases were used for the sound pressure level to predict power levels. These were microphone position 8 with the closed test section and microphone position 7 with the anechoic chamber. The power levels from the microphone position 7 agrees well with the calibrated power level. However, the data from microphone position 8 does not agree with the calibrated curve. This fact indicates that the simple theory used here is not suitable for application in the complex environment of the wind tunnel.

## V. CONCLUSIONS

The body of this report contains an evaluation of existing aeroacoustic facilities, a review of theory which may offer some guidance, and a summary of experimental data on the acoustic response of wind tunnels. From this rather scanty body of knowledge, one is faced with arriving at a decision regarding the suitability of using a conventional wind tunnel for aeroacoustic research. It is concluded, with some qualification, that meaningful data can be collected in a low speed facility such as the USAAMRDL 7 x 10 wind tunnel. The reservation is that extensive acoustic treatment is required, special data acquisitions techniques are necessary and careful consideration must be given to the selection of model scaling and the types of experiments that can be accomplished successfully.

As far as is possible, specific suggestions are given concerning the type of acoustic treatment required. In certain areas, specific data on the USAAMRDL facility are lacking and problem areas can only be anticipated without offering specific solutions. A discussion of facility limitations and suggestions for further work are also given.

### Recommendations for Tunnel Modifications

Any modification program should be aimed at the test section. Based on all that is known, acoustic treatment in this area will reap the most benefit. In considering what should be done, there are several factors that must be considered. Consideration should be given to a balanced design, i.e., all possible uses of the tunnel should be considered. Aeroacoustic research may only be a fraction of the test program. With this in mind, any modifications should not result in a loss of capability

for testing in other aerodynamic fields. Secondly, the modifications should provide a quantum change in the acoustic properties of the tunnel as it now stands. Thirdly, the whole program should be carried out at reasonable cost.

The approach that most closely satisfies the constraints involved appears to be the use of a closed test section with resonant absorber type treatment as developed in the NASA Quiet Engine Program. This treatment would be backed by standard fiberglass absorptive material to insure treatment over a wide frequency range. Of the eleven aeroacoustic facilities cited in Table II, none have used this approach. With this in mind, the pro and cons of the various avenues of approach should be considered in detail.

It has been accepted without question that an open jet facility with an anechoic test section is the best possible solution. There are however many problems associated with this type of facility which should be kept in mind.

The aerodynamic properties of a given wind tunnel will change drastically if converted from a closed test section to an open jet mode. Severe flow instability can be encountered and has been experienced in some facilities. This problem is overcome through proper collector cowl design. Not to be discounted is the extensive region of turbulent flow induced in the mixing zone of the jet. Large scale velocity fluctuations are sensed even at the centerline of the jet. Measurements of Von Frank (23) shown in Figure 47 indicate that an open jet leaving the nozzle with only a 0.07% turbulence level has a turbulence level of 1.25% at the centerline at 2 diameters from the nozzle. This is due to the intermittent incursion of large scale eddies from the mixing zone. Measured values of near field

pressure in an open jet, reported by Barefoot (24) are shown in Figure 48. The numbers in parentheses are the sound pressure levels equivalent to a jet velocity of 100 meters per second. The upper portion of the diagram corresponds to data obtained in a jet with a 10:1 ellipsoid of revolution placed in the potential core. The lower portion of the graph contains data for an unperturbed jet. Inspection of these data indicate that microphone placement within the anechoic test section will be severely limited and complete directivity patterns will be difficult if not impossible to obtain. Further problems with an open jet are evidenced in the refraction effects suffered by the sound field passing through the shear region surrounding the jet. Experimental data demonstrating this effect were presented in Section III (Figures 16 and 17). Under certain conditions refraction corrections would be necessary which for the complicated source system associated with a rotor will be very unwieldy. The refraction correction is a function of the type and orientation of elementary sound sources. Any analytical correction would necessarily be a function of the test object and it would be difficult to predict.

Another problem that has been experienced in open test section configurations is inter-collector resonance. This problem has been experienced in the NSRDC Anechoic Wind Tunnel and the United Aircraft Research Laboratories Acoustic Wind Tunnel which is described in Section II. The edge tone mechanism occurs when a disturbance originally generated at the nozzle tip is convected downstream in time to impinge on the collector cowl and generate a new disturbance which propagates back in phase with another disturbance being generated at the nozzle. The problem was resolved for the NSRDC wind tunnel by modifying the collector cowl.

The modified collector reduced the size of the secondary vortex so that interactions between it and the nozzle were reduced, but they were not completely eliminated. One solution suggested by the UARL staff was to vary the length of the jet since the edge tone is a strong function of jet length. However, this possibility was excluded because the length would have to be reduced to a point where the collector and nozzle would interfere with directivity patterns due to scattering. The final solution used in the UARL wind tunnel was to use a tab arrangement to break up the disturbances at the nozzle. This reduced the background noise in the range below 3000 Hz but increased the background noise by 3dB above this range, as shown in Figure 3. The inter-collector resonance was a critical problem in the NSRDC and UARL wind tunnels until some type of solution was found to minimize it. Other open test sections probably have a similar effect but it is minimal due to a fortuitous combination of jet length, jet velocity and collector shape. The edge tone occurrence will have an effect which may or may not be minimized. In addition to the turbulence and refraction effects, the open jet induces a circular pattern of flow within the anechoic chamber which can induce self noise at the microphone.

Further problems with open jet configurations are evidenced when testing high lift systems. Jet deflection occurs, which in some cases is severe, producing a flow situation in the test section which is distinctly non-uniform resulting in additional background noise, flow instability and self noise at the microphone. It is also difficult to correctly model the aerodynamics of a high lift system in an open jet. A quote from Heyson's (25) study of jet boundary corrections for V/STOL aircraft models illustrates the problem: "Under similar conditions with an open floor, large distortions of the lower boundary will occur so that, in

F



practice, the corrections will be indeterminate. For this reason the use of completely open wind tunnels for low speed and high lift coefficient testing is not recommended".

The jet deflection will cause further problems by increasing the background noise levels. This has been investigated at the UARL Wind Tunnel and results are shown in Figure 5. This results in a 10 dB increase for a 4 degree deflection. The mechanism for this increase is the fact that higher velocity portions of the shear layer impinge on the collector lip. For a model rotor system deflections will be much higher than the 4 degrees tested in the UARL wind tunnel. For this reason the method of correcting this problem at UARL will probably not work when a high lift system is being tested. The method used at UARL was to increase the area of the collector. For a substantial deflection a very large area increase would be necessary.

One advantage with an open test section configuration is the fact that it is easy to provide an anechoic test section. Because it is open the sound radiates away spherically and anechoic conditions can be provided by "wrapping" an anechoic chamber around the test section. This also allows placement of microphones at relatively large distances from the model.

Another disadvantage to be considered with an open test section is the instrumentation. Noise measurements in an open test section/anechoic chamber can be made outside the flow. This can be done with standard microphones without developing a special probe to be used in flow. There may be some self-noise or pseudo-sound due to the large eddy structure within the anechoic chamber. This eddy structure is shown in Figure 49 after Brownell (26), and has been confirmed in the Aerospace Wind Tunnel by probing with a tuft on a rod. A nose cone would not

be much help because it would be difficult to align with the flow. However, the velocities should be low enough not to cause high self noise problems.

Finally, the noise measurement constraints for this configuration must be considered,

- a) Microphone should be kept at least one wavelength, of the lowest frequency sound being measured, away from the source.
- b) Microphone should be kept one quarter wavelength away from the wedges of the anechoic chamber.
- c) Microphone should avoid the corners of the nozzle and collector to prevent scattering.
- d) Microphones should be kept out of the flow since standard instrumentation is used.
- e) Microphones should be kept out of the nozzle and diffuser to avoid reverberant problems.

The alternative to the cited problems with an open jet configuration is of course retention of a closed test section if the tunnel is already so equipped. Without treatment, the reverberation effects will be too severe to consider any serious acoustic testing. However, considerable strides have been made in developing hard wall surfaces with good sound absorption characteristics. Treatment in a closed test section might consist of a porous wall backed by a resonant chamber for low frequency attenuation and a fiberglass blanket for high frequency attenuation. The frequency range of the low frequency treatment can be broadened by tuning adjacent walls for different frequencies as shown in Figure 14. The results of the calculated absorption in the AMRDL 7 x 10 foot wind tunnel using the procedure of Beranek (18) are shown in Figure 50. Here the predicted

increase in hall radius is shown as a function of frequency. This calculation is based on the predicted change in absorption in Sabines over that found from reverberant decay measurements with an impulsive sound source. This type of comparison is qualitative at best, since the definition of hall radius is based on the idea of a semi-reverberant room. The region within the hall radius is dominated by the direct field and presumably measurements within this region contain little contamination from reverberation effects.

Another problem with a closed test section is the fact that all measurements must be made within the flow. Additional problems then are the self noise of the microphone and the pseudo-sound inherent with natural turbulence in the flow. Figure 51 contains a comparison between the measured background level in the AMRDL 7 x 10 foot wind tunnel and the reported (27) self noise of a B & K Model 4131 microphone with nose cone. In this particular case improvements in tunnel background noise would have to be followed by improvements in instrumentation. The frequency distribution of this self noise is rather flat as seen in Figure 52. Here a comparison is made between the 1/3 octave spectrum of the B & K microphone, the background level in a rather noisy wind tunnel and the predicted pseudo-sound due to a 1% turbulence level. The pseudo-sound is estimated from the pressure intensity in isotropic flow:

$$\sqrt{p'^2} = 1.4 \rho \sqrt{u'^2}$$

A flat spectrum is assumed over 3 decades and corrected to equivalent 1/3 octave bands. In this case substantial reductions in background noise may be made without the necessity to improve the instrumentation at low frequencies. At high frequencies improvements in instrumentation are

necessary but would be in vain due to the pseudo-sound noise floor. In other words, a balanced approach to the problems of wind tunnel design involves both the wind tunnel itself, and the instrumentation.

Several authors cite pressure measurements in turbulent flows which are summarized by Barefoot (24). It is believed that some of this experience can be directed toward the problem of noise measurements in flow. One problem appears to be the use of a screen covered opening in the design of most wind screens. This induces turbulent flow and resulting self noise. Experience shows that four equally spaced holes around the periphery of a streamlined pressure probe perform the same function of space averaging the pressure field. The lack of sensitivity to flow angle for such a probe as measured by Barefoot (24), is shown in Figure 53. The idea here is to keep the flow laminar over the body. At high flow velocities a body with a favorable pressure gradient over a considerable length is necessary. Such bodies can be easily developed. An example is shown in Figure 54 from Eisenberg (28). This body has the same shape as the cavity behind a disk in supercavitating liquid flow. Since the walls of the cavity are a constant pressure surface, a similar shaped body has the same pressure distribution. Bodies of similar shape may be useful for enclosing microphones. The authors believe an improved probe can be developed along these lines that would give a 20 dB improvement in self noise over a standard microphone with nose cone.

Another major consideration is that the far field is at least one wave length away from the source. This places restrictions on the model scale in certain positions. The confining walls of the test section limit the distance a microphone can be positioned from the source. However, a properly designed closed jet test section will allow sound measurements in the region of the tunnel centerline which are usually not possible with

an open jet configuration. Again the idea of balanced design crops up. Treatment at the wall should be such that the hall radius, possible microphone positioning and typical scale-frequency combinations all be considered together. By this it is meant that if the physical size of the test section places a lower limit on frequency, then it is not practical to go to the expense of providing acoustic treatment for much lower frequencies. (The major expense in acoustic treatment being the problem of absorption in the low frequency range).

In considering the pros and cons of the two types of test sections, the authors believe that a closed jet test section provides a cost effective alternate to the more or less standard open jet configuration. The technology for hard wall acoustic treatment can be drawn from other fields, i.e., the NASA Quiet Engine Program. Constraints on model scaling and directivity information are outweighed by the utility of the closed jet configuration in areas other than aeroacoustic. Objections to measurements within the flow can be overcome with the development of instrumentation that is within the state of the art.

Another portion of the wind tunnel that requires treatment is all four corner sections. Treatment is recommended here for both the end walls and the turning vanes. It is suggested that all end walls around the turning vanes be treated. Here end walls refer to all flat surfaces in the corners, i.e., walls, floor and ceiling. Recommended treatment is fiberglass blankets or boards covered with some combination of perforated metal, screen and mylar to prevent flow erosion of the fiberglass. The fiberglass covering material to be used depends on the

flow velocity in a particular corner. This treatment could be mounted in two configurations. One configuration would be to mount the fiberglass and covering on existing wind tunnel surfaces. However, this is prohibitive due to added tunnel blockage and also more extensive covering would be required. The second mounting would be to remove existing surfaces in the corner and mount the covering flush with the walls with the fiberglass behind this. The walls would then be replaced behind the fiberglass as a hard backing and support for the treatment. The disadvantage of this type mounting would be the expense of removing the walls and replacing them behind the treatment. However, this second type of mounting does not restrict the thickness of the fiberglass which will determine the amount and frequency range of attenuation. The recommendation by the authors is the use of 2 to 4 inch thick fiberglass mounted on the existing walls. Removing these walls to flush mount the treatment would not be cost effective. The screening to prevent flow erosion should closely follow Table 10.8 of Beranek (18), Figure 55 herein. This table lists necessary protection for fiberglass treatments for flow velocities up to 300 feet per second. Appendix C lists various manufacturers of standard fiberglass treatment and screen coverings.

The functions of this treatment differs for the front and back corners of the wind tunnel. The front corners, at the end of the test section leg of the wind tunnel, are treated to reduce reflection of sound from the source back to the test section, thus providing more nearly anechoic conditions in the axial directions. The back corners, at the end of the fan leg of the tunnel, are treated to attenuate background noise from the fan and prevent most of this sound from reaching

the test section. The treated front corners will also reduce the fan noise and other background sources to some extent. The treated corners will reduce secondary decay modes and the decay "bumps" described in the experimental section of this report. This type of corner treatment will also reduce the tunnel reverberant response.

#### Corrections to Specific Problems

This section serves as a guideline to correct specific problems that may or may not exist after the test section and tunnel elbow modifications have been made. The data that is presently available is not sufficient to determine if certain problems will exist in the USAAMRDL 7-x10-foot wind tunnel. However, testing in the one tenth model of this facility may help in determining if there are any aerodynamic problems associated with the proposed modifications.

If the background spectra in the test section are higher than desired in the upper frequency range and if the source of this noise is determined to be the fan, then turning vane treatment is required. The turning vanes will tend to focus high frequency sound around corners without allowing it to be absorbed by the end wall treatment. This treatment could be in the form of porous acoustic material which could take on an airfoil shape as cited by Bauer and Widnall (4). Damping material could be used to prevent "singing" of the turning vanes if this should be a problem.

If low to midrange frequency background noise from the fan or other sources is found in the test section and if most of this noise is found to be propagating to the test section from the downstream direction, then it

is recommended that the diffuser be redesigned and a muffler be added to the diffuser. If this problem does exist most of the noise will be propagating from the downstream direction. The nozzle reflects lower frequencies away from the test section. This is demonstrated by Schultz (14). The type and design of the muffler will depend on what frequency range is troublesome.

If there is a high background sound level in the test section from sources other than the fan, then fiberglass treatment is necessary in selected areas. These areas depend on the source and magnitude of the background noise and must be selected by experiment in the wind tunnel or model tunnel. The covering of the fiberglass should be selected from Figure 55 from Beranek (18).

If there is a high background sound level from the fan for specific ranges of fan parameter, then the problem is that part of the fan is stalling. A number of corrections to this problem are possible. First, corresponding test section velocities can be avoided. Fan pitch control and fan speed control may be necessary. The fan could also be redesigned for low noise and high efficiency over a large velocity range. If this background noise is pure tone in nature, then the distance between the rotor and stators should be increased. The effect this will have is shown in Figure 56.

A panel excited vibration can be corrected by reinforcing or sandloading the troublesome panels. If the source of panel excitation is determined to be secondary corner flows, then corner fillets will eliminate the excitation source. If the vibrations are excited by the



fan or powerplant, then vibration isolation and vibration decoupling the source is necessary. If the source of vibration is something foreign then the tunnel should be vibration isolated from the foundation.

The problems outlined above are the most probable ones that might be found in the 7-x10-foot wind tunnel. Other problems would probably be related or be treatable by the methods outlined above. All recommendations are reiterated in Table IV.

#### Experimental Procedures

To facilitate making noise measurements in a wind tunnel various experimental procedures are recommended. By proper scaling techniques, the noise from a model rotor can be scaled into the frequency range where the acoustic treatment provides optimum performance. This would insure maximum benefit from any acoustic treatment. Correlation techniques described in this report may prove extremely useful in extracting the rotor noise signature from the background noise.

The use of microphone probes within the flow has not reached the peak of possible development. Recently Arndt and Nagel (29) reported the use of a pressure probe to obtain near field data. These data gave considerable information about rotor noise harmonics not evident in the far field signal. Figure 57 and 58 present a comparison of near field and far field data obtained under comparable conditions. The microphone probe was positioned upstream of the rotor in such a manner that contamination from broadband components of the rotor noise are almost eliminated. Note the higher harmonics in the near field spectrum which are masked by broadband components in the far field noise signature. Arndt, et al., (30) and Barefoot (24) have successfully

used such probes to measure pressure intensity and cross correlation of the pressure field in the mixing zone of an open jet. This type of probe appears to be far more satisfactory than the use of conventional microphones with wind screens.

#### Data Correction

Perfect acoustic properties will not be achieved with any reasonable modification of an existing wind tunnel. However, data correction procedures, such as first suggested by Hartman and Soderman (5) and revised to include frequency dependence by Arndt and Boxwell (11) may be proved valid after treatment reduces the magnitude of the correction. Several correction techniques discussed in the previous sections may also prove suitable. Aerodynamic corrections discussed in this section will also be necessary.

#### Limitations on Experimental Research

Although the state of the art in acoustic treatment, aerodynamic theory, correlation analysis, etc., can be utilized to achieve reasonable success in a rotor acoustic research program, it should be emphasized that certain limits will exist after full utilization of the suggestions in this report. Cost constraints will limit the amount that background noise and reverberant buildup can be reduced. This will set a lower limit on the noise level of a model rotor. Further theoretical analysis is also required to gain confidence in the correlation techniques just now being reported in the literature.

### Suggestions for Further Work

Although the data base is limited, there appears to be enough evidence to indicate that the USAAMRDL 7-x10-foot wind tunnel can be modified to permit aeroacoustic testing. Therefore it is suggested that a detailed design study be initiated at this stage, incorporating the suggestions contained in this report. Coincident with this study there should be a test program to evaluate the aerodynamic and acoustic properties of the test section. Aerodynamic tests can evaluate the influence of slots or holes in the test section walls with regard to possible surging, boundary layer buildup and its influence on diffuser performance, etc. This work can be carried out in the 1:10 model of the subject wind tunnel.

A study should be made to include but not to be limited to, selection of hard wall acoustic treatment with maximum attenuation in the frequency range where reverberation effects are at a maximum, an in-depth study of acoustic modelling including the additional effects of air absorption due to frequency shift, variations in materials, and the frequency dependent absorption characteristics of acoustic treatment. Consideration should be given to modelling the effects of reverberation in the tunnel circuit on the acoustic properties of the test section. A model scale should then be selected and a model designed.

At the present time a 1:2 scale would appear to be best for acoustic tests. The influence of reverberation could be handled by designing the model such that ends can have either anechoic (with

wedges) or hardwall termination. Data should be collected to first evaluate the accuracy of the tuned chamber design procedure and to study the influence of additional absorptive material in the chamber. The extremes of anechoic and hardwall termination should give an estimate of the overall effect of the treated test section when coupled to the entire wind tunnel circuit. Information should be gathered on the relative influence of wall porosity and configuration such as holes or slots. This work should be coincident with the aerodynamic testing.

Finally, an assessment of the probable types of vehicles that will be tested in the future should be made to obtain an intensity-frequency envelope in which noise measurements will probably be made. This will determine the type of probe design that would be necessary for use in a closed jet wind tunnel. This is an important consideration since the decision to use a closed jet test section should be based both on acoustic performance of the tunnel and the ability to collect acoustic data within a flow.

Summary

The present use of conventional wind tunnels in aeroacoustic research is probably limited to qualitative evaluations of relative noise levels from various configurations. The acoustical properties of such facilities are extremely complex and simple correction procedures based on the simple theory for a semi-reverberant enclosure do not lead to accurate answers for complex acoustic problems. Suitable acoustic treatment can lead to an acceptable aeroacoustic facility. It is suggested that consideration be given to a treated closed jet configuration.

In conjunction with any acoustic modifications, improvements are necessary in the types of microphone probes used to collect acoustic data in a flowing media. Proper selection of model size is necessary to insure that the frequency range of interest falls within the acoustic capabilities of the facility. Further research is also necessary to improve acoustic signal detection techniques to allow measurement of directivity and spectral density in a less than ideal acoustic environment.

REFERENCES

1. Paterson, R. W., Vogt, P. G., and Foley, W. M., "Design and Development to the United Aircraft Research Laboratories Acoustic Research Tunnel," AIAA Paper No. 72-1005, September 13-15, 1972.
2. Heyson, H., "Jet-Boundary Corrections for Lifting Rotors Centered in Rectangular Wind Tunnels," NASA TR R-71, 1962.
3. Hanson, Carl E., "The Design and Construction of a Low Noise, Low Turbulence Wind Tunnel," MIT Department of Mechanical Engineering, DSR 79611-1, January 13, 1969.
4. Bauer, Paul and Widnall, S., "The Development of a Wind Tunnel Facility for the Study of V/STOL Noise" MIT, FTL Report R-72-6, August 1972.
5. Hartmann, J. R. and Soderman, P. T., "Determination of the Acoustical Properties of the NASA Ames 40- by 80-Foot Wind Tunnel", Ames Research Center, Working Paper No. 237, August 1967.
6. Hickey, David H., Soderman, P. T. and Kelly, Mark W., "Noise Measurements in Wind Tunnels", NASA SP-207, July 1969, pp. 399-408.
7. Cox, C. R., "Full Scale Helicopter Rotor Noise Measurements in the Ames 40- by 80-Foot Wind Tunnel", Bell Helicopter Report 576-099-052, October 1967.
8. Cox, C. R., "Rotor Noise Measurements in Wind Tunnels", Proc. Third CAL/AVLabs Symposium, Vol. 1, June 1969.
9. Arndt, R. E. A. and Borgman, D. C., "Noise Radiation from Helicopters Operating at High Tip Mach Number", Jour. A.H.S., January 1971.
10. Bies, David Alan, "Investigation of the Feasibility of Making Model Acoustic Measurements in the NASA Ames 40- by 80-Foot Wind Tunnel", NASA CR-114352, July 1970.
11. Arndt, R. E. A. and Boxwell, Donald A., "A Preliminary Analysis of the Feasibility of Rotor Noise Measurements in the AMRDL-Ames 7- x 10-Foot Wind Tunnel", Unpublished Report.
12. Ver, I. L., Malme Charles I. and Meyer, E. B., "Acoustical Evaluation of the NASA Langley Full-Scale Wind Tunnel", NASA CR-111868, January 1971.
13. Schultz, G., "On the Measurements of Noise in the Neighborhood of Bodies in Subsonic Wind Tunnels. Part I", DLR FB 68-43, DVL Report No. 772, July 1968, (RAE Library Translation 1352).

G

REFERENCES CON'T

14. Schultz, G., "On the Measurements of Noise in the Neighborhood of Bodies in Subsonic Wind Tunnels. Part II", DLR-FB 69-86, November 1969, (RAE Library Translation 1465).
15. Smith, Preston W., Jr. and Lyon, Richard H., "Sound and Structural Vibrations", NASA CR-160, March 1965.
16. Mangiarotty, R. A., March, Alan, H. and Feder, Ernest, "Duct Lining Materials and Concepts", NASA SP-189, Paper No. 5, October 1968.
17. Eversman, Walter, "The Effect of Mach Number on the Tuning of an Acoustic Lining in a Flow Duct", J. Acoust. Soc. Am., Vol. 48, No. 2 (Part 1), 1970.
18. Beranek, L. L., Noise and Vibration Control, McGraw Hill, New York, 1971.
19. Atvars, J., Schubert, L. K., Grande, E., Ribner, H. S., "Refraction of Sound by Jet Flow or Jet Temperature", NASA CR-494, January 1965.
20. Arai, Masaaki, "Correlation Methods for Estimating Radiated Acoustic Power", 6th International Congress on Acoustics, Tokyo, Japan, F-1-4, August 21-26, 1966.
21. Cook, B. D., "Acoustic Modeling of Noise Sources Utilizing Correlation Techniques", Presented at 83rd Meeting of the Acoustical Society of America, Buffalo, New York, April 18-21, 1972.
22. Arndt, R. E. A., "Some Considerations of Rotor Noise", Unpublished Report, August 1969.
23. Von Frank, E., "Turbulence Characteristics in the Mixing Zone of a Perturbed and Unperturbed Round Free Jet", M.S. Thesis, Penn State University, June 1970.
24. Barefoot, G. L., "Fluctuating Pressure Characteristics in the Mixing Region of a Perturbed and Unperturbed Round Free Jet", M.S. Thesis, Department of Aerospace Engineering, The Pennsylvania State University, to be published, 1972.
25. Heyson, H., "Linearized Theory of Wind Tunnel Jet-Boundary Corrections and Ground Effect for VTOL-STOL Aircraft", NASA TR R-124, 1962.
26. Brownell, W. F., "An Anechoic Test Facility Design for the Naval Ship Research and Development Center", NSRDC Report 2924, September 1968.

REFERENCES (CON'T)

27. Bruel, P., "Windscreens", Bruel & Kjaer Technical Review, November 2, 1960.
28. Eisenberg, P., "On the Mechanism and Prevention of Cavitation", David Taylor Model Basin, Report 712, July 1950.
29. Arndt, R. E. A. and Nagel, Robert T., "Effect of Leading Edge Serrations and Noise Radiation from a Model Rotor", AIAA Paper No. 72-655, June 20-28, 1972.
30. Arndt, R. E. A., Tran, Nam and Barefoot, Galen L., "Turbulence and Acoustic Characteristics of Screen Perturbed Jets", AIAA Paper No. 72-644, June 26-28, 1972.
31. Lowson, M. V. and Ollerhead, J. B., "Studies of Helicopter Rotor Noise", USAAVLABS Technical Report 68-60, January 1969.



BIBLIOGRAPHY

Aerodynamic Noise, edited by Arnold Goldberg, AIAA Selected Reprint Series, Volume XI.

Architectural File, Sweet's Catalog Service, F. W. Dodge Corp., New York, 1971.

ASHRAE Guide and Data Book, Fundamentals and Equipment Volume, Chapter 14, Sound Control, 1965 and 1966.

Atvars, J., Schubert, L. K. Grande, E. and Ribner, H. S., "Refraction of Sound by Jet Flow and Jet Temperature", NASA CR-494, May 1966.

Atvars, J., Schubert, L. K. and Ribner, H. S., "Refraction of Sound from a Point Source Placed in an Air Jet", J. Acoust. Soc. Am., Vol. 37, January 1965, pp. 168-170.

Benzakein, M. J. and Hochheiser, R. M., "Some Results of Fan/Compressor Noise Research," ASME 70 WA/GT-12, August 1970.

Beranek, L. L., Noise Reduction, McGraw Hill, New York, 1960.

Block, James A., Runstadler, Peter W., Jr., and Dean, Robert C., Jr., "Low Speed of Sound Modeling of a High Pressure Ratio Centrifugal Compressor", Creare, Inc., TN-146, June 1972.

Bommes, Leonhard, "Effect of Fan Configuration on the Variation of Fan Sound Generation with Operating Conditions", ASHRAE Transactions, No. 2057, 1967.

Cremer, Lothar, "Theorie Der Luftschall-Dampfung in Rechteckkanal mit Schluckender Wand and Das Sich Dabei Ergebende Hochste Damfungsmass", Acustica, Vol. 3, 1953, pp. 249-263.

Grande, E., "Refraction of Sound by Jet Flow and Jet Temperature", NASA CR-840, August 1967.

Groff, G. C., Schreiner, J. R. and Bullock, C. E., "Centrifugal Fan Sound Power Level Prediction", ASHRAE Transactions, No. 2058, 1967.

Hanson, Carl E., "The Design and Construction of a Low Noise, Low Turbulence Wind Tunnel", M.I.T., Department of Mechanical Engineering, DSR 79611-1, January 13, 1969.

Harris, Cyril M., Handbook of Noise Control, McGraw Hill, New York, 1957.

BIBLIOGRAPHY (CON.)

Irani, P. A. and Sridhar, Ya K., "Aerodynamic Noise in Aircraft and Wind Tunnels", Natl. Aeronaut. Lab., Bangalore Sci. Rept. AE-2-63, August 1963.

Kinsler, Lawrence E. and Frey, A. R., Fundamentals of Acoustics, John Wiley & Sons, Inc., New York, 1962.

Kraichman, R. H., "The Scattering of Sound in a Turbulent Medium", J. Acoust. Soc. Am., Vol. 25, 1953, pp. 1096-1104.

Marsh, Alan H., "Study of Acoustic Treatments for Jet Engine Nacelles", J. Acoust. Soc. Am., Vol. 43, 1968, pp. 1137-1156.

Morse, P. M. and Ingard, K. V., Theoretical Acoustics, McGraw Hill, New York, 1968.

NASA Acoustically Treated Nacelle Program, NASA SP-220, October 1969.

Pankhurst, R. and Holder, D. W., Wind-Tunnel Techniques, Pitman, London, 1952.

Pope, Alan, Low-Speed Wind Tunnel Testing, John Wiley & Sons, Inc., New York, 1966.

Pope, Alan, Wind Tunnel Testing, John Wiley & Sons, Inc., New York, 1947.

Progress of NASA Research Relating to Noise Alleviation of Large Subsonic Jet Aircraft, NASA SP-189, October 1968.

Richards, E. J. and Mead, D. J., Noise and Acoustic Fatigue in Aeronautics, John Wiley & Sons, Inc., New York, 1968.

Schmidt, D. W., "Recent Experimental Investigations on the Scattering of Sound by Turbulence", AGARD Report 461, April 1963.

## T A B L E I

PROBLEM AREAS ASSOCIATED WITH AEROACOUSTIC RESEARCHBackground Noise

Environmental Sources - machinery in the vicinity of the wind tunnel

Mechanical Sources - powerplant  
tunnel fan

mechanically induced vibrations

Aerodynamic Sources - flow separation

secondary flows in corners

periodic flows from turning vanes or collector cone

turbulent fluctuations in shear layer

along interior walls

mixing region of an open jet

Instrumentation Source- pseudosound from microphone in flow

periodic flows produced by instrumentation, i.e, microphone tripod

Model Noise Distortion

Reverberation - reflections from all confining surfaces

Refraction - in case of an open jet

Scattering

Scaling

Aerodynamic Scaling

Acoustic Scaling

T A B L E II

## Facilities Used for Aeroacoustic Research

<u>Facility</u>	<u>Size</u>	<u>Speed</u>	<u>Circuit</u>	<u>Test Section</u>	<u>Acoustic Treatment</u>	<u>Remarks</u>
MIT Dept of A/A	5'x7 1/2'	115 fps	Closed	Open	Anechoic Chamber, Treated Collection Cowl, Acoustic Wedges, Turning Vanes (pressure surface) treated, Vibration isolated anechoic chamber	
MIT Ac. & Vib. Lab.	15'x15"	180 fps	Open	Open-Closed	Honeycomb (soda straws) inlet & outlet, Screens, Treated nozzle & collector, Reverberant/Anechoic chamber, Muffler- Diffuser.	Low turbulence 0.05% - 0.2%
Penn State Aero Tunnel	4'x5'	150 fps	Closed	Open-Closed	Anechoic Chamber, Treated Endwalls	
DVL (Germany)	11'x10'	300 fps	Closed	Open	Treated Diffuser, Muffler, Paired Corners, Treated Collector Cone, Treated Corners	Fan located just past 1st corner
NASA Langley	30'x60'	110 fps	Double Closed	Open	None	2 Fans Correction approach
NASA Ames	40'x80'	340 fps	Closed	Closed	None	6 Fans
NSRDC	8'x8'	200 fps	Closed	Open-Closed	2 Mufflers, Anechoic Chamber, Vibration isolation from foundation, Wall treatment (selected areas), Damping material on turning vanes, (Closed partially treated test section)	Specially designed for optimum performance and low noise
UARL	5 ft <sup>2</sup> 10 ft <sup>2</sup>	650 fps 300 fps	Open	Open	Honeycomb & Screens, Anechoic Chamber, Muffler between fan & diffuser, Serrations on nozzle lip.	Variety of final nozzle & contraction sections & collector pieces.

<u>Facility</u>	<u>Size</u>	<u>Speed</u>	<u>Circuit</u>	<u>Test Section</u>	<u>Acoustic Treatment</u>	<u>Remarks</u>
BBN	16" x 16" 18" dia	120 fps	Open	Open	Treated inlet & outlet, Plywood chamber with cotton batting.	Large chamber w/small
RAE United Kingdom			Closed	Open	Anechoic Chamber, Muffler in settling chamber or treated corners, Treated diffuser, Splitter in diffuser, Splitters connecting turning vanes, Low noise fan.	
AV3DL (Ares)	7'x10'	410 fps	Closed	Closed	None	

# TABLE III

## SCALING PARAMETERS FOR A DIMENSIONALLY SCALED MODEL

### Aerodynamic Parameters

- (1) Mach Number Criteria  $M_t = \omega R_o / a_o$ ,  $M_s = V_s / a_o$ ,  $\mu = M_s / M_t$

The forward velocity should be the same for model and prototype.

The advance ratio should be the same in model and prototype.

The rotor speed should increase with the decrease in rotor size.

- (2) Lock Number Criteria  $L = \rho / \rho_o \quad 1 / (t/c) \sigma$

The density of the blade and prototype must be the same for equality at Lock number.

- (3) Reynolds Number Criteria  $R = \omega R_o c / \nu$

The kinematic viscosity must be decreased in proportion to the model scale, i.e., a pressurized tunnel is required.

### Acoustic Parameters

- (1) Frequency

The frequency of model noise increases with rotor speed

- (2) RMS Pressure

The pressure is proportional to  $R_o / r$

The pressure is related to tip Mach Number for rotational, vortex and thickness like  $M_t^5$ ,  $M_t^3$ , and  $M_t^4$  respectively

- (3) Directivity of Sound

The directivity of sound is the same for model and prototype and:

For vortex interaction

$$\propto \cos \delta \sin^2 \delta$$

For shockwave formation

$$\propto \sin^2 \delta$$

For vortex noise

$$\propto \cos \delta$$

For thickness noise

$$\propto \sin^2 \delta$$

# TABLE IV

## RECOMMENDATIONS FOR TUNNEL MODIFICATION

- (1) Closed test section treated with resonant type treatment including fiberglass within the honey combs.
- (2) End wall treatment of 2 to 4 inches of fiberglass covered as shown in Figure 55.

### Corrections to Specific Problems

- |                                                                |   |                                                                     |
|----------------------------------------------------------------|---|---------------------------------------------------------------------|
| (1) High frequency background noise from fan                   | - | turning vane treatment                                              |
| (2) "Singing" turning vanes                                    | - | damping material on turning vanes                                   |
| (3) Low or mid-range background noise from fan                 | - | redesign diffuser incorporating muffler                             |
| (4) Background noise from sources other than fan               | - | fiberglass treatment in selected areas with covering from Figure 55 |
| (5) Background noise from fan for specific ranges of fan speed | - | avoid corresponding test section velocities                         |
| (a) Broadband                                                  | - | fan pitch control and fan speed control                             |
|                                                                | - | redesign fan for low noise and high efficiency                      |
| (b) Pure tone                                                  | - | over large range of test section velocities                         |
|                                                                | - | separate rotor and stators                                          |
| (6) Panel excited vibration                                    | - | reinforce or sandload panels                                        |
| (a) excitation by secondary corner flows                       | - | add corner fillets                                                  |
| (b) excitation by fan or powerplant                            | - | vibration isolation and/or vibration decoupling                     |
| (c) excitation by source other than tunnel                     | - | vibration isolate tunnel from foundation                            |
|                                                                | - | vibration isolate source from foundation and/or enclose source      |

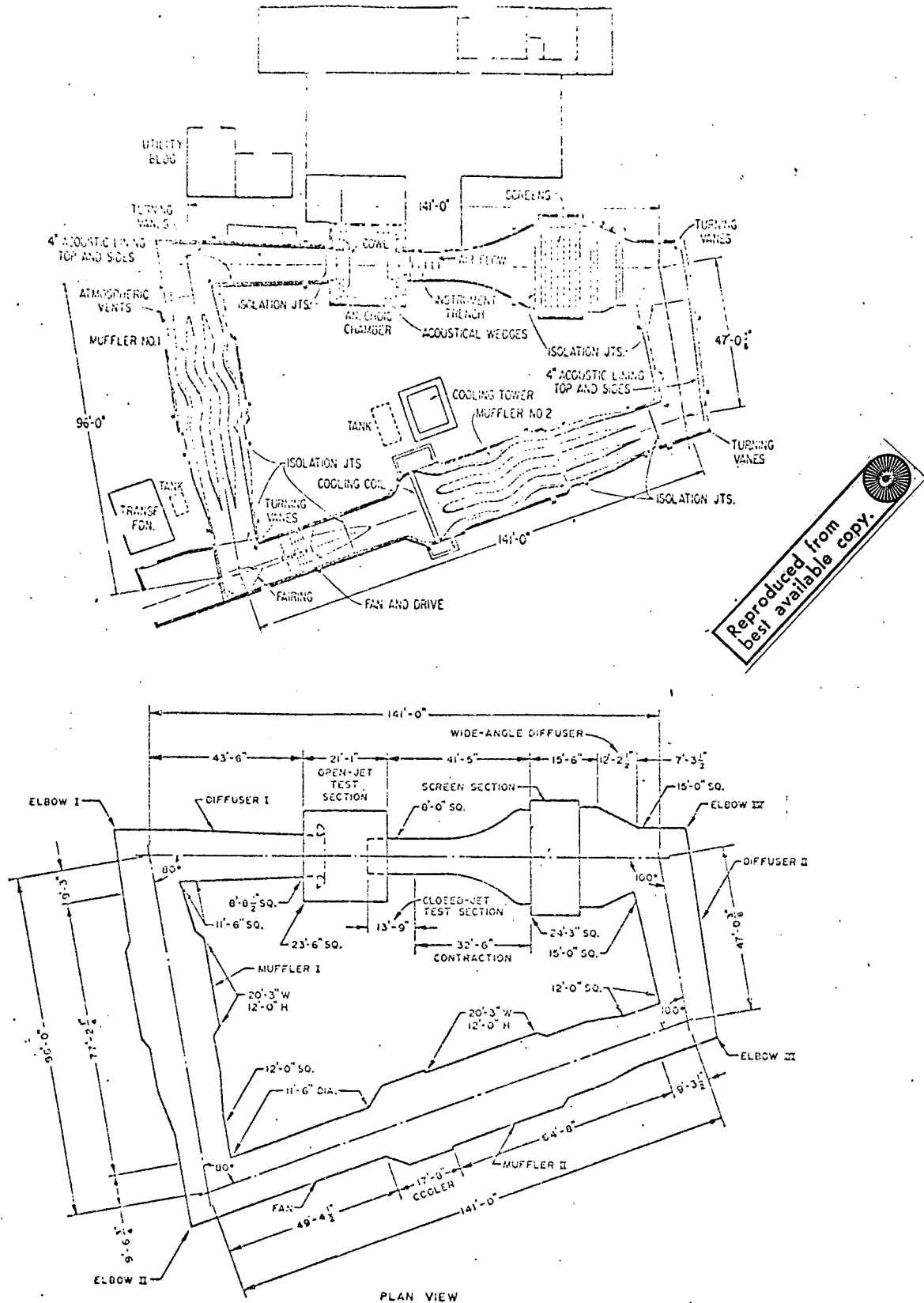


Figure 1. NSRDC Anechoic Wind Tunnel



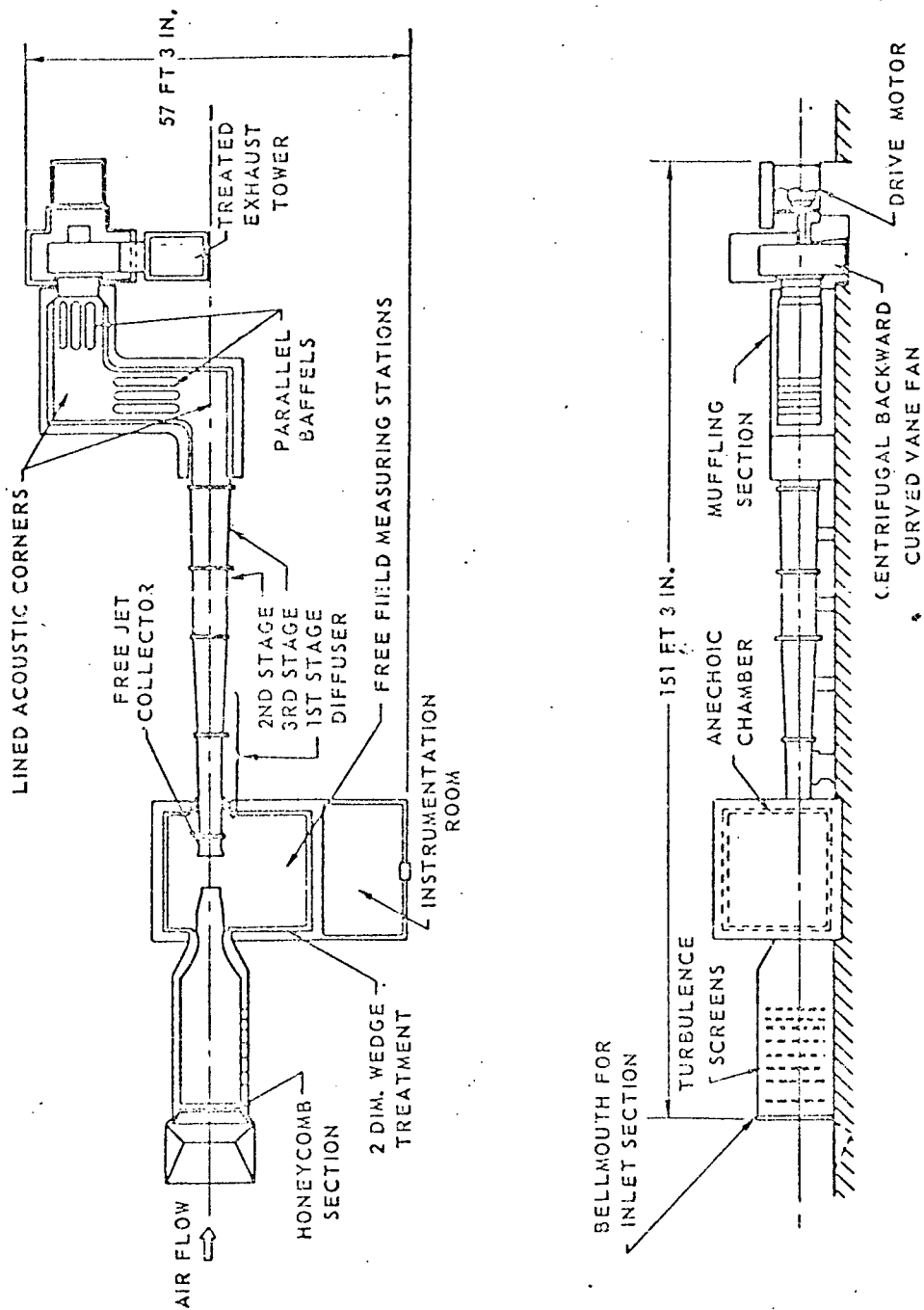


Figure 2. United Aircraft Research Laboratories Acoustic Research Tunnel

MEASUREMENT 7 FT ABOVE TEST SECTION CENTERLINE  
 30 IN. SEMI-OPEN JET LENGTH  
 $V=575$  FT/SEC

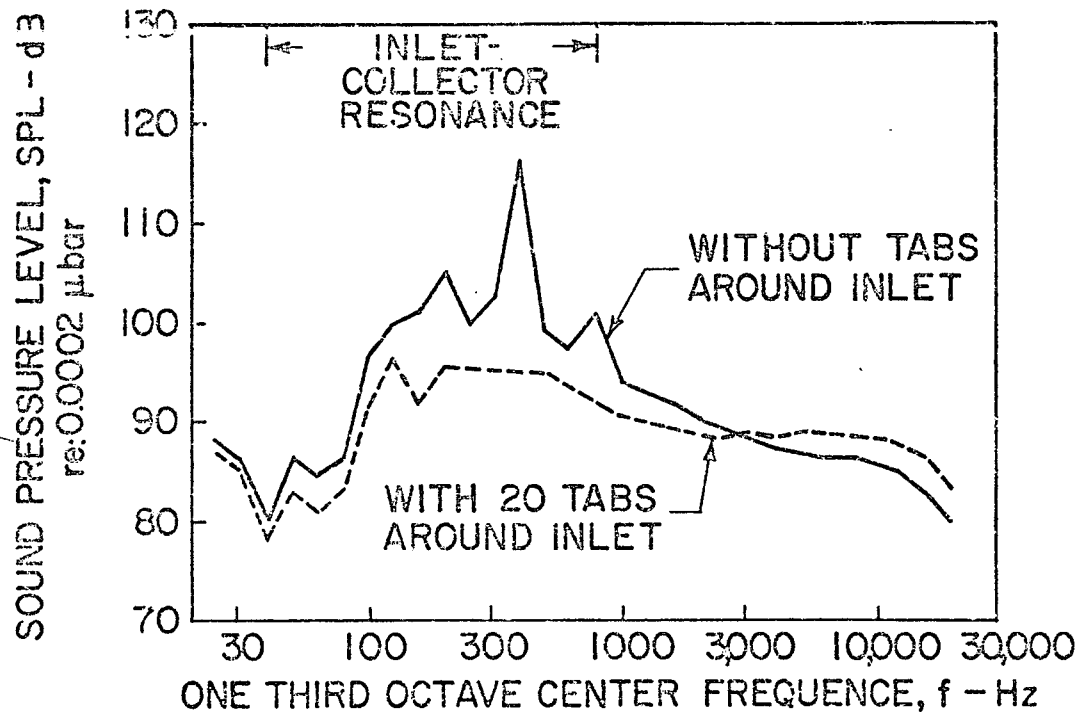
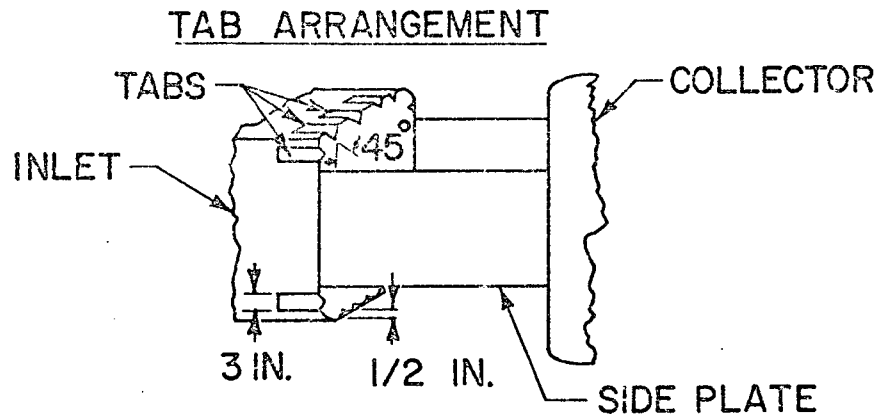


Figure 3. Effect of Inlet Tabs on Background Noise Spectra  
 (After Paterson, et al (1))

MEASUREMENT 7 FT ABOVE TEST SECTION CENTERLINE  
WITHOUT TABS AROUND INLET

$V = 575 \text{ FT/SEC}$

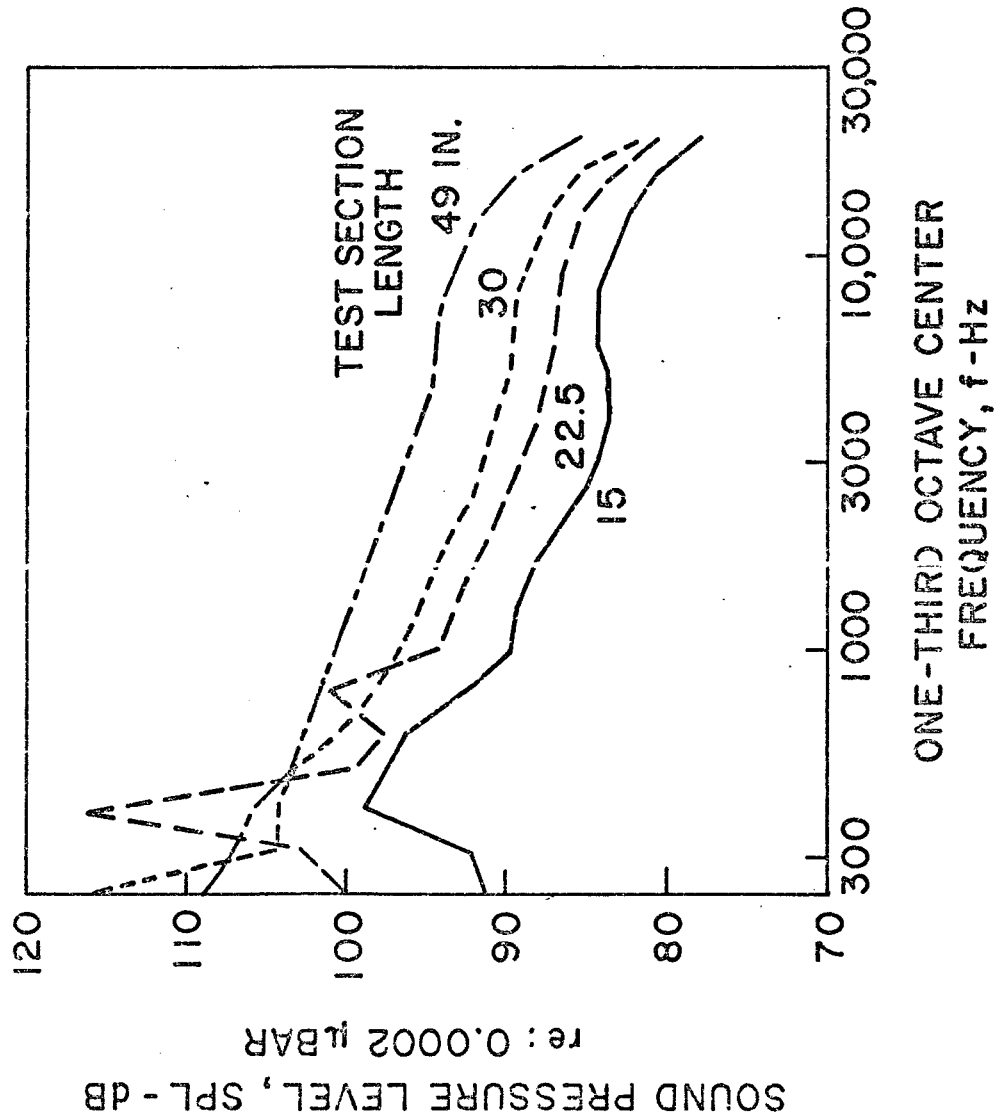
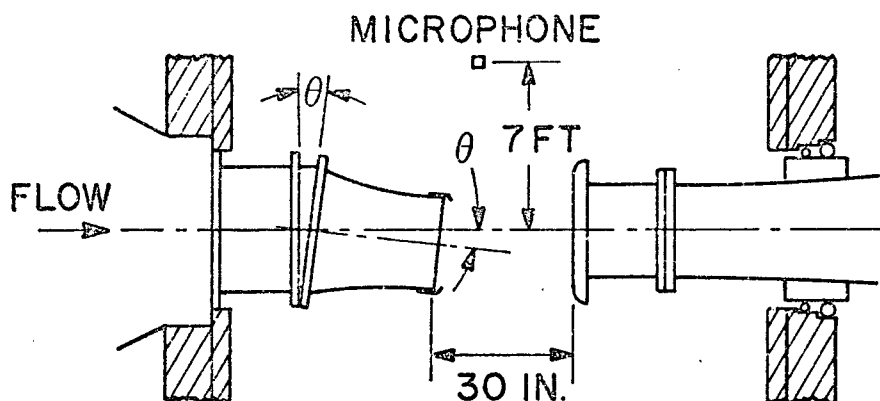


Figure 4. Effect of Test Section Length on Background Noise Spectra (After Paterson et al (1))

## a. SCHEMATIC OF DEFLECTED JET



## b. SOUND SPECTRA FOR VARIOUS DEFLECTION ANGLES

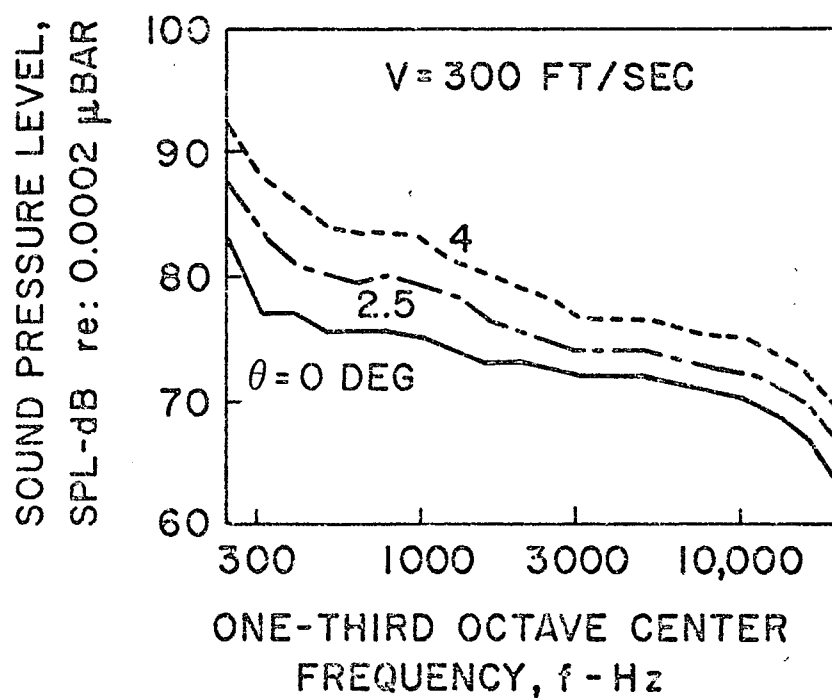


Figure 5. Investigation of Deflected Jet Noise  
(After Paterson, et al (1))

C<sup>2</sup>

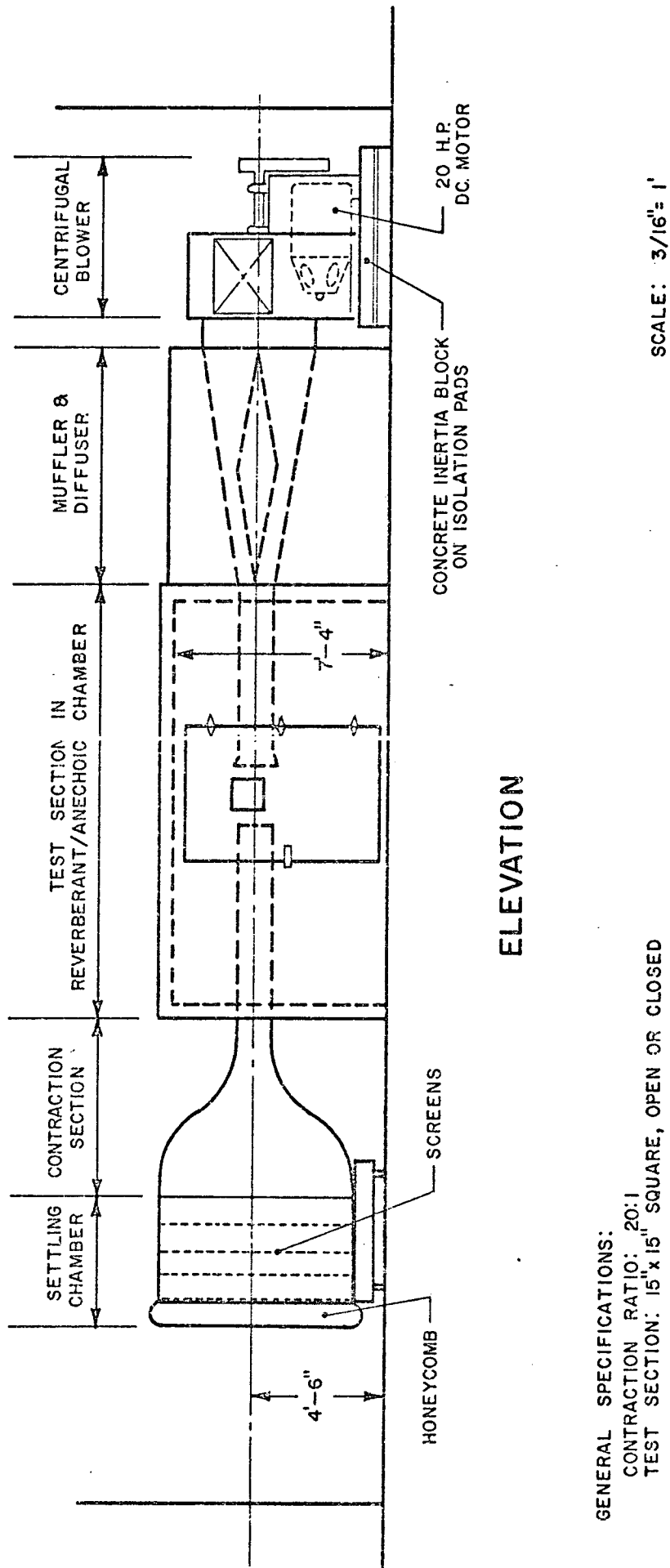


Figure 6. M.I.T. Acoustics and Vibration Laboratory Anechoic Wind Tunnel

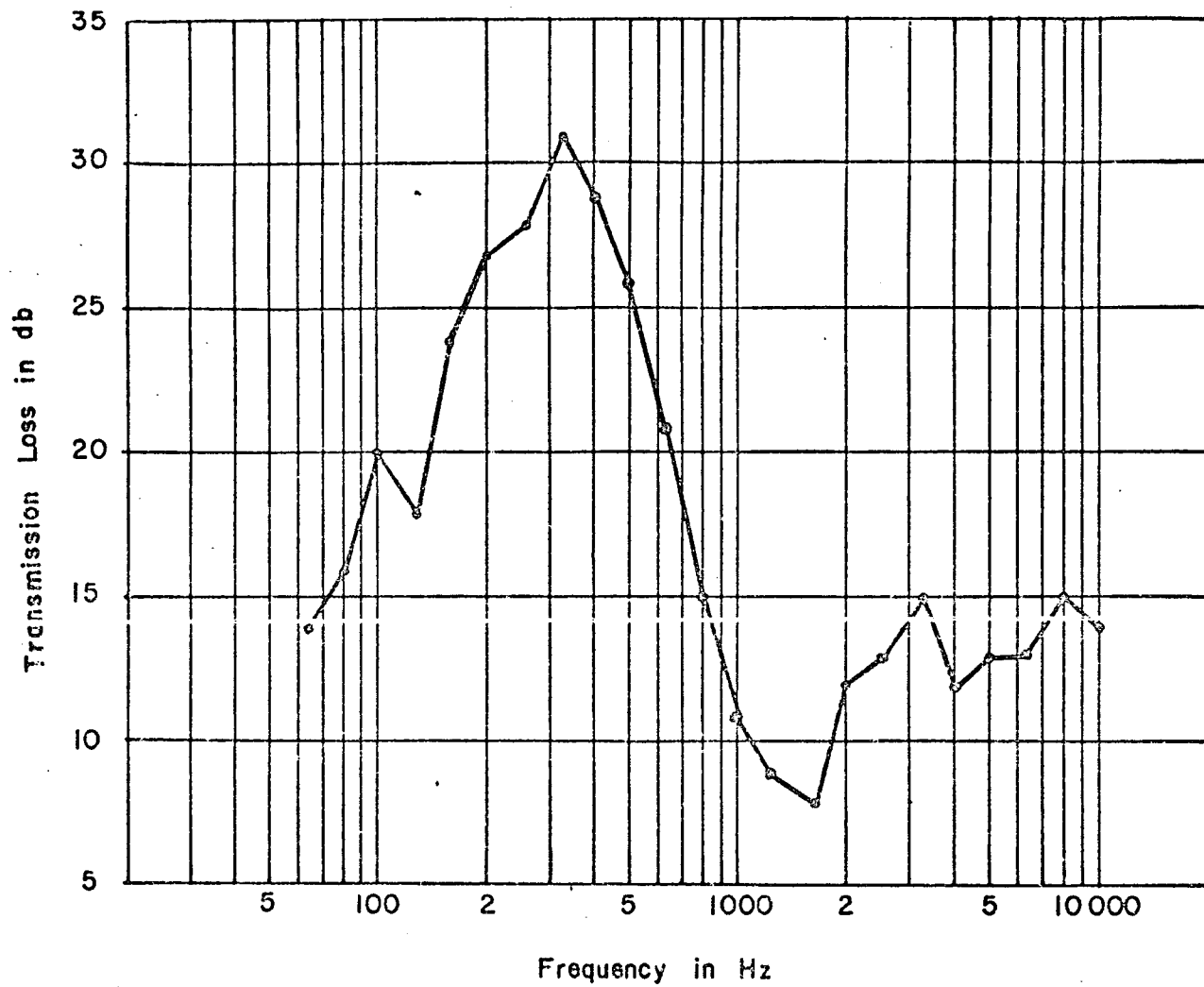


Figure 7. Muffler Transmission Loss between Inlet and Exit Measured in 1/3 Octave Bands

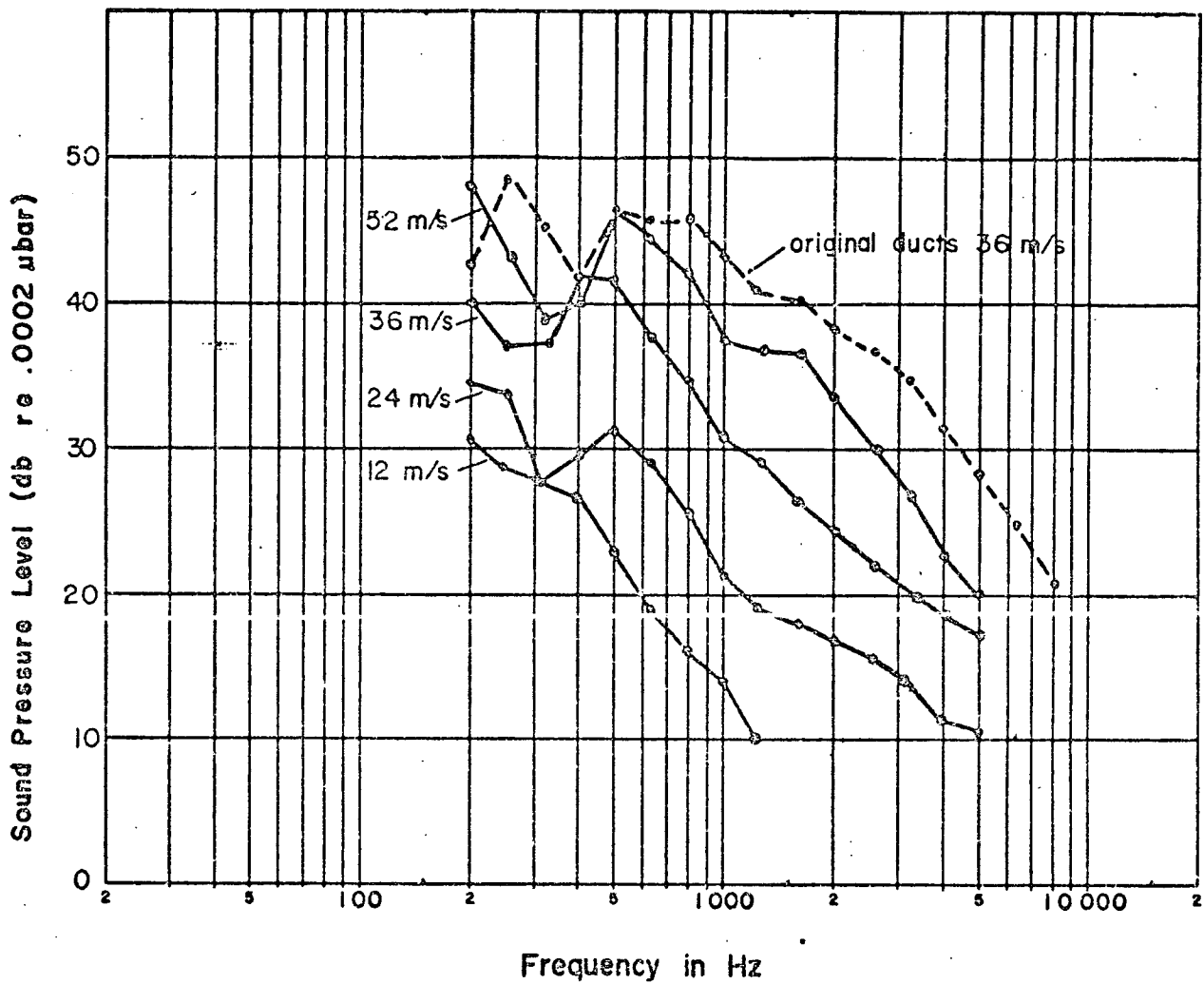
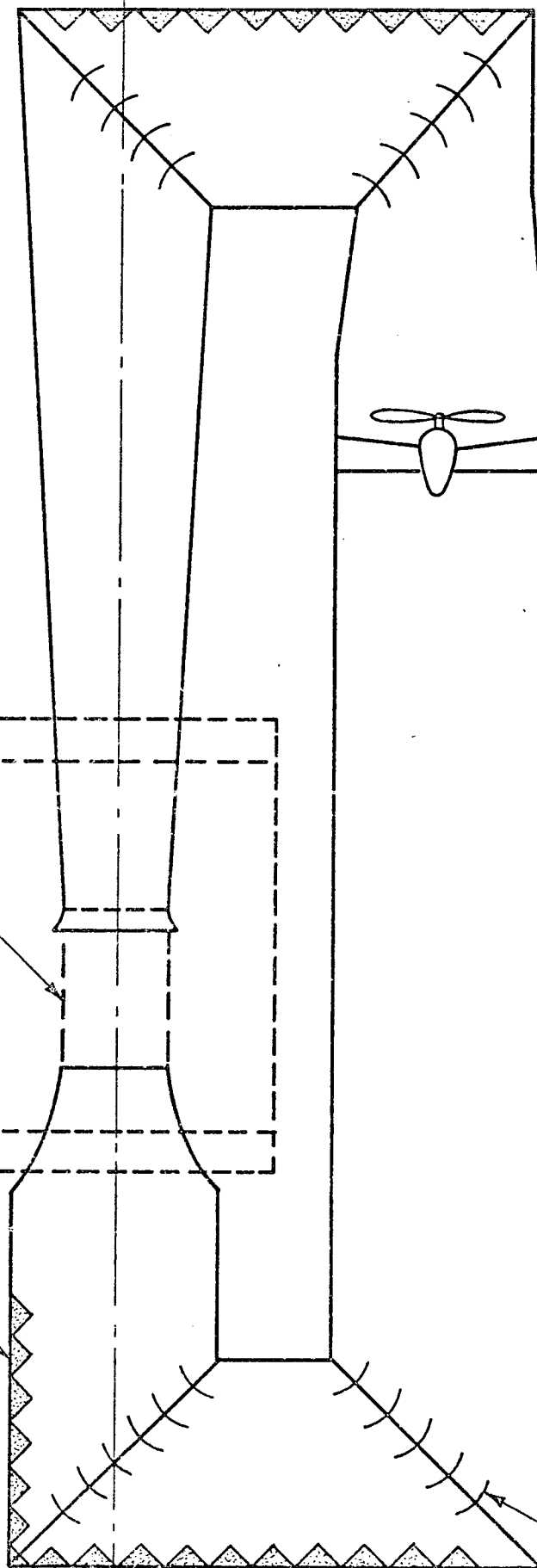


Figure 8. Background Noise Level in 1/3 Octave Bands  
in Reverberant Chamber with Closed Duct  
Test Section

ANECHOIC CHAMBER

4-1/2 x 7-1/2 TEST SECTION (REMOVED)

ACOUSTIC  
TREATMENT



ACOUSTICALLY TREATED  
VANES

SCALE: 3/16" = 1'

Figure 9. M.I.T. Department of Aeronautics and Astronautics Wind Tunnel



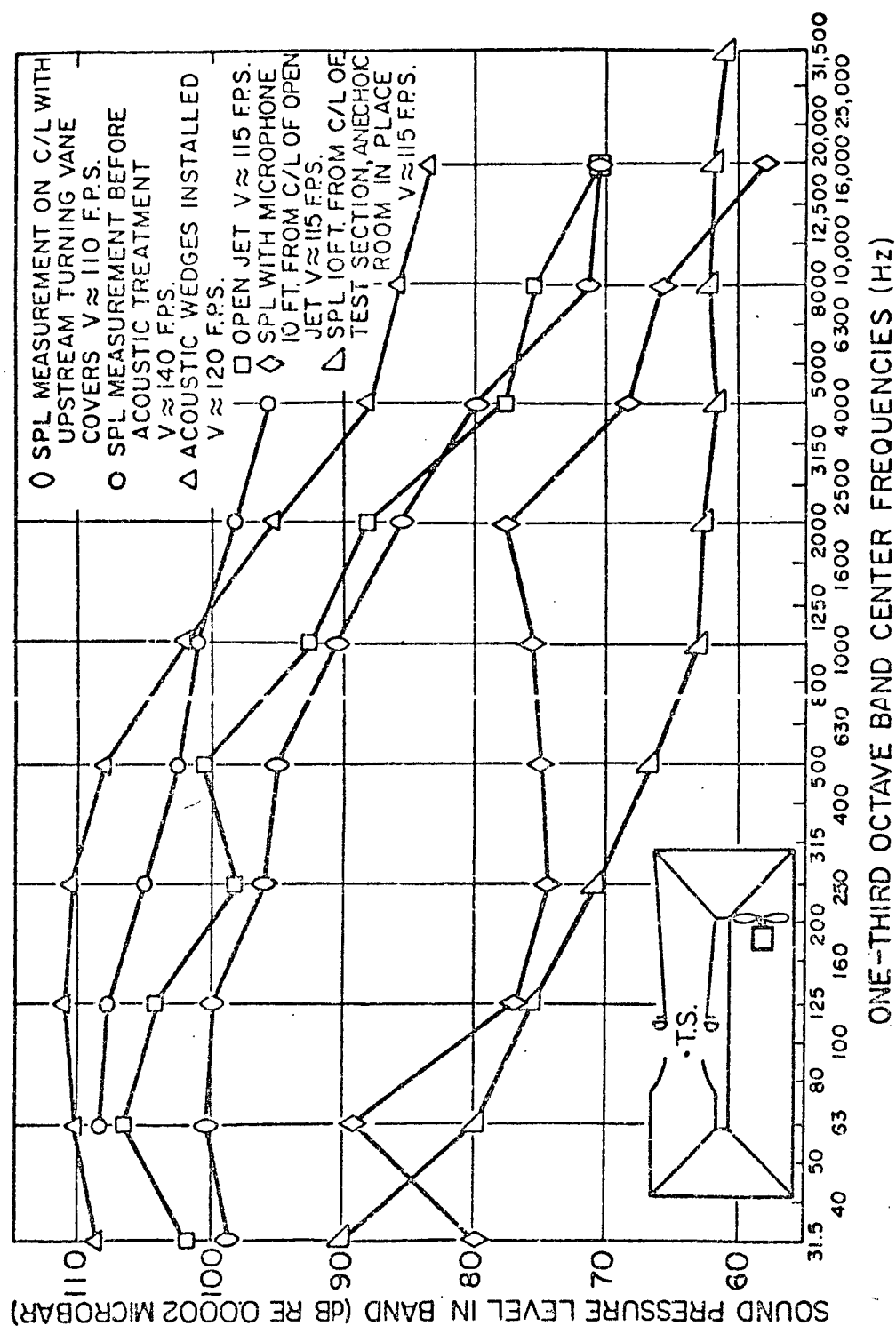


Figure 10. SPL Measurements of Background Noise in Test Section Corrected to 1/3 Octave Bandwidth

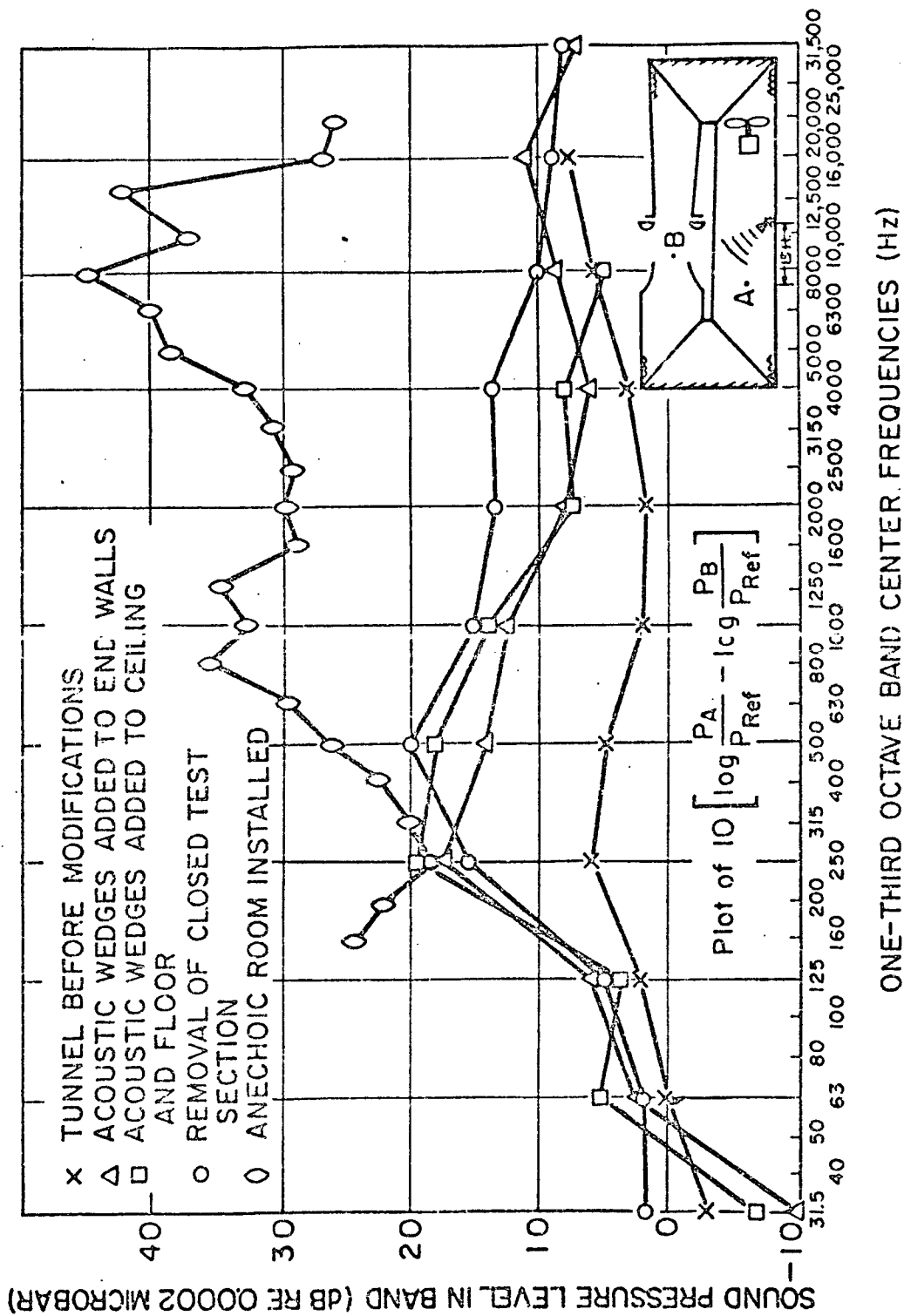


Figure 11. Measurement of the Attenuation of a Noise Source Located in the Return Section

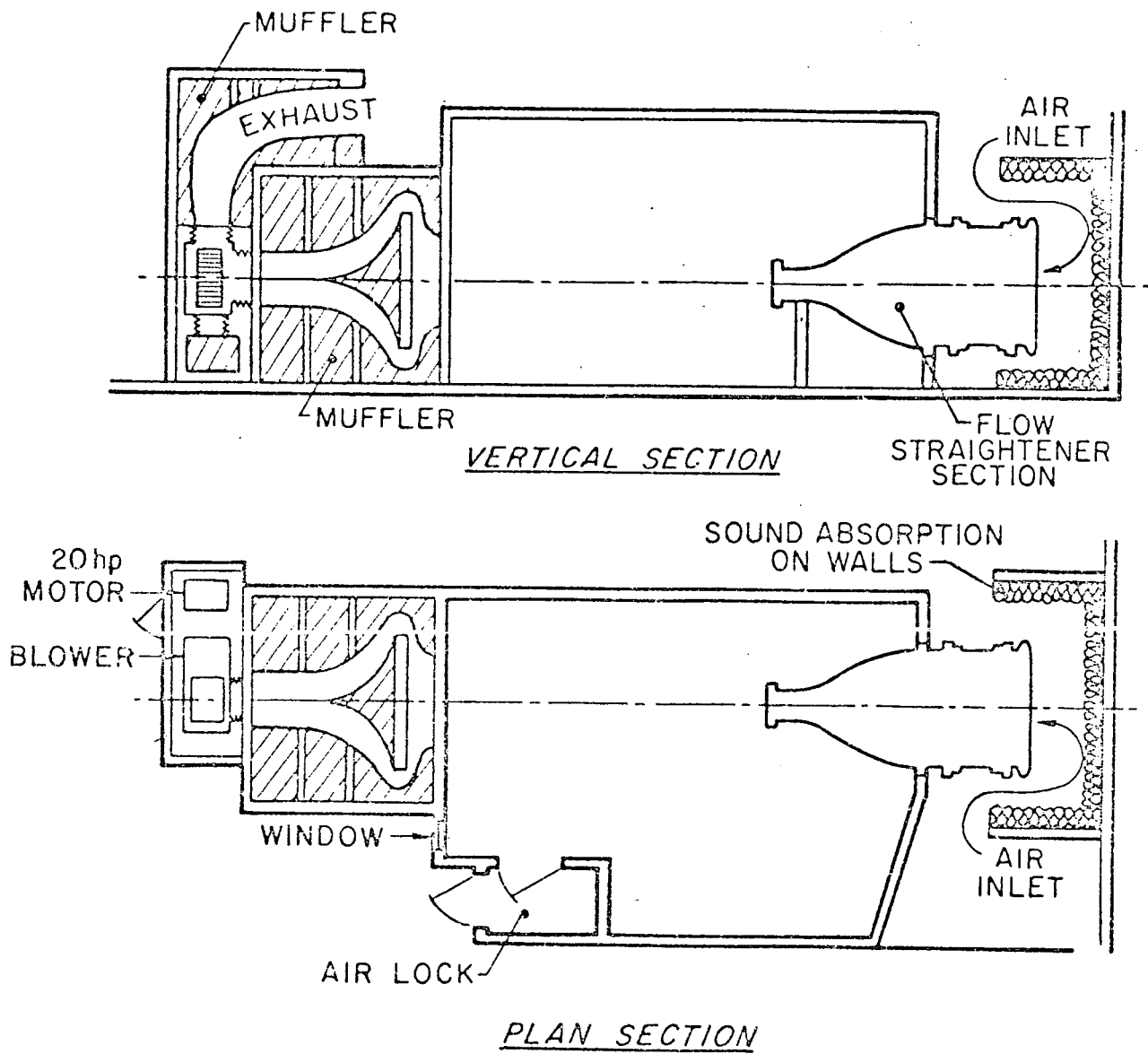


Figure 12. BB & N Quiet Wind Tunnel

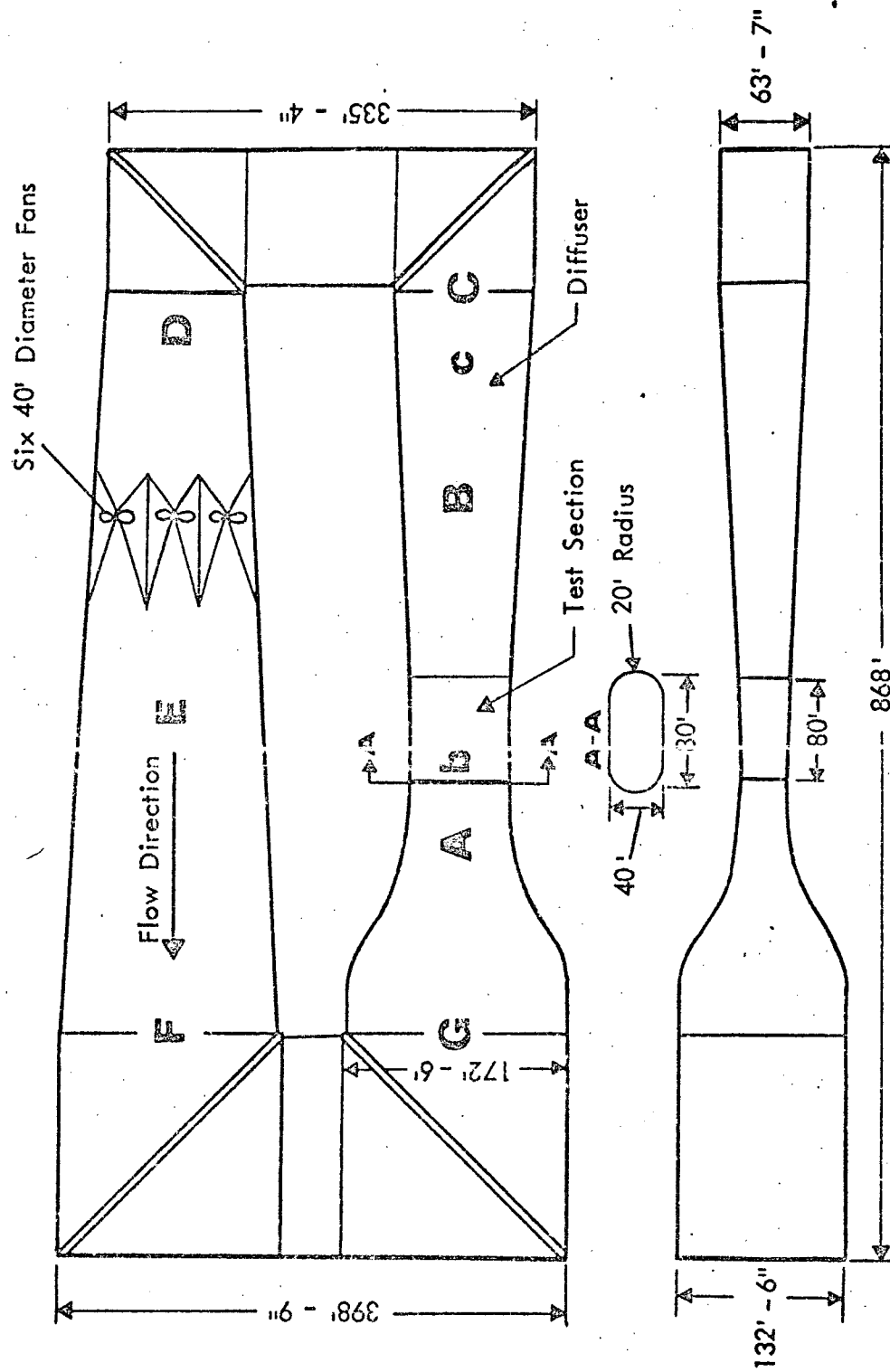
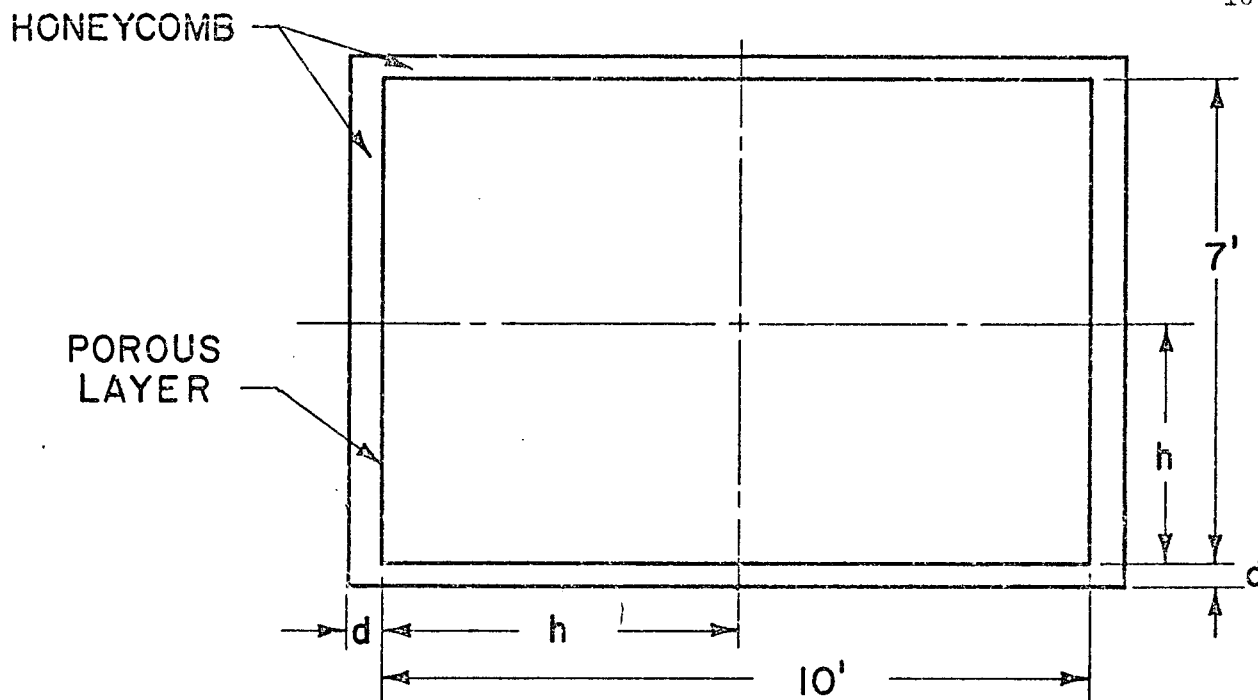


Figure 13. NASA Ames 40- x 80-Foot Wind Tunnel



#### TREATMENT ON FLOOR AND CEILING

$$h = 3.5'$$

$$f_0 = 400 \text{ Hz}$$

$$L = 15.6'$$

$$d = 2.93''$$

$$t < .282'$$

$$\delta < .72'$$

$$\left( \frac{R_f}{\rho a_0} \right)_{\text{opt}} = 2.29$$

$$R_l > 1.09 \times 10^4 \text{ mks rays/m}$$

#### TREATMENT ON WALLS

$$h = 5.0'$$

$$f_0 = 250 \text{ Hz}$$

$$L = 15.6'$$

$$d = 5.25''$$

$$t < .453'$$

$$\delta < 1.13'$$

$$\left( \frac{R_f}{\rho a_0} \right)_{\text{opt}} = 2.04$$

$$R_l > 6.05 \times 10^3 \text{ mks rays/m}$$

Figure 14. Results of Sample Calculations of Design  
Procedure for AMRDL 7- x 10-Foot Wind Tunnel

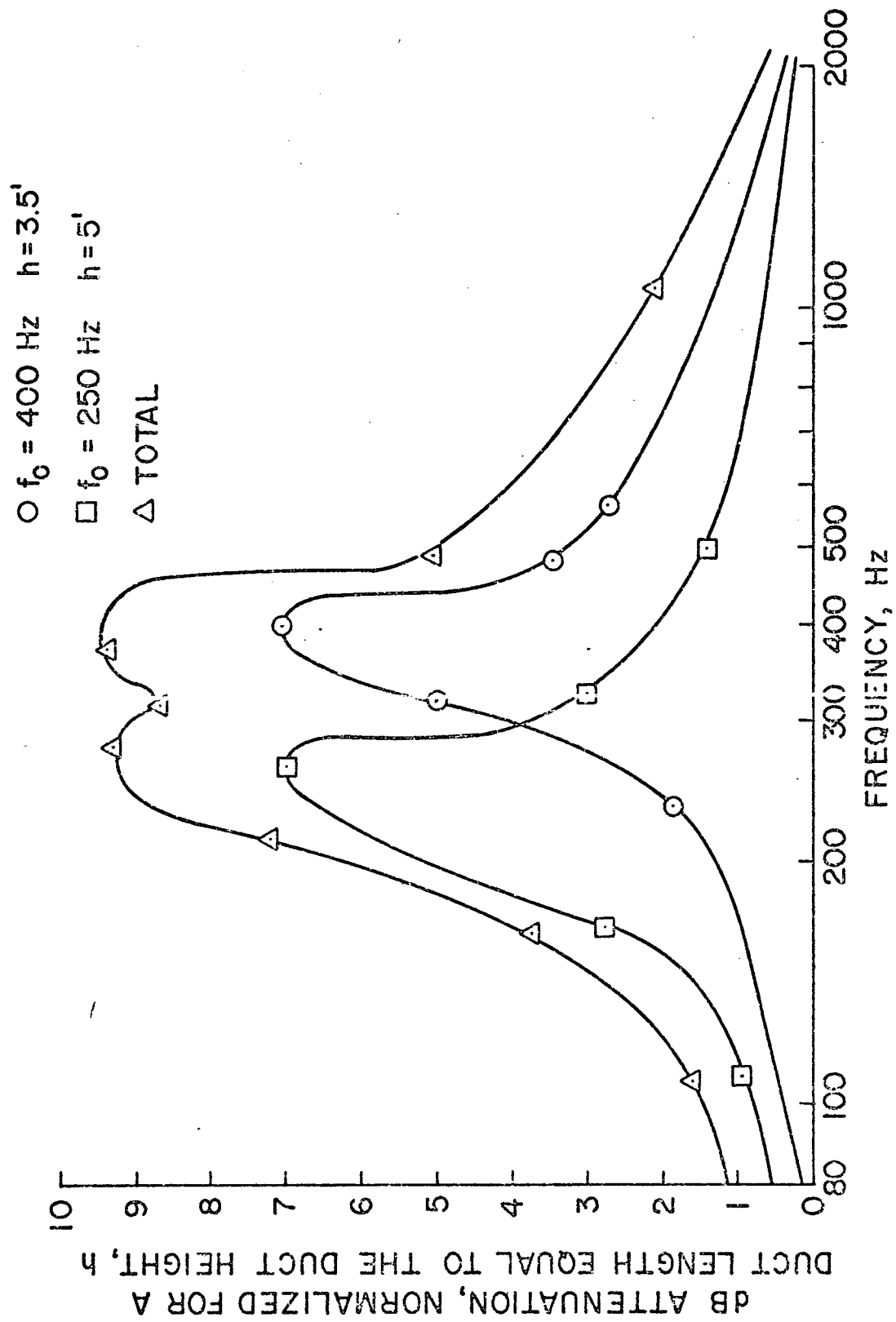


Figure 15. Results of Sample Calculations of Design Procedure of AMRDL 7- x 10-Foot Wind Tunnel

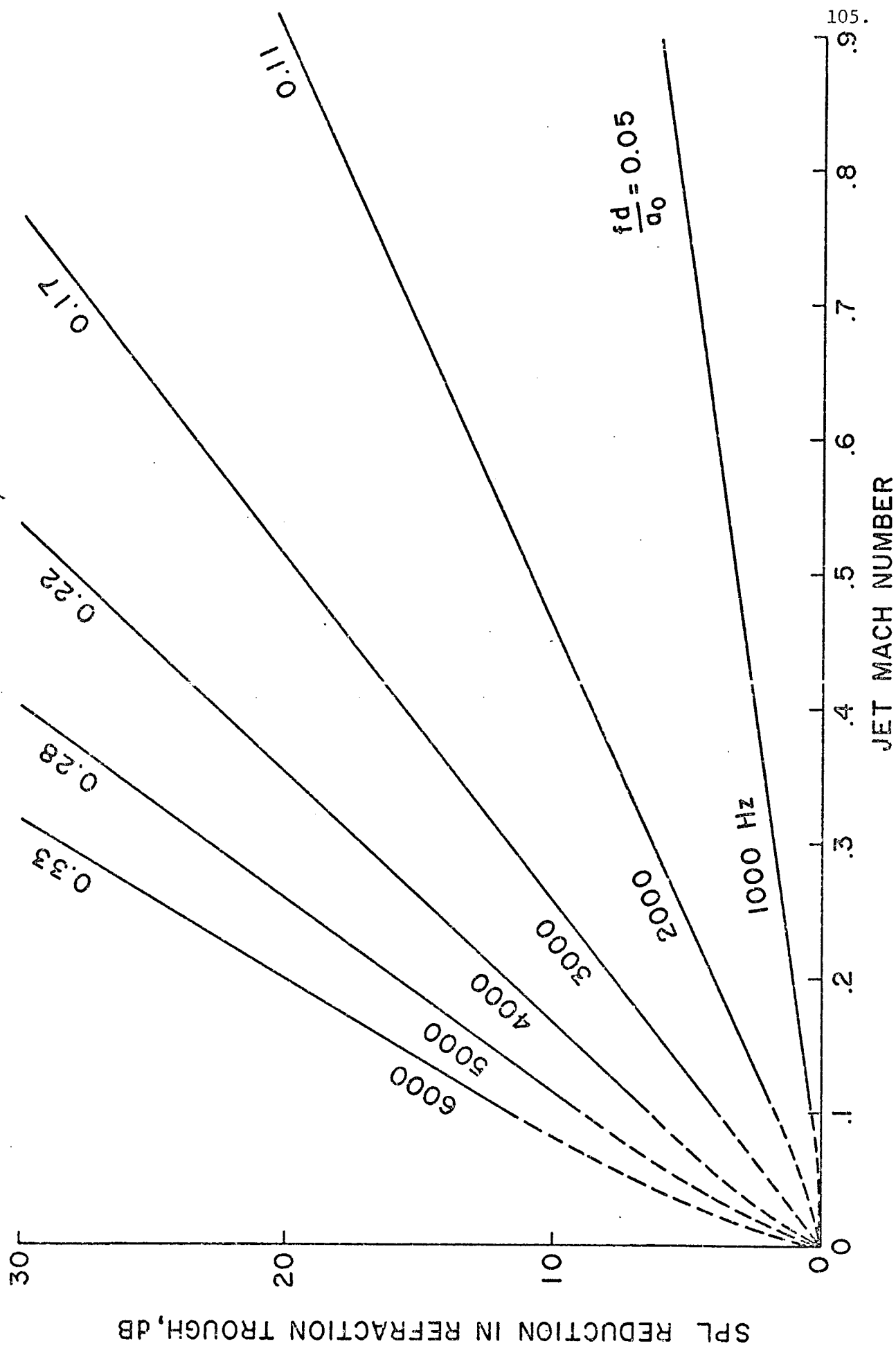


Figure 16. Jet Refraction Effects

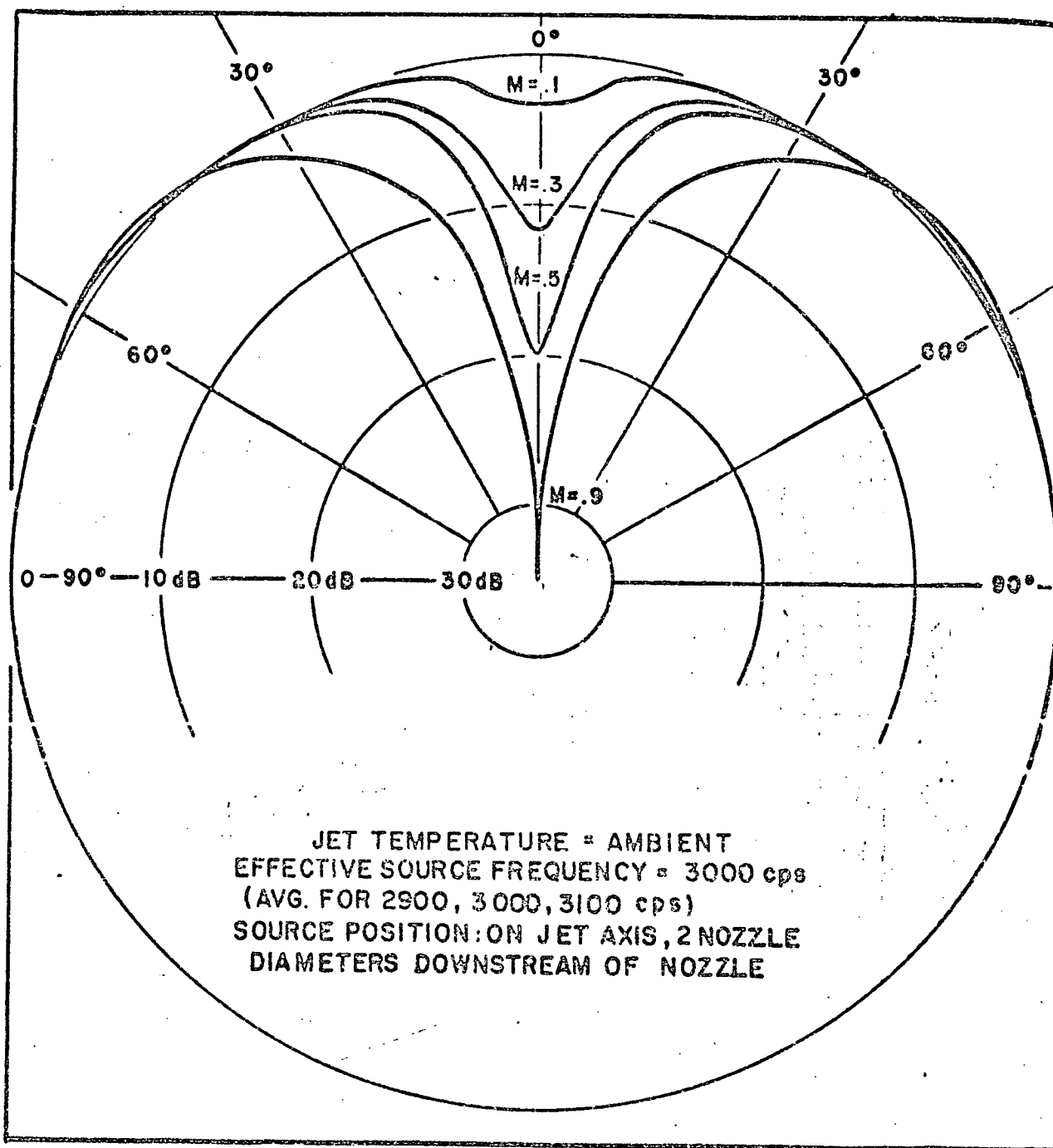


Figure 17. Effect of Jet Velocity on Directivity



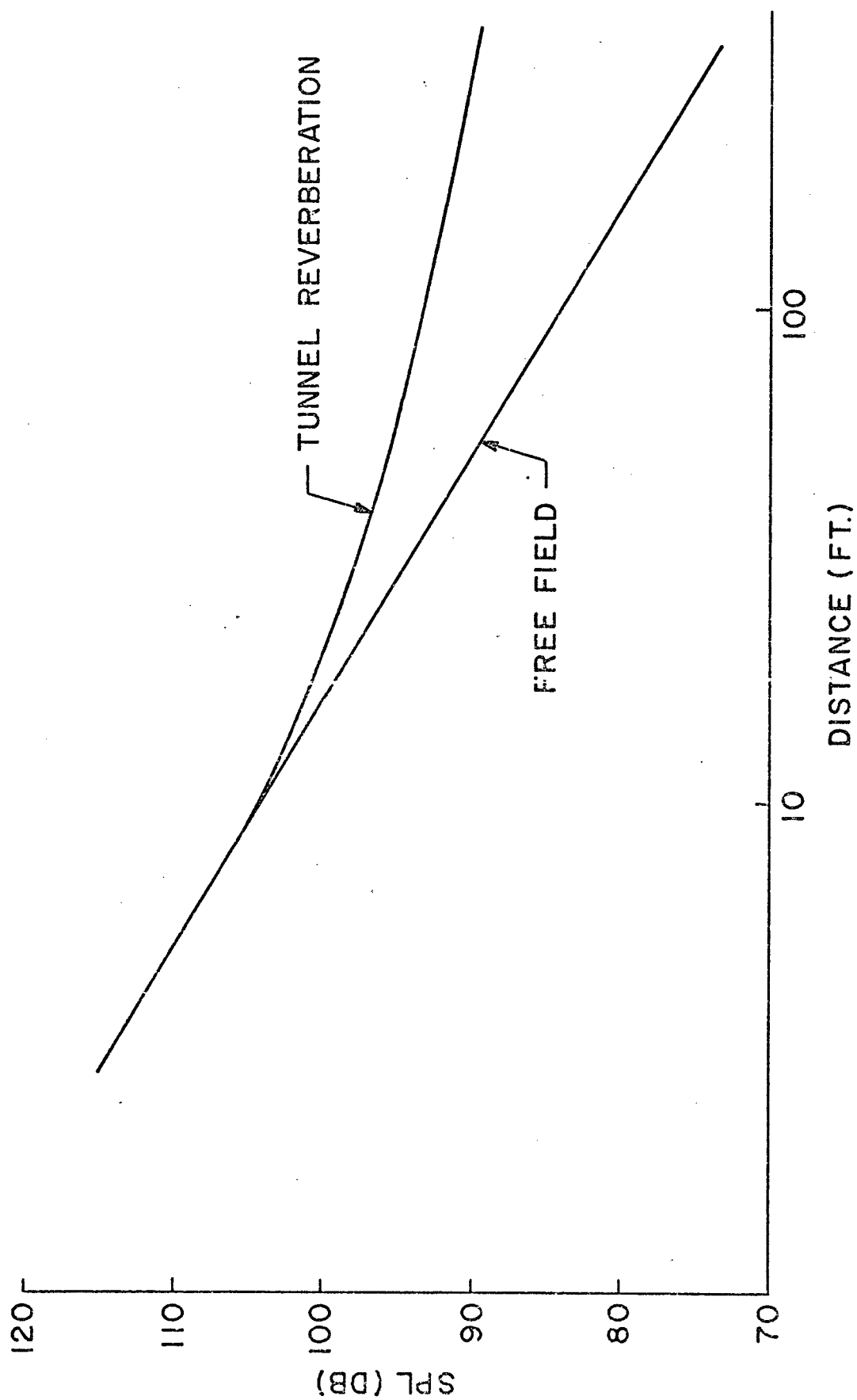


Figure 18. Reverberation Correction

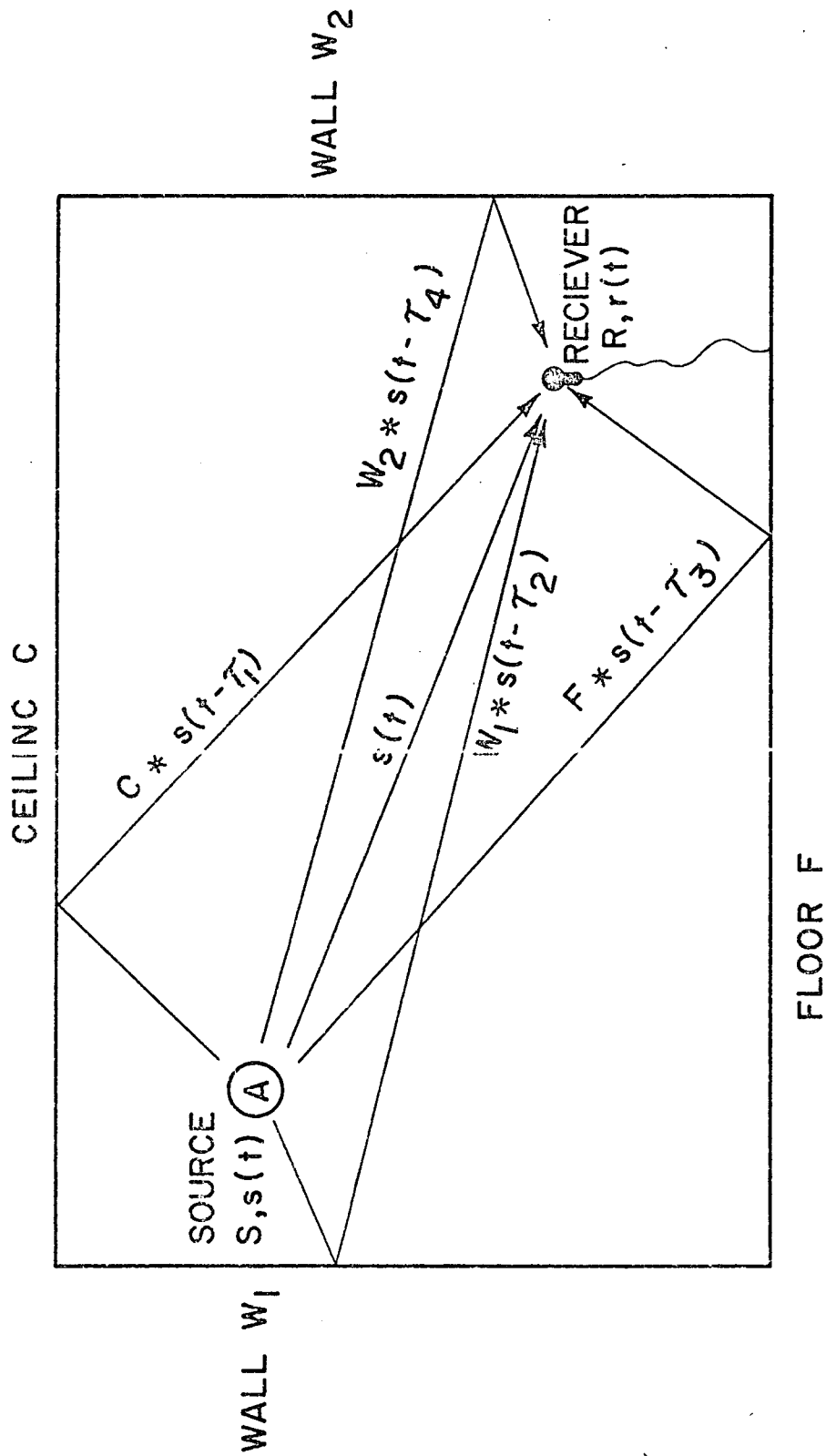


Figure 19. Schematic of Correlation Technique  
(After Cook (21))

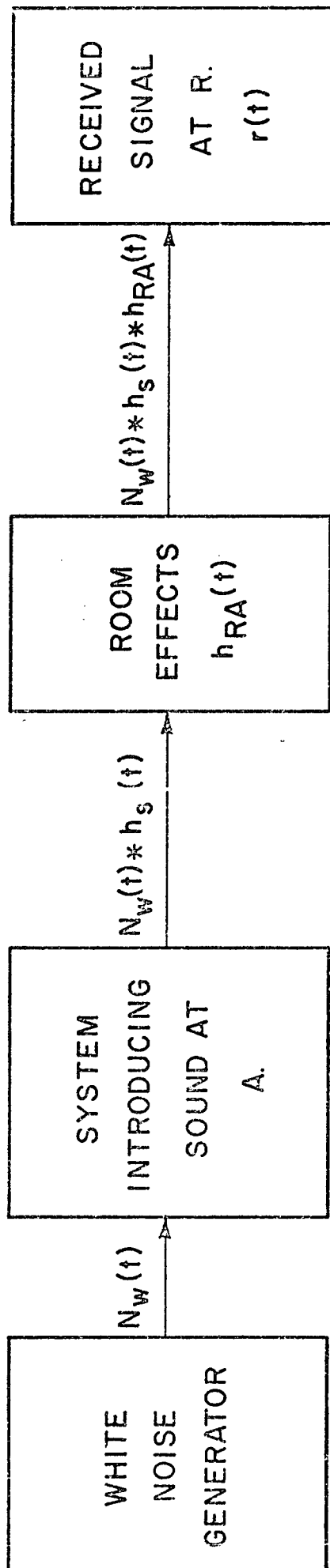
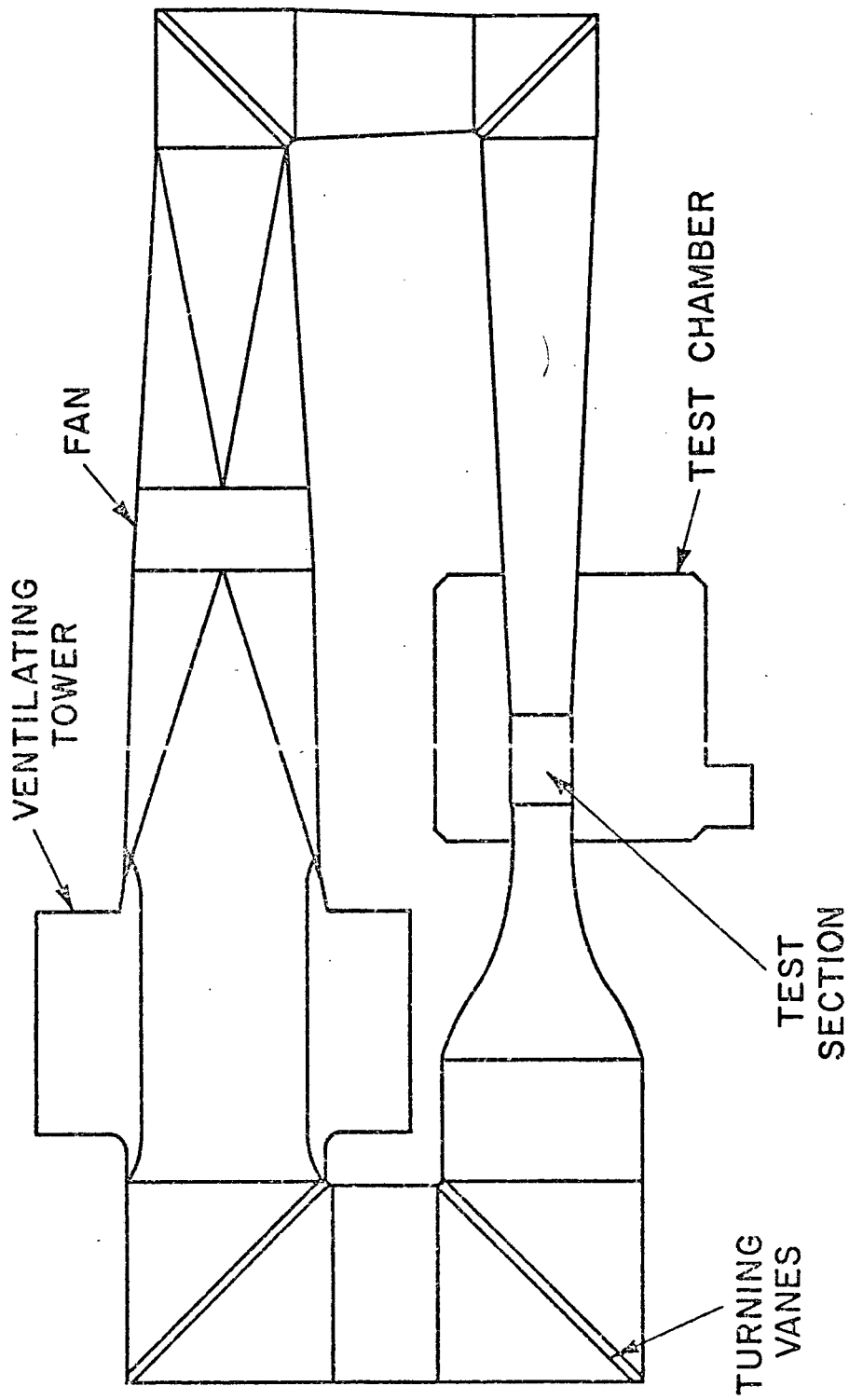


Figure 20. Block Diagram of Correlation Technique  
(After Cook (21))



SCALE - 1" ~ 30'

Figure 21. AMRDL 7- x 10-Foot Wind Tunnel

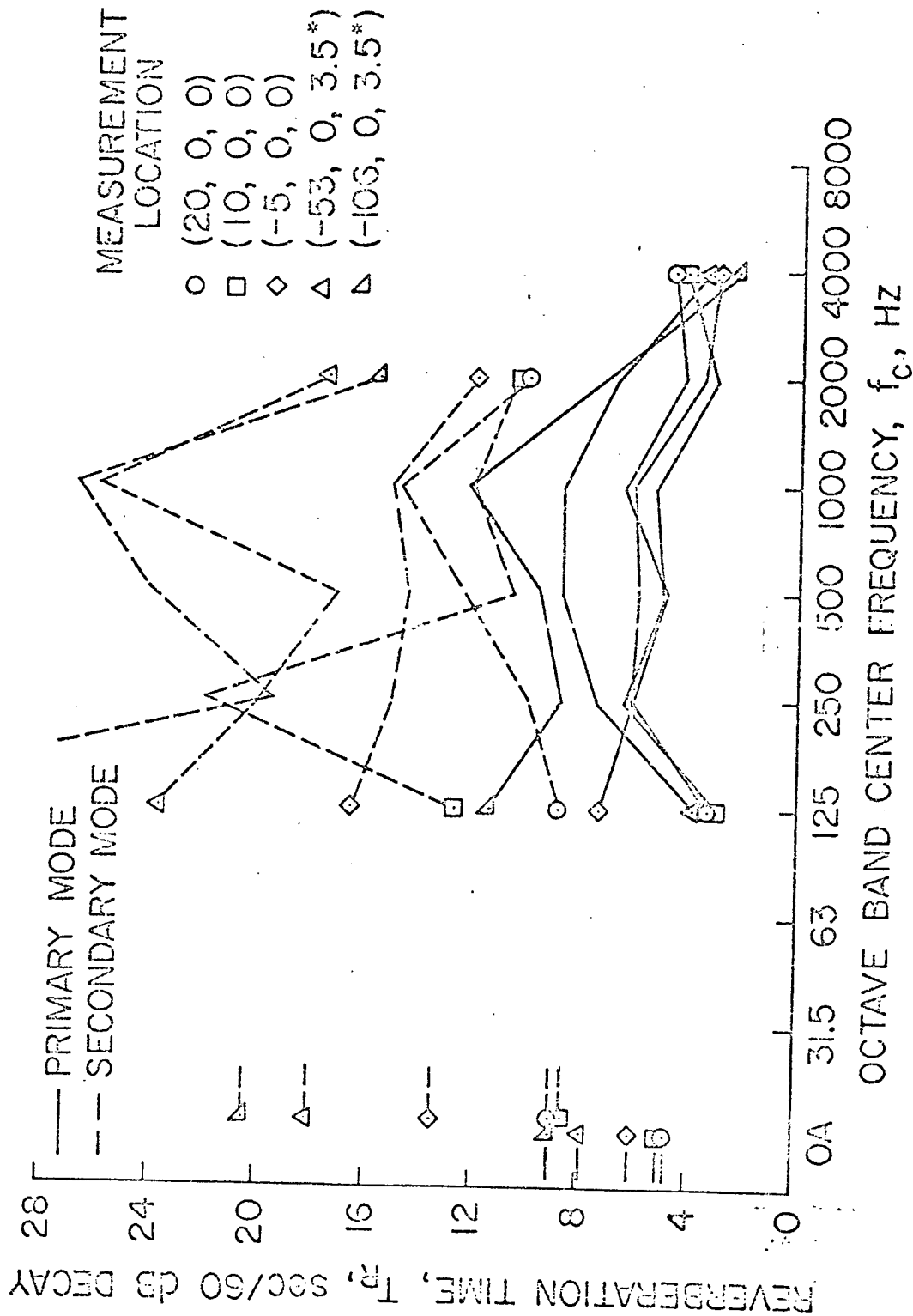


Figure 22. AMRDL, Reverberation Time vs Frequency

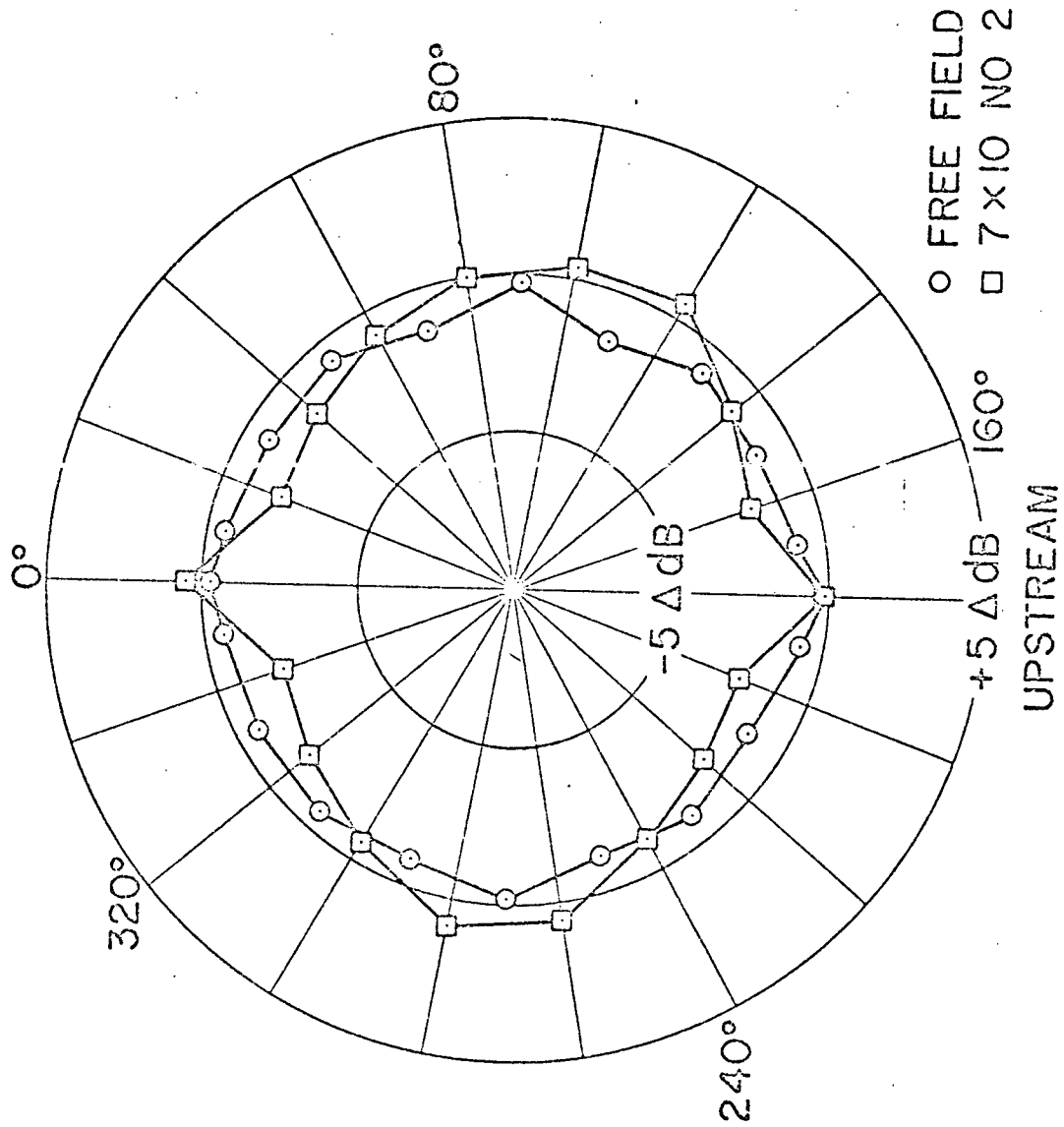


Figure 23 AMRDL, Broadband Noise Directivity Free Field and 7- x 10-Foot Wind Tunnel

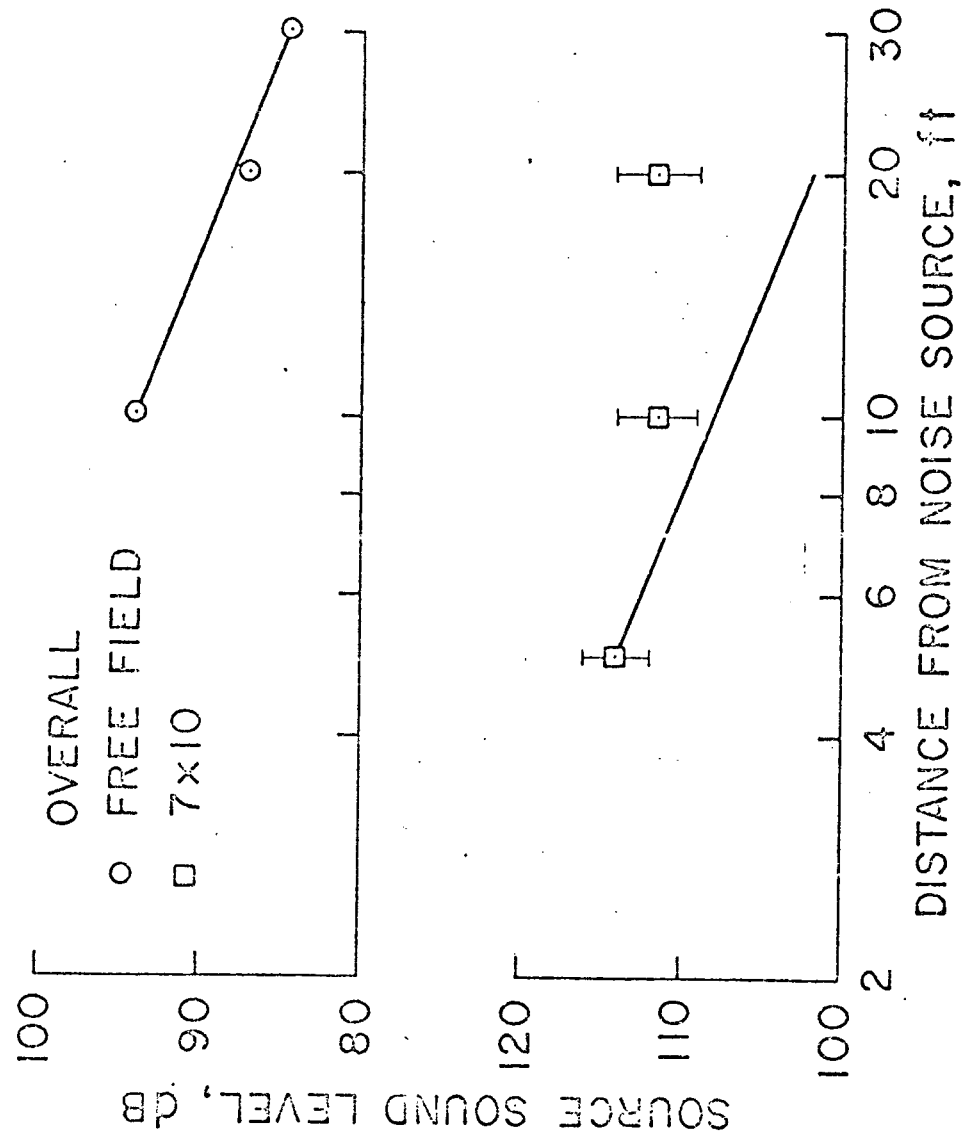


Figure 24. AMRDL, Free Field and Tunnel Broadband Noise Level vs Distance

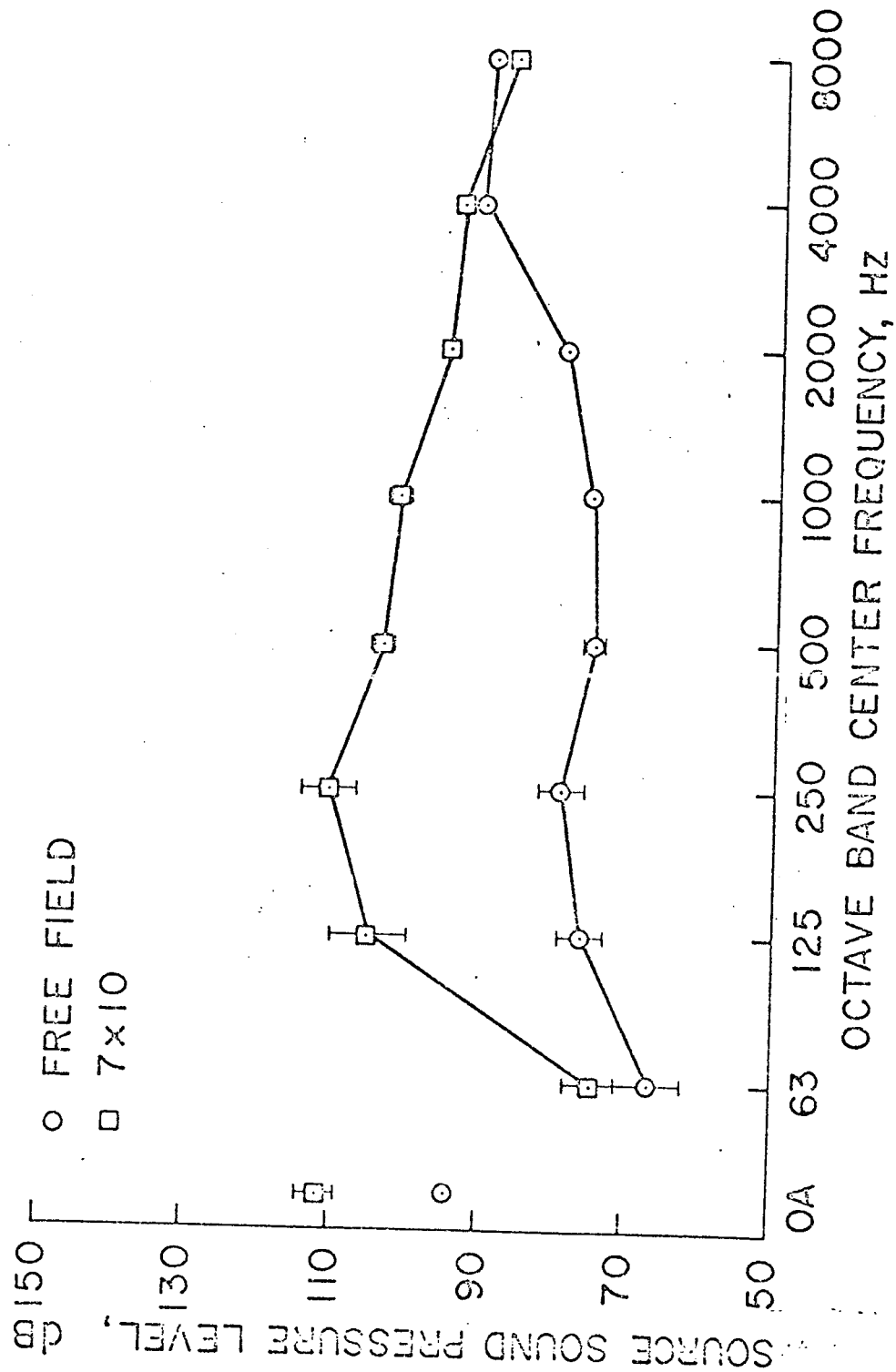


Figure 25 AMRDL, Comparison of Sound Pressure Level Measurement in Tunnel and Free Field Ten Feet from Source



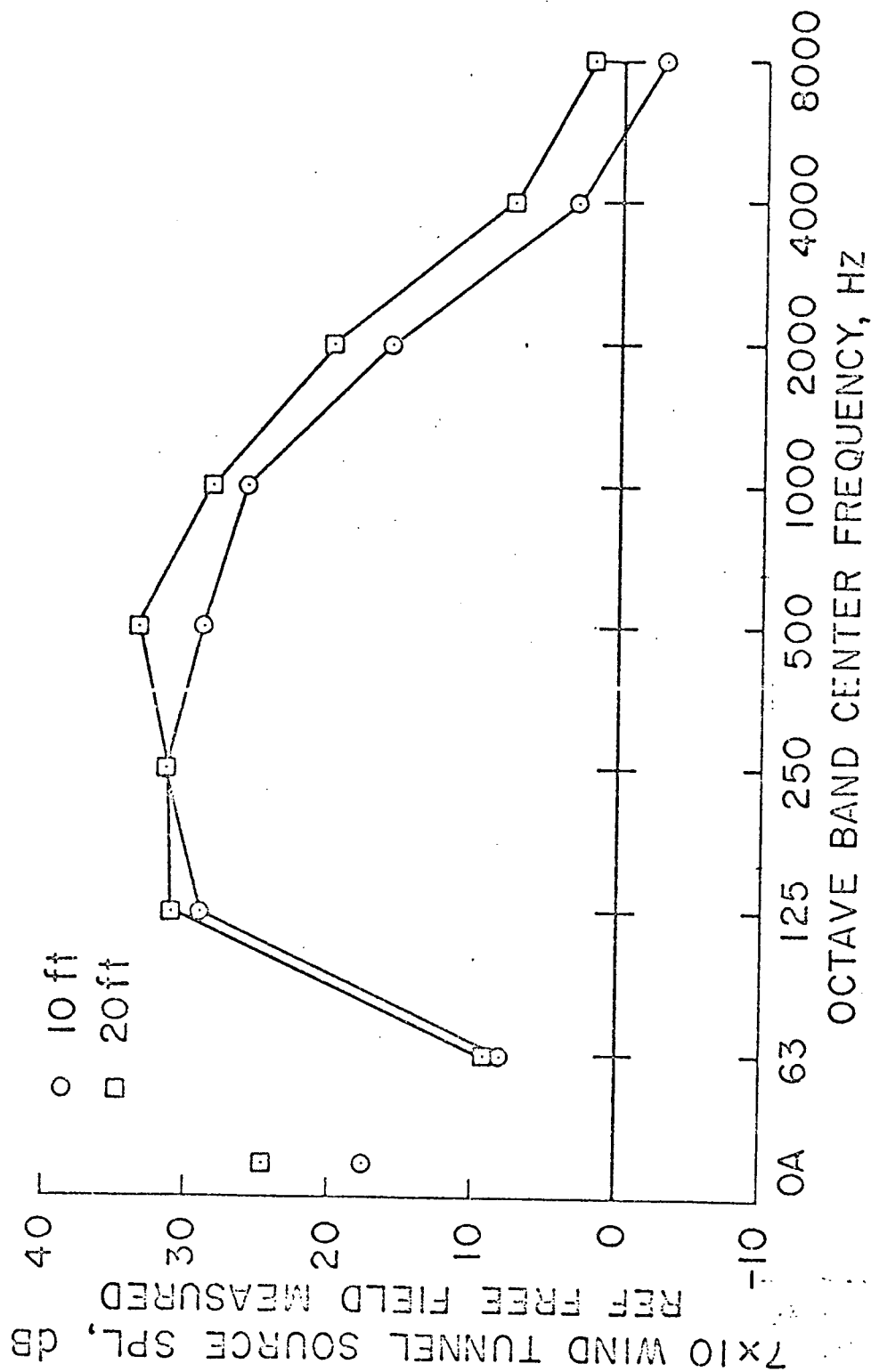


Figure 26. AMRDL, Wind Tunnel and Free Field SPL Measurement Difference as a Function of Frequency and Distance

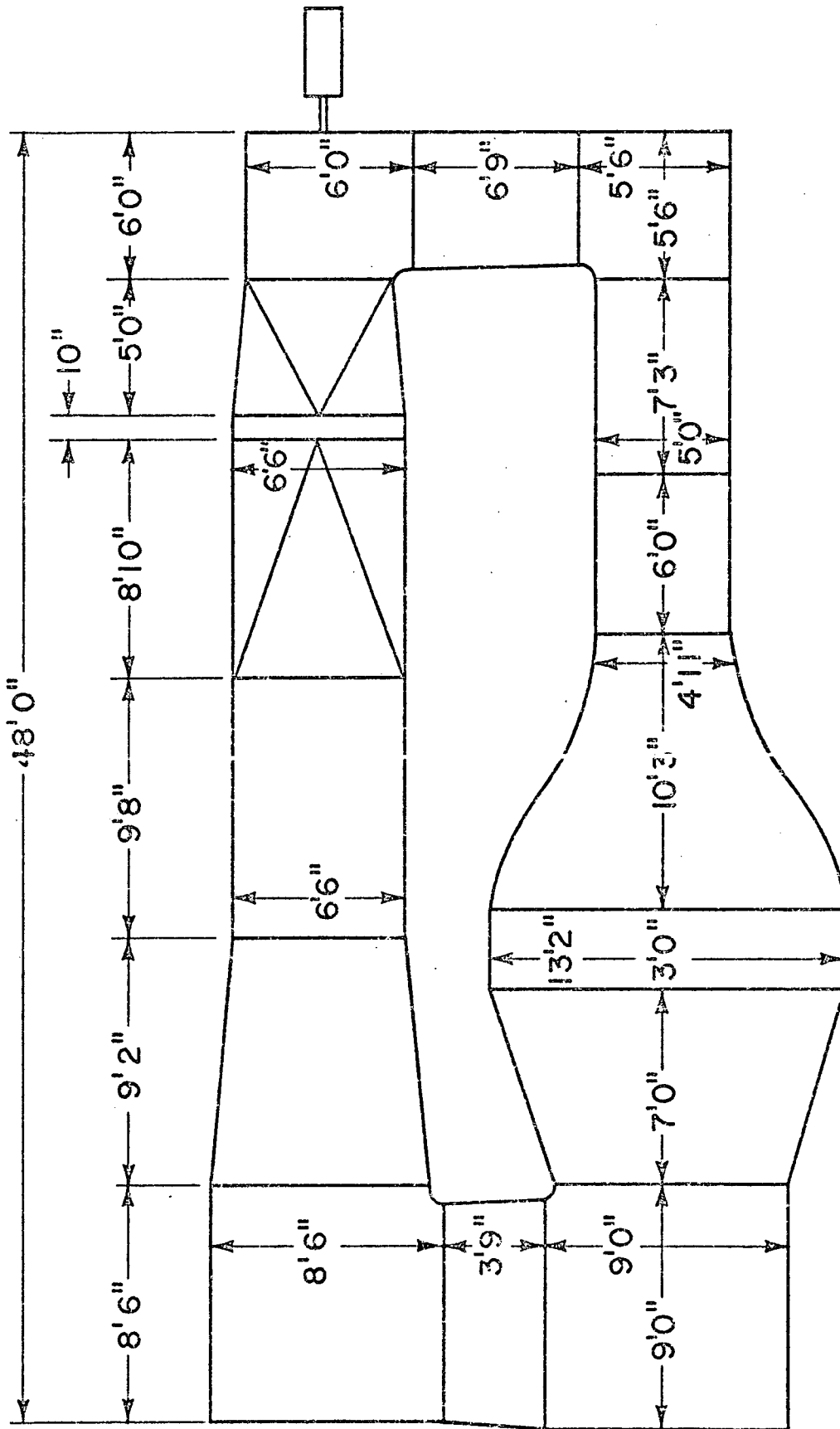


Figure 27. Penn State Aerospace Department Wind Tunnel

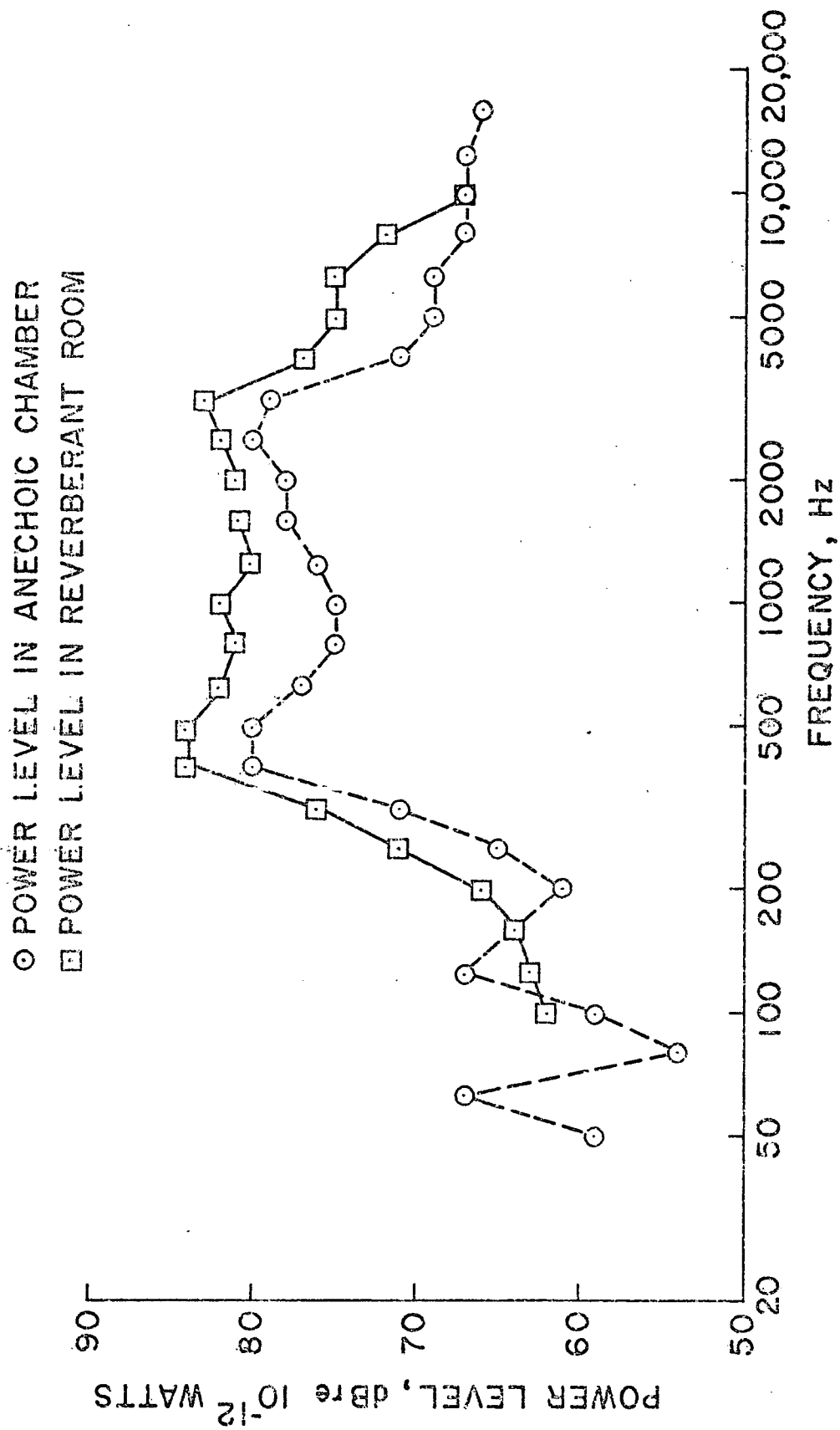


Figure 28. Calibrated Power Curves

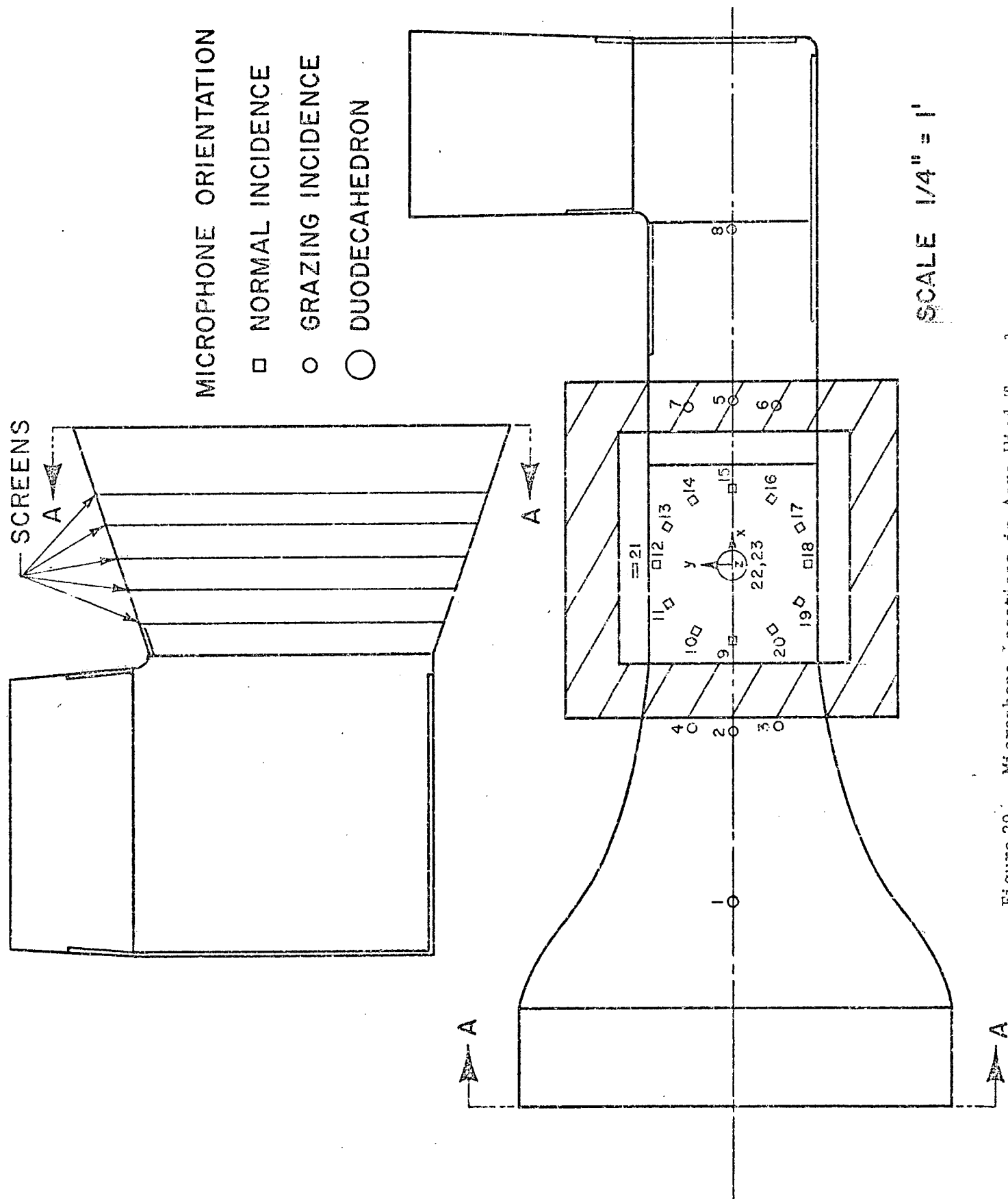


Figure 29. Microphone Locations in Aero Wind Tunnel

## MIKE POSITION 22

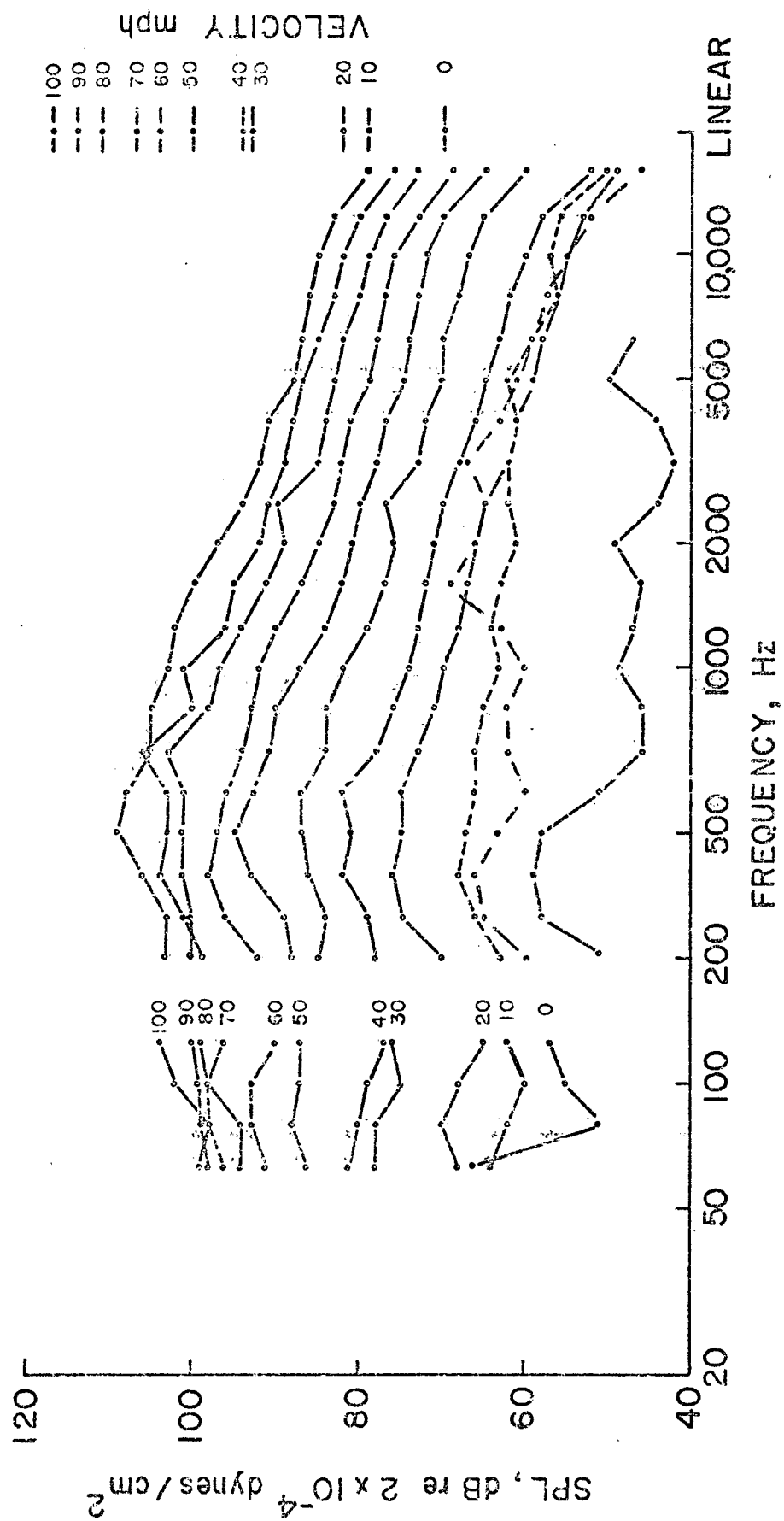


Figure 30. Background Spectra with Flow with Closed Test Section

## MIKE POSITION 22

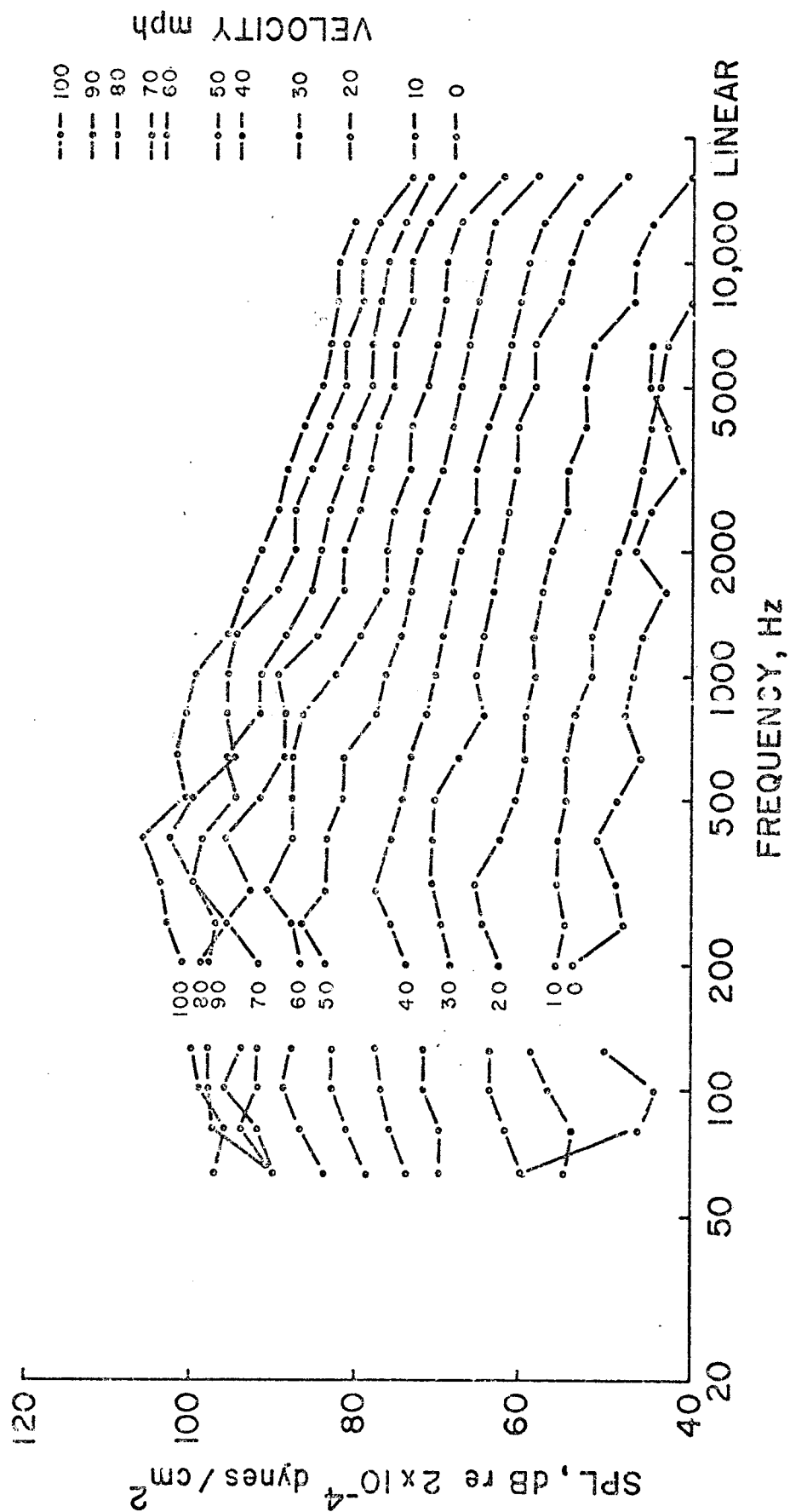


Figure 31. Background Spectra with Flow with Anechoic Chamber

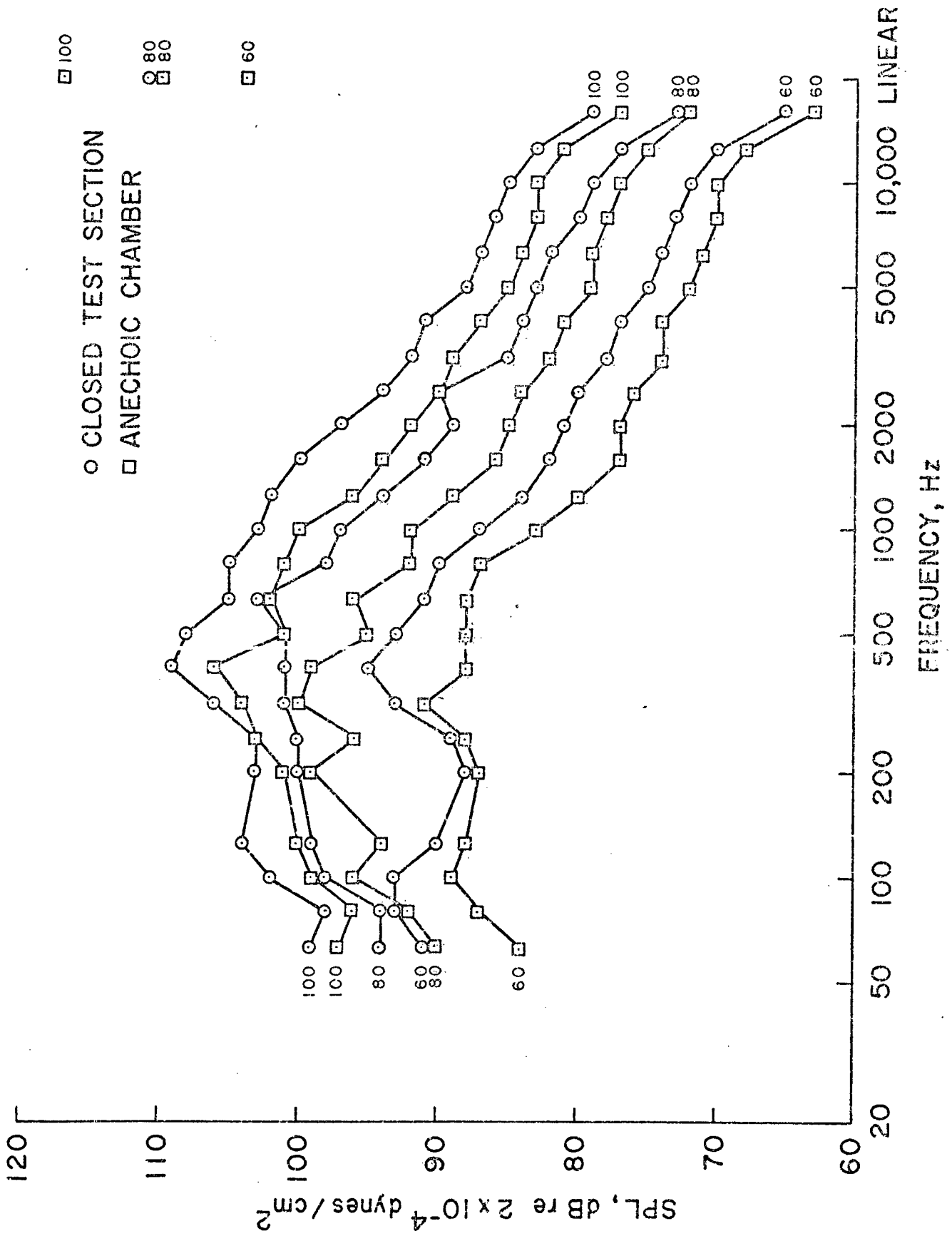


Figure 32. Background Spectra with Flow

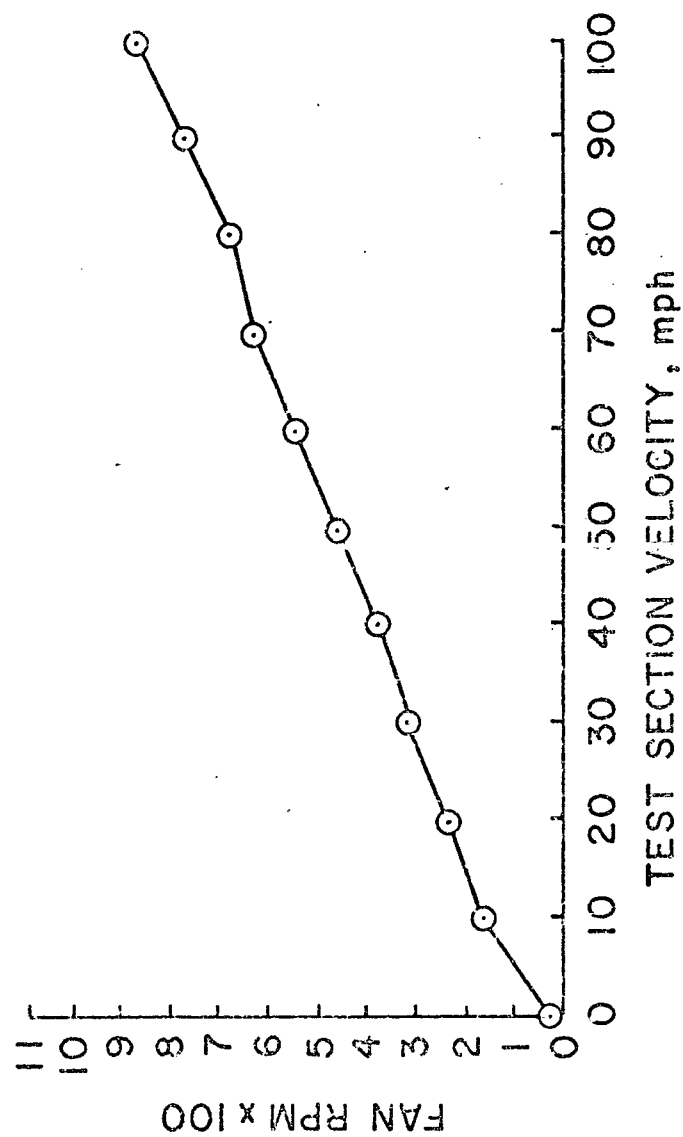


Figure 33. Test Section Velocity vs Fan RPM



○ CLOSED TEST SECTION  
 □ ANECHOIC CHAMBER

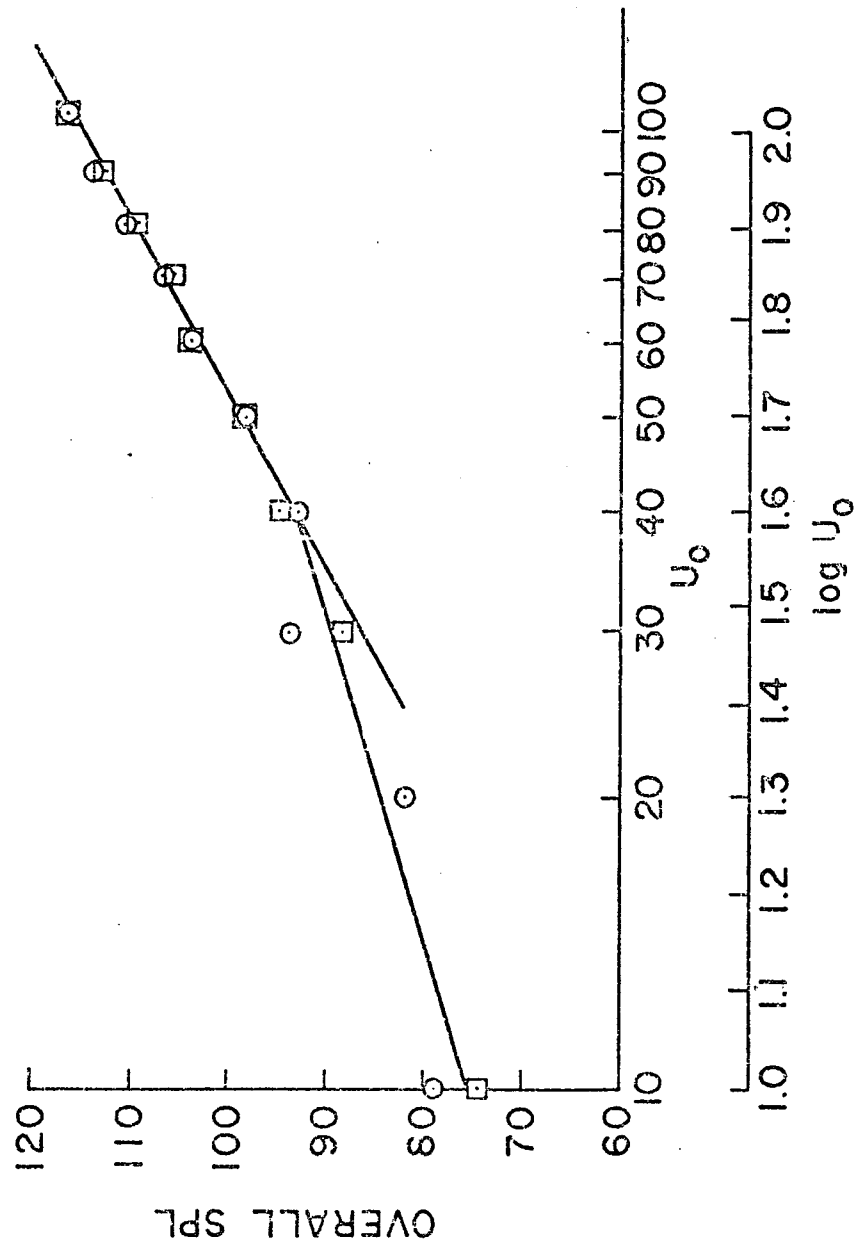


Figure 34. Overall SPL vs Logarithm of Test Section Velocity

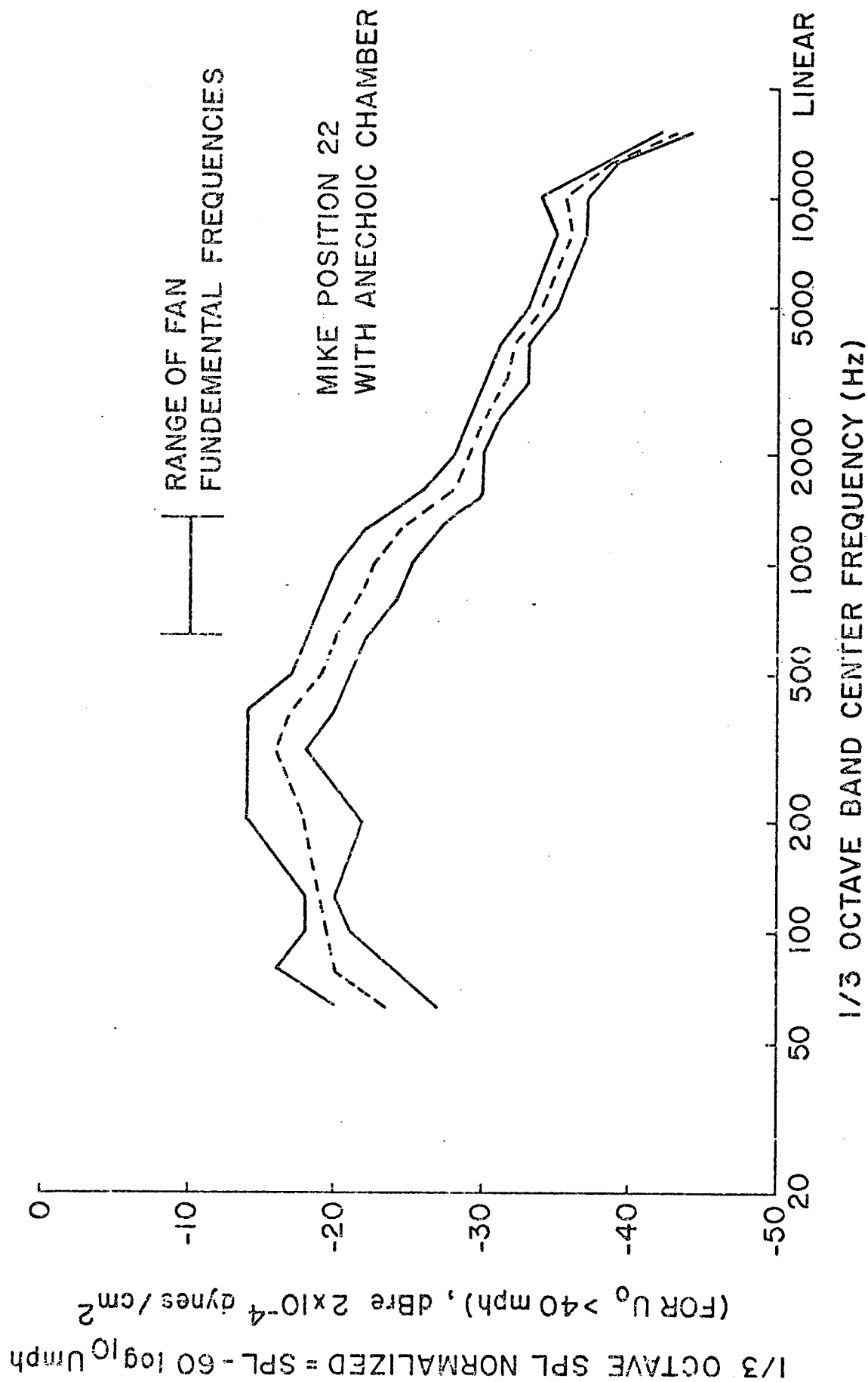


Figure 35. Range of Normalized Background Noise Levels

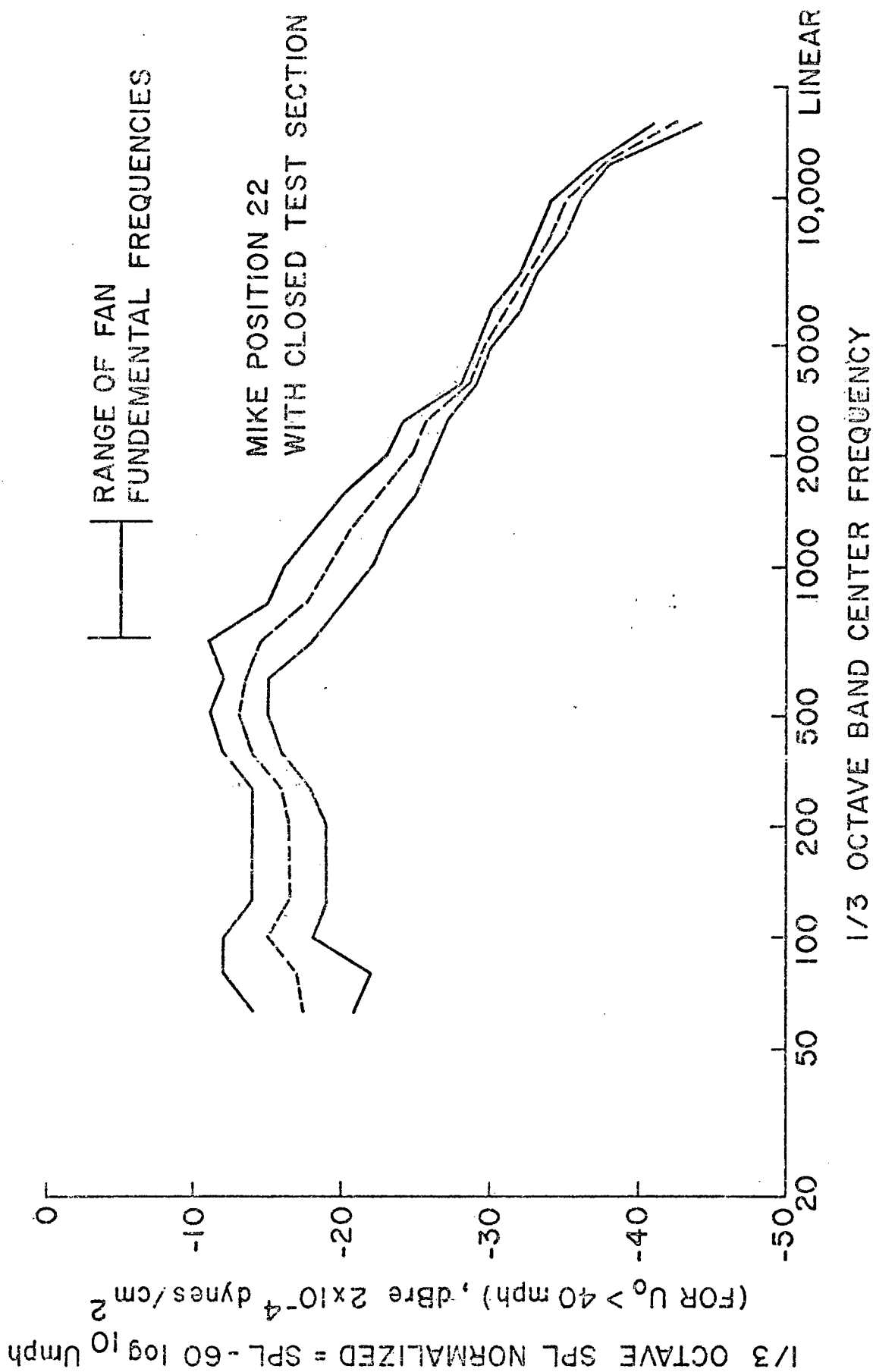


Figure 36. Range of Normalized Background Noise Levels

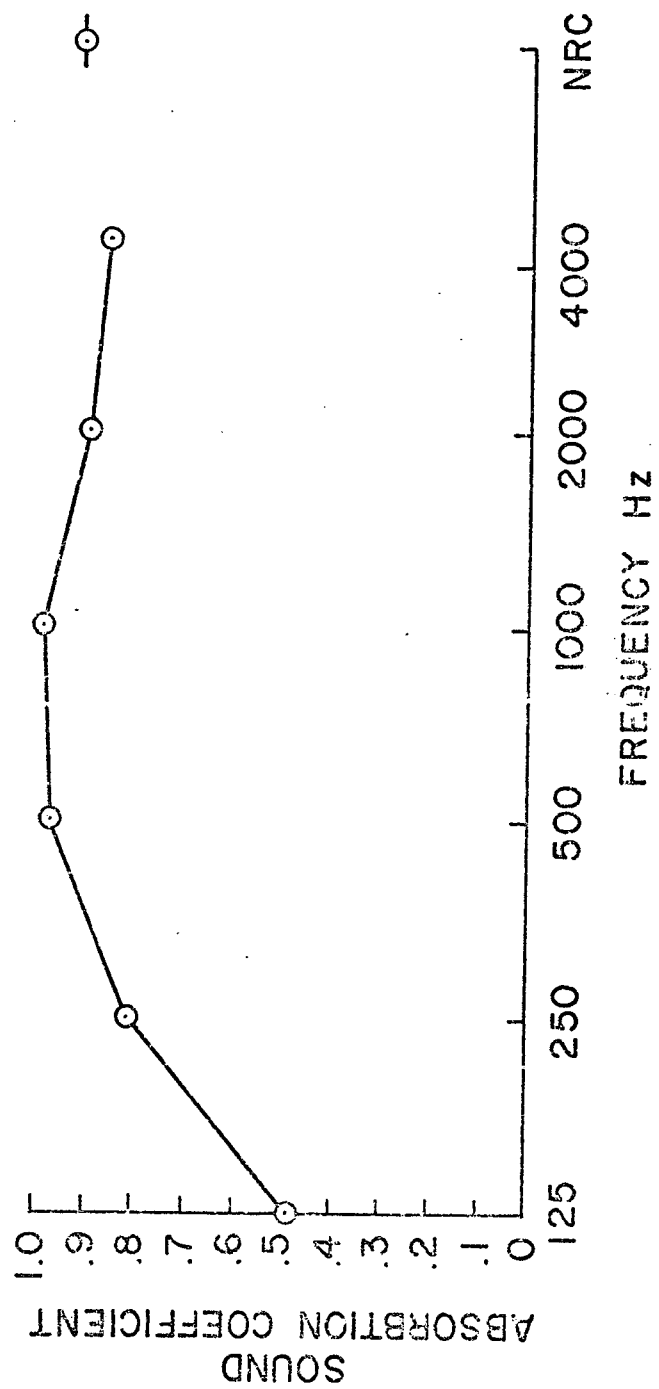


Figure 37. Sound Absorption of Owens/Corning Fiberglass, Type 705

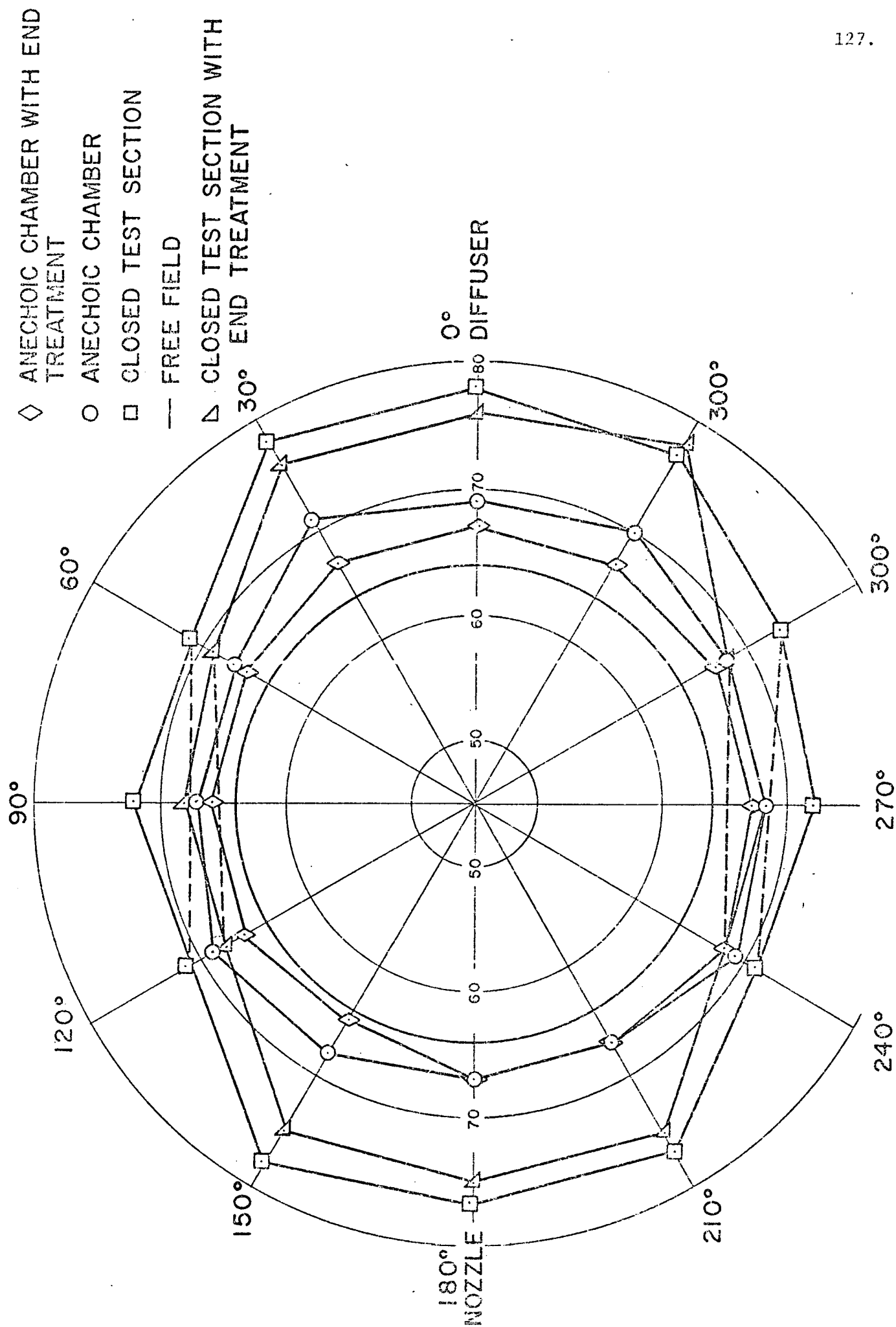


Figure 38. SPL Directivity Pattern, 500 Hz 1/3 Octave Band

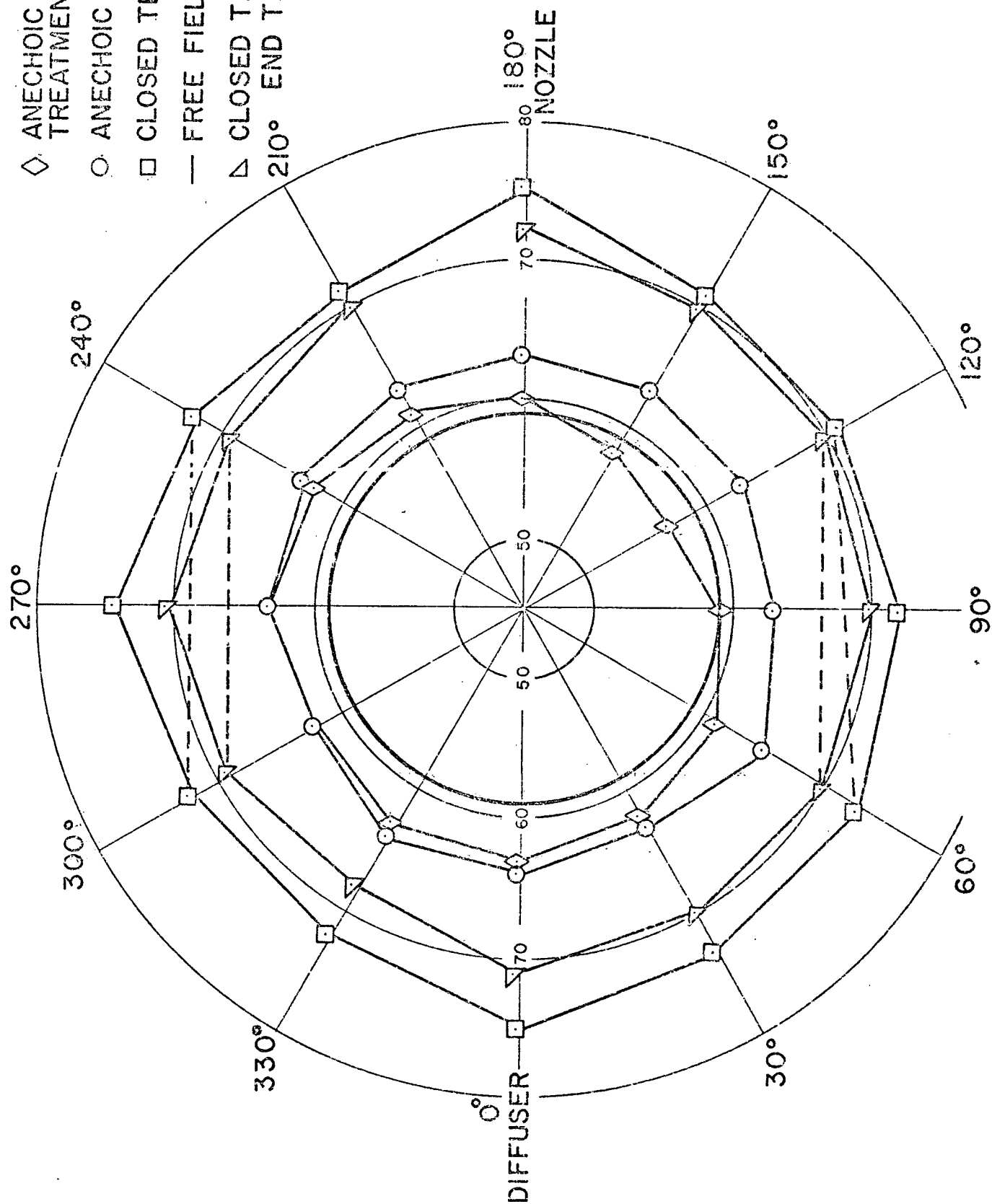


Figure 20. SPL Directivity Pattern, 1000 Hz 1/3 Octave Band

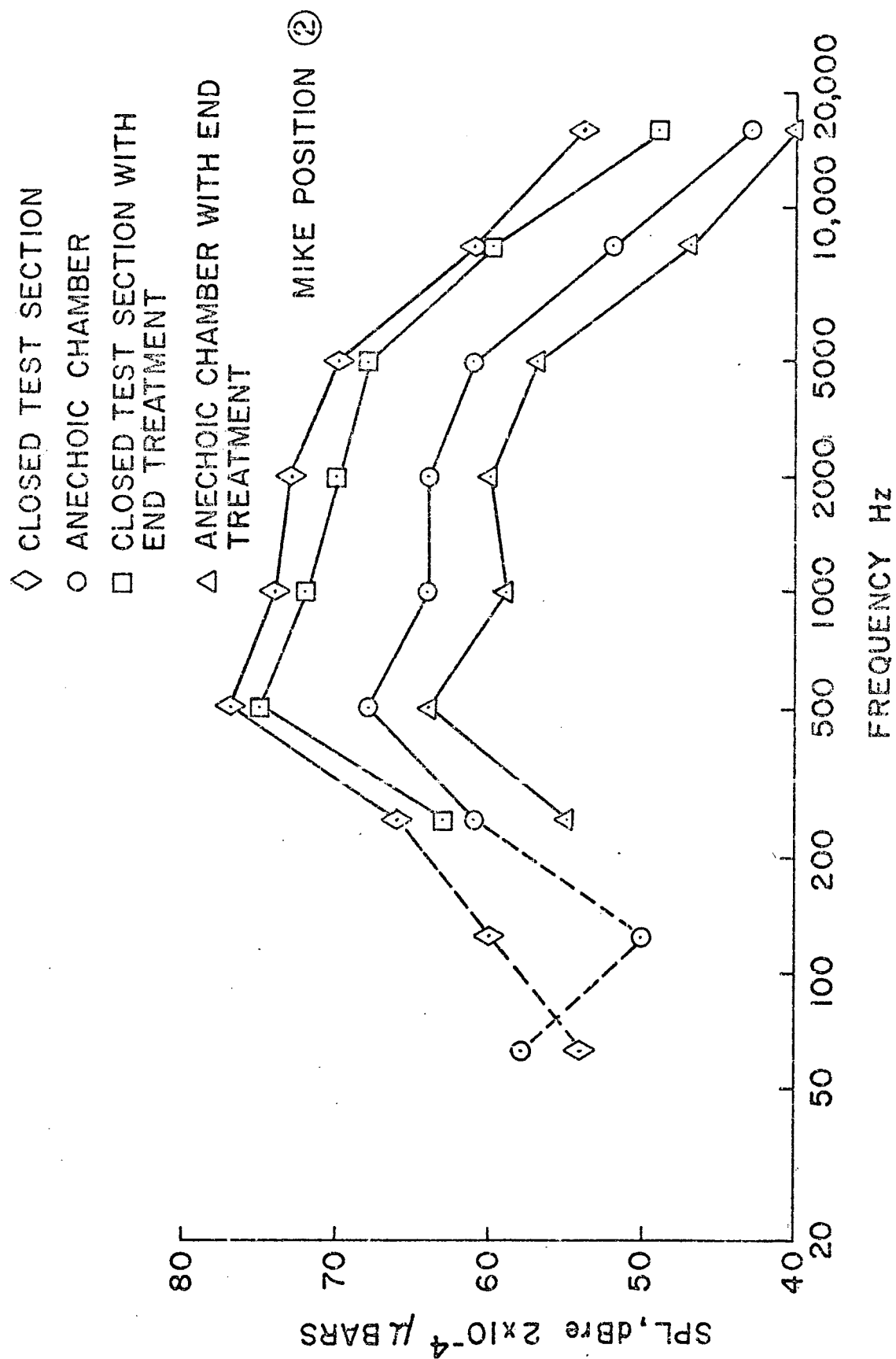


Figure 40. SPL Spectra at Microphone Position 2

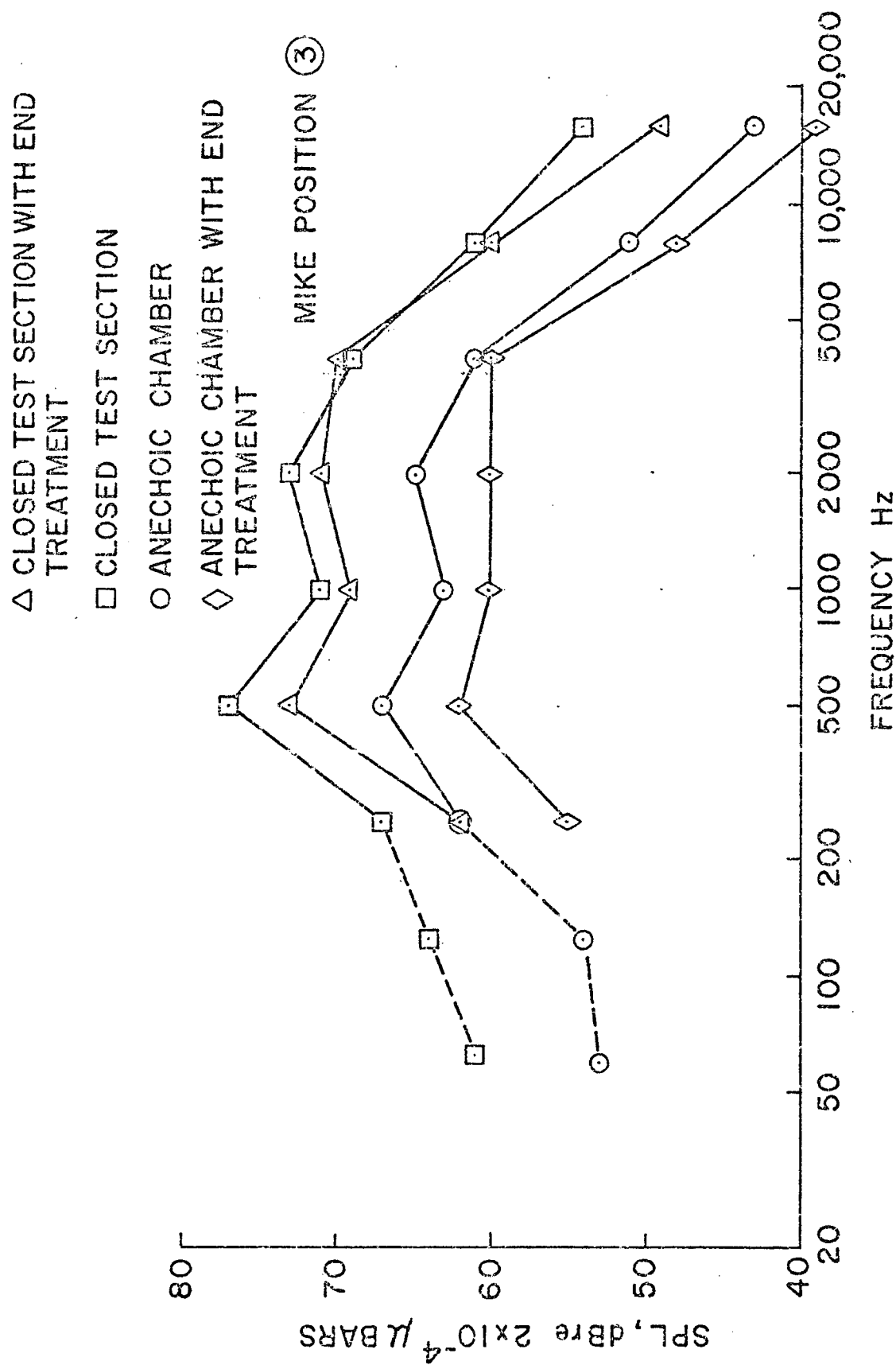


Figure 41. SPL Spectra at Microphone Position 3



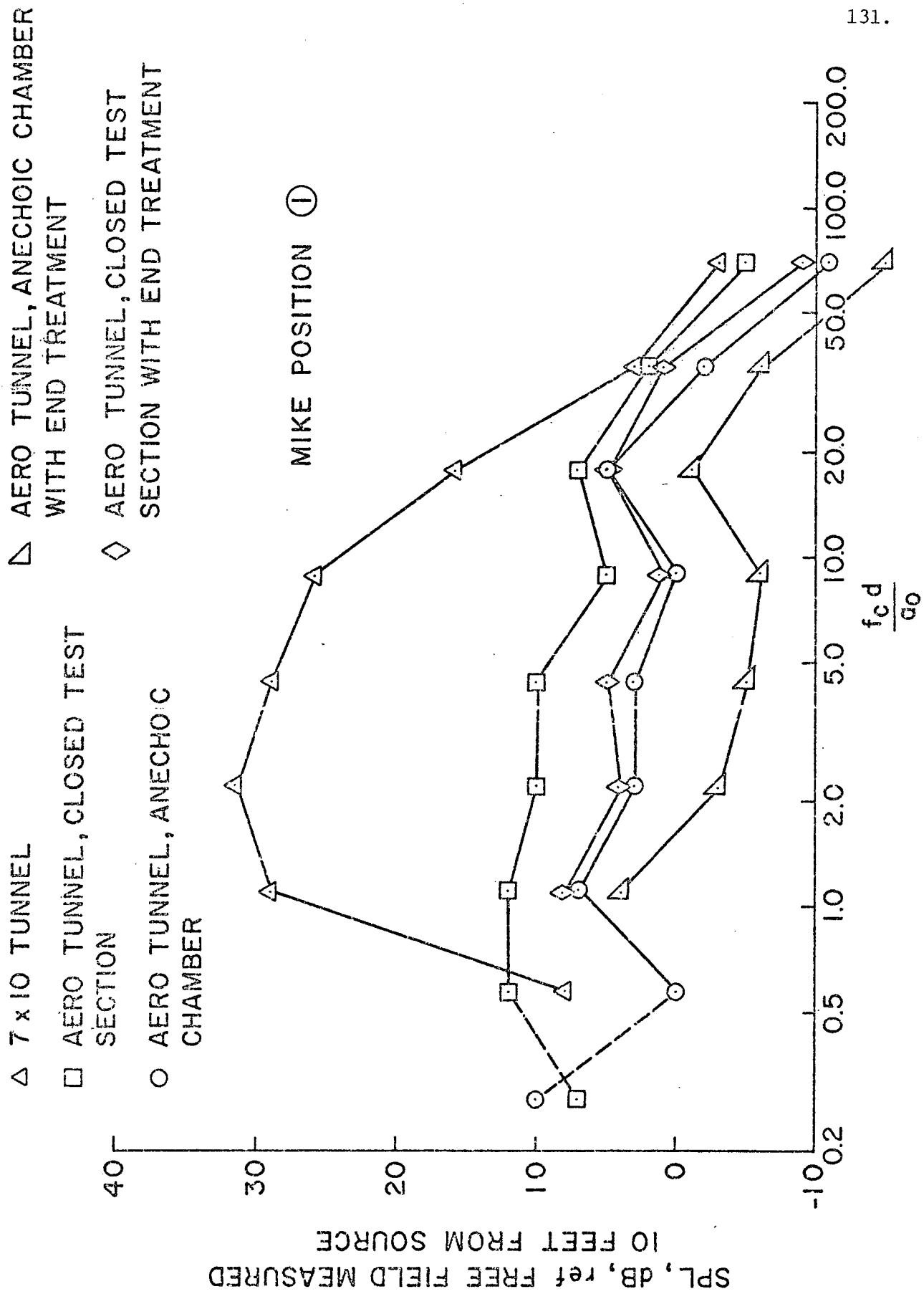


Figure 42. Non-Dimensional Spectra for AMRDL and Aero Wind Tunnel

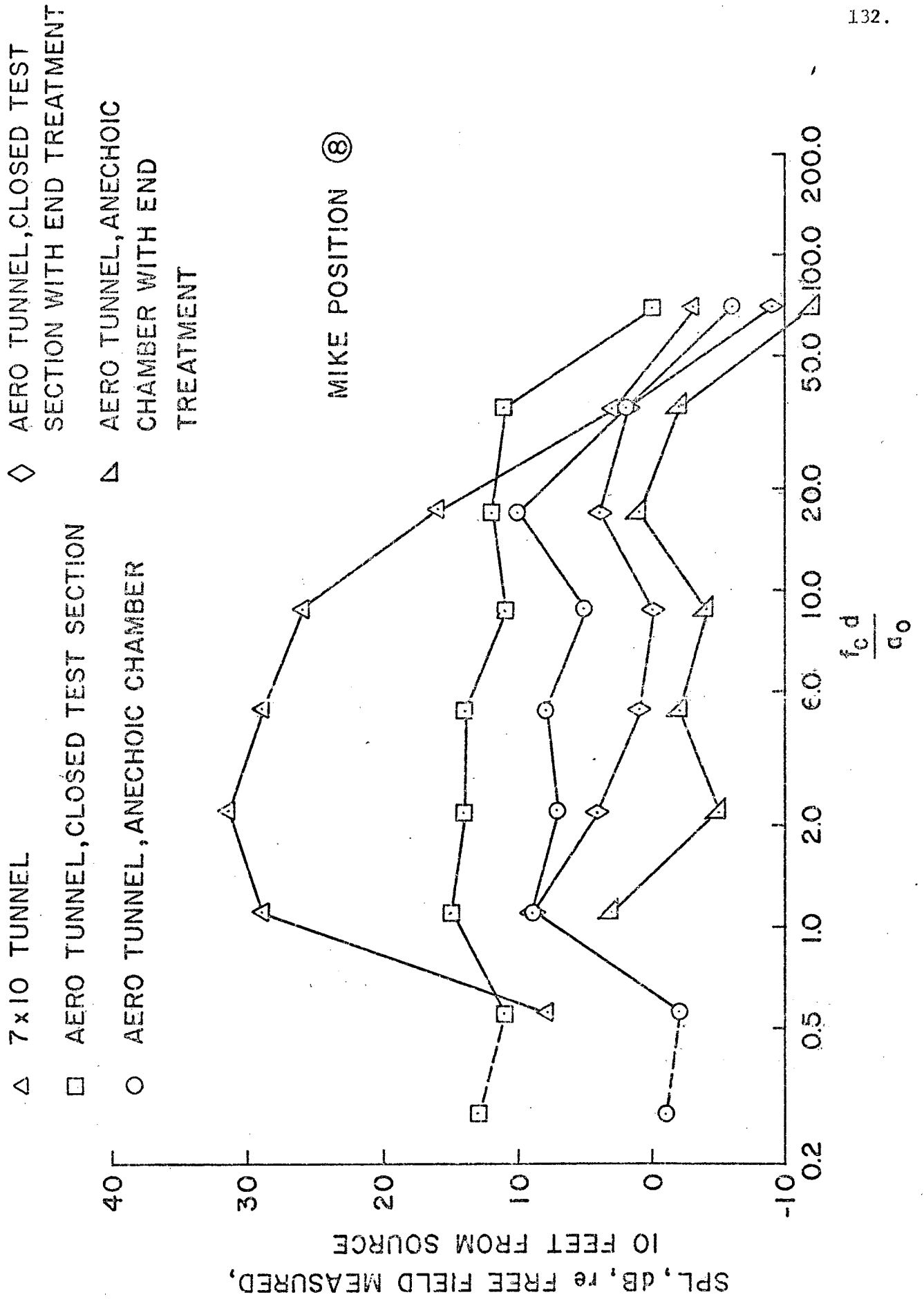


Figure 43. Non-Dimensional Spectra for AMRDL and Aero Wind Tunnel

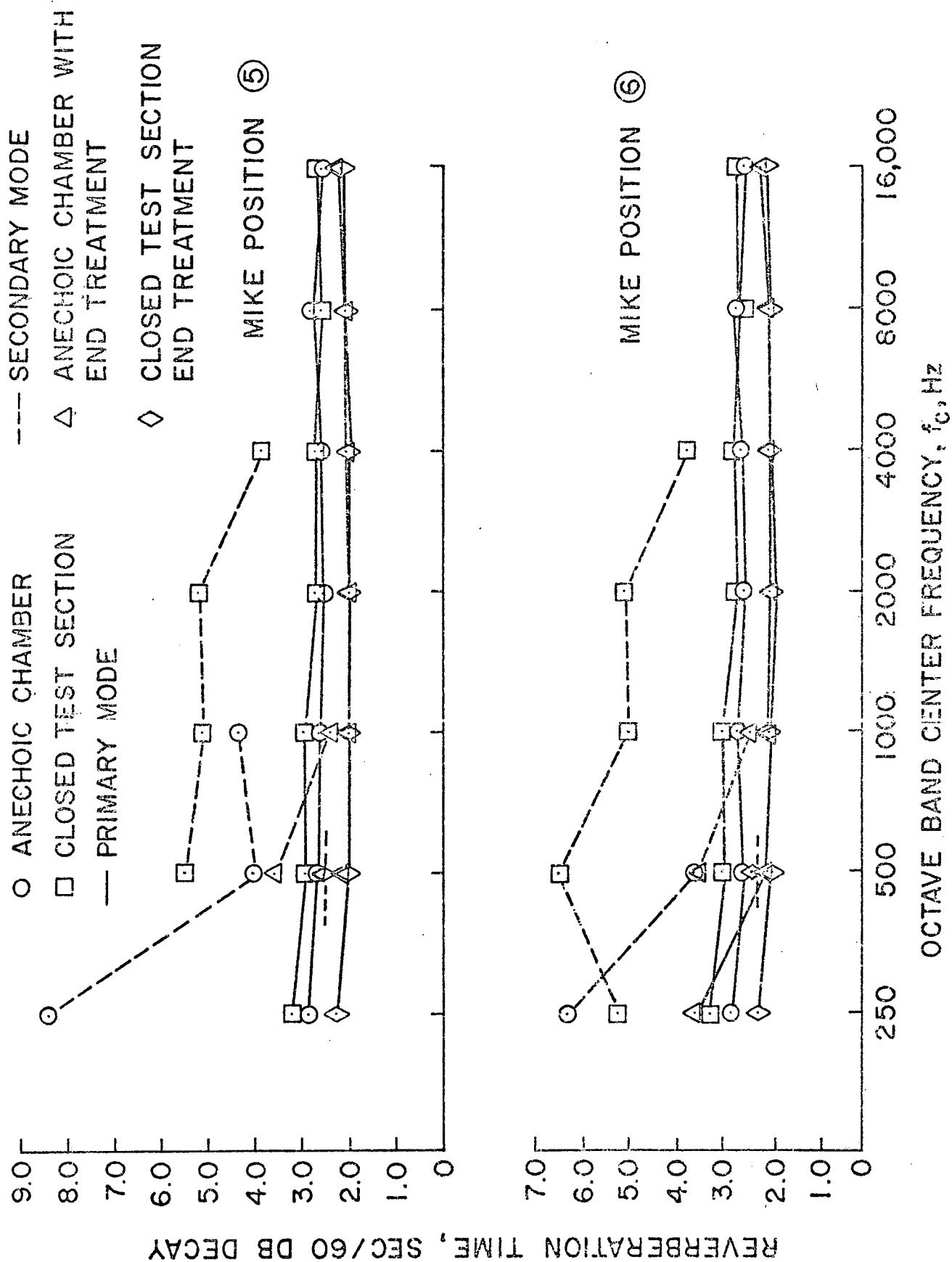


Figure 44. Reverberation Times at Microphone Positions 5 and 6

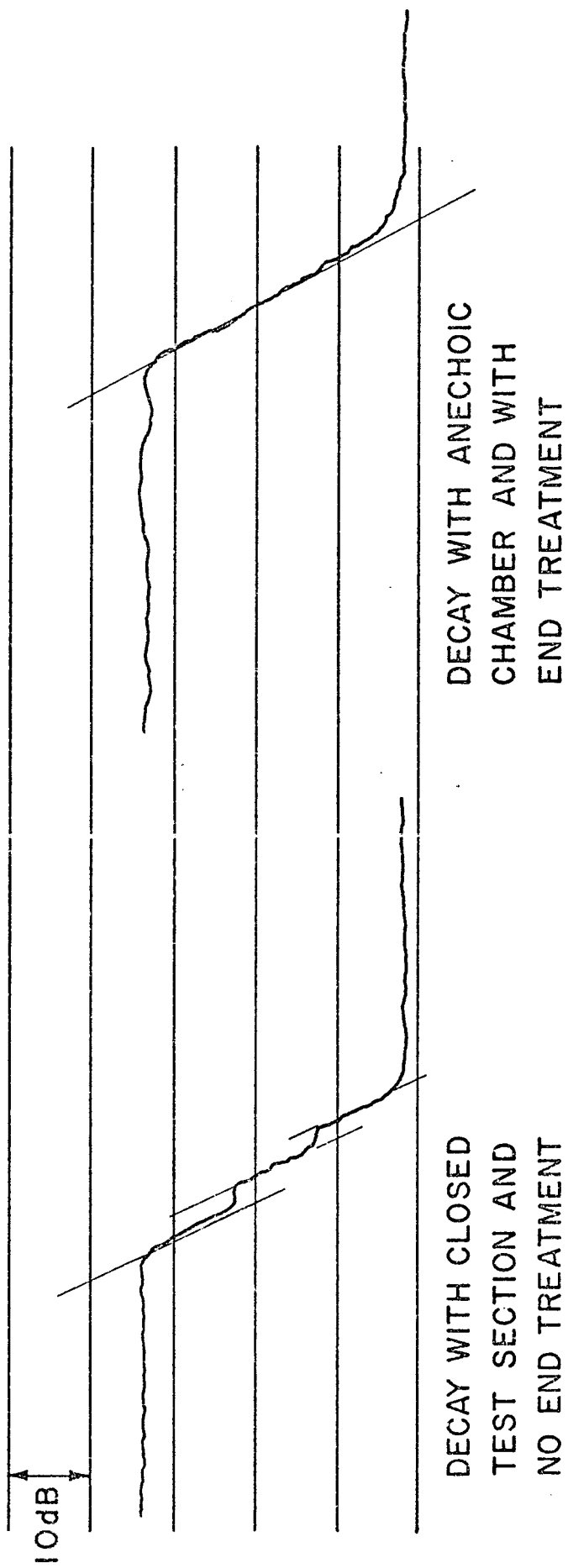


Figure 45. Typical SPL Decays

- AVERAGE POWER LEVEL
- PREDICTED POWER LEVEL FROM SPL AT MIKE POSITION 8 WITH CLOSED TEST SECTION
- △ PREDICTED POWER LEVEL FROM SPL AT MIKE POSITION 7 WITH ANECHOIC CHAMBER

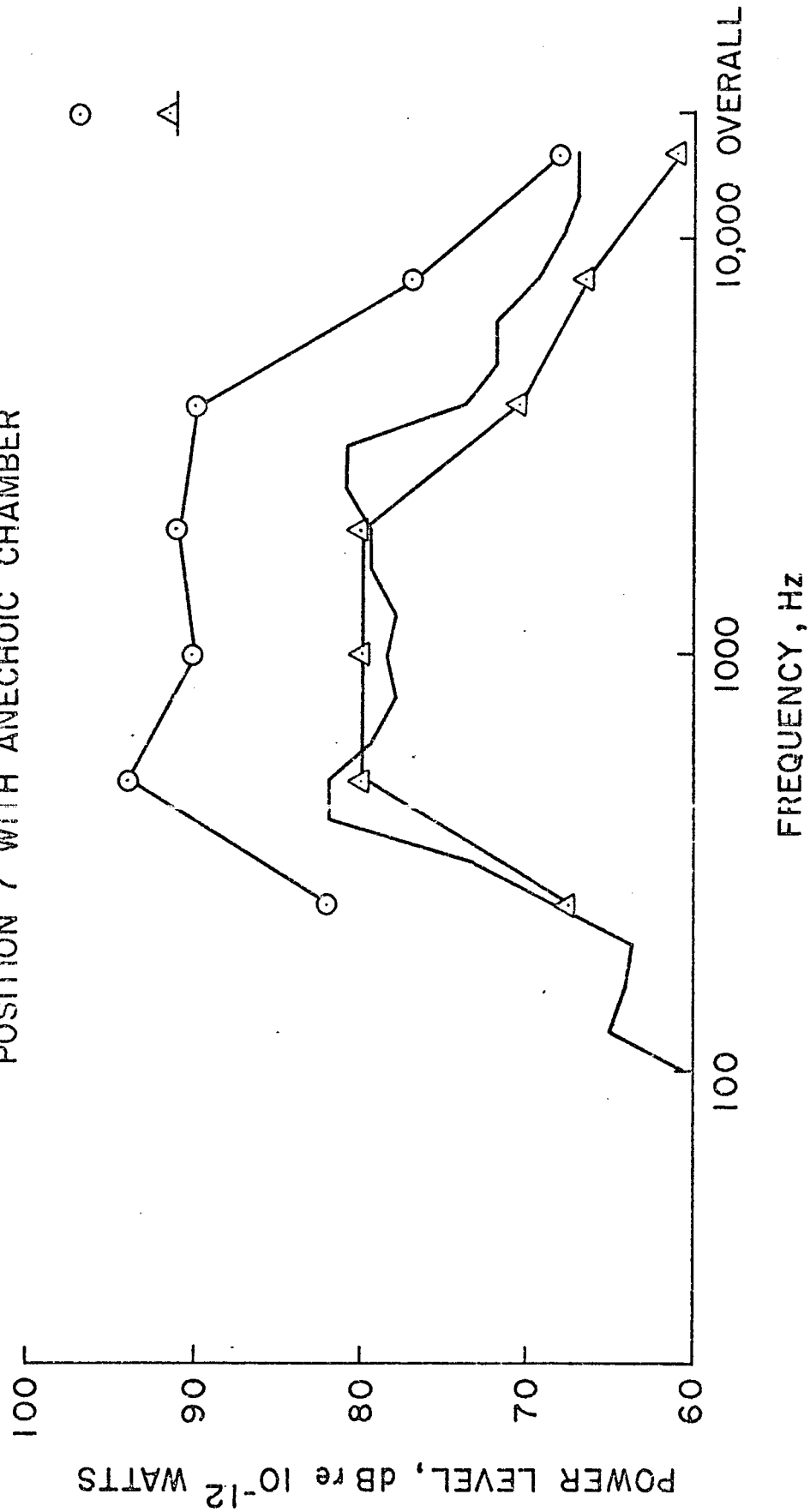


Figure 46. Predicted Power Levels

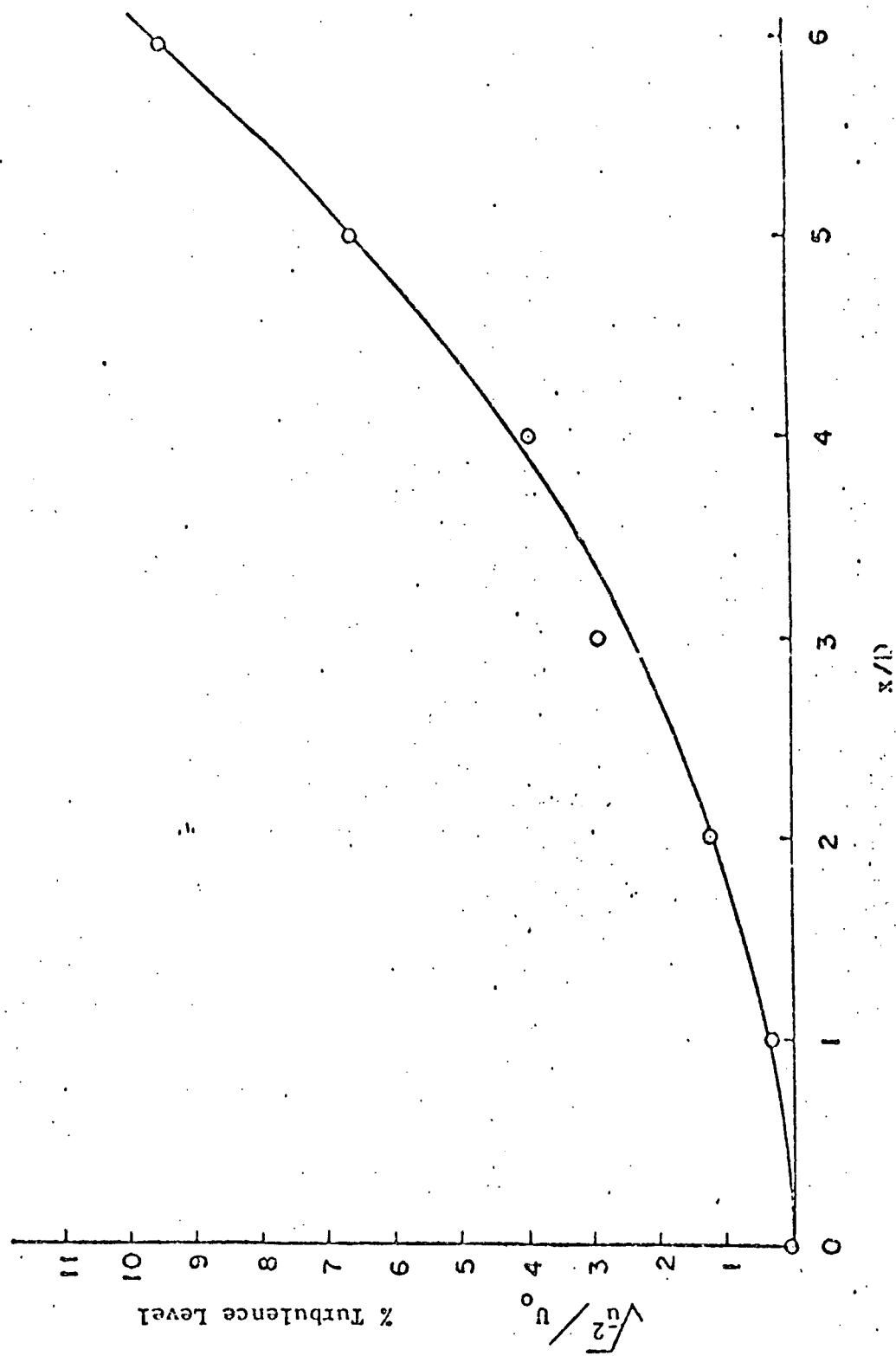


Figure 47. Growth of Axial Intensity Along Axis of an Unperturbed Jet  
(After Von Frank (23))

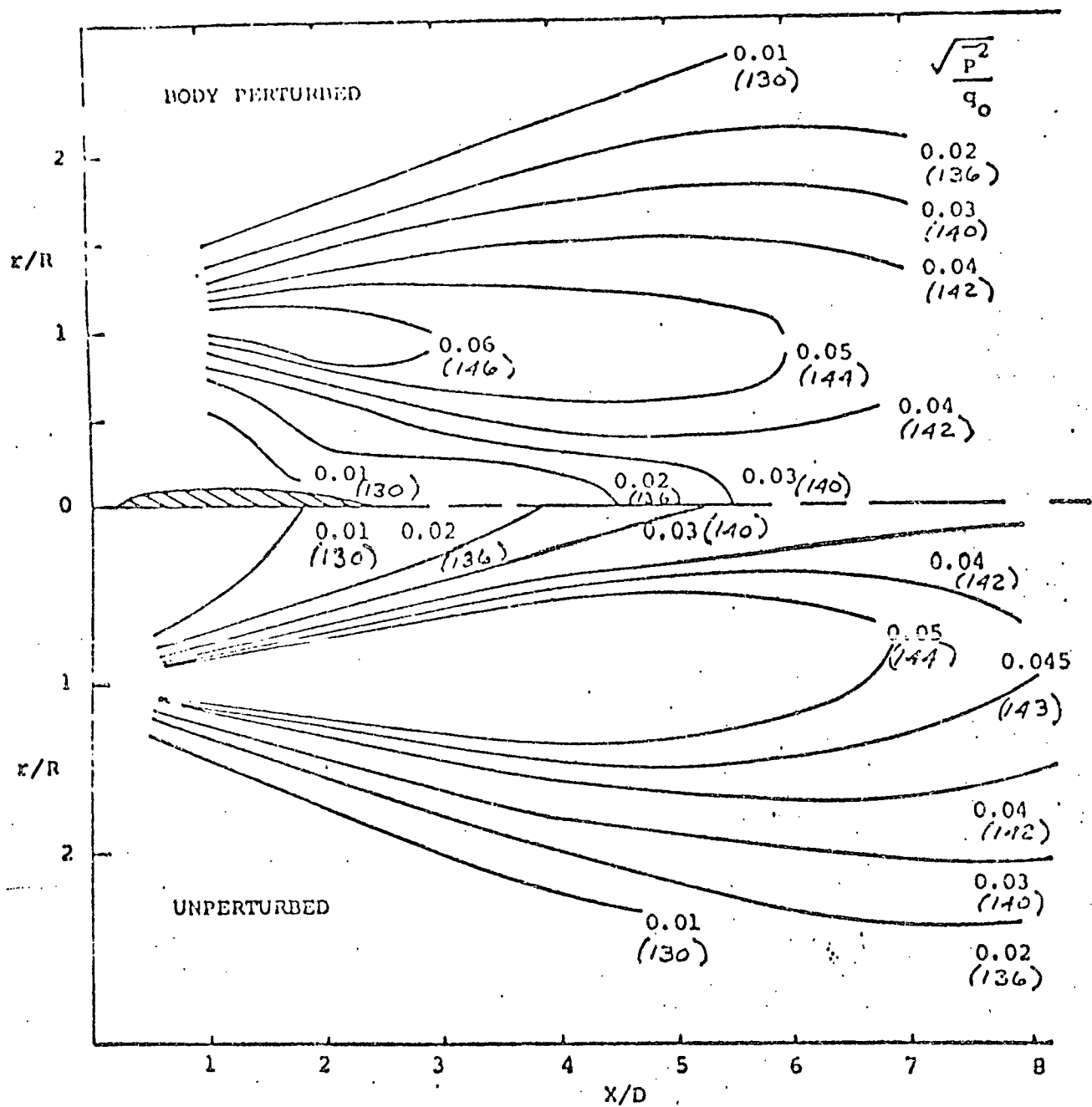


Figure 48. Pressure Field in Unperturbed and Body Perturbed Jets

Note: Numbers in parentheses correspond to SPL in dB re:  $2 \times 10^{-4}$  dynes/cm<sup>2</sup> at a tunnel speed of 100 meters/sec. (After Barefoot (24))

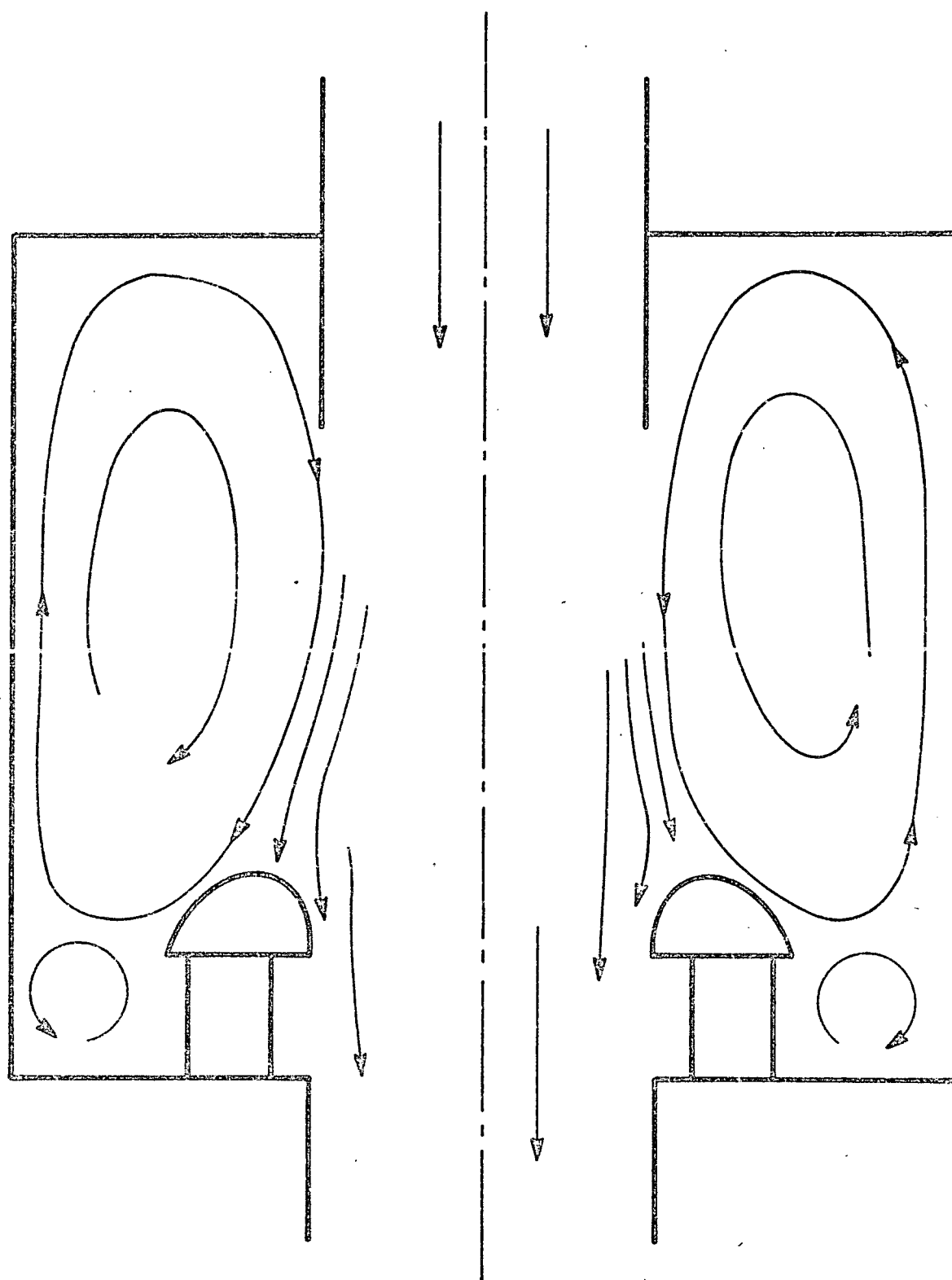


Figure 49. Flow Pattern Inside Open Jet  
Test Section (After Brownell (25))



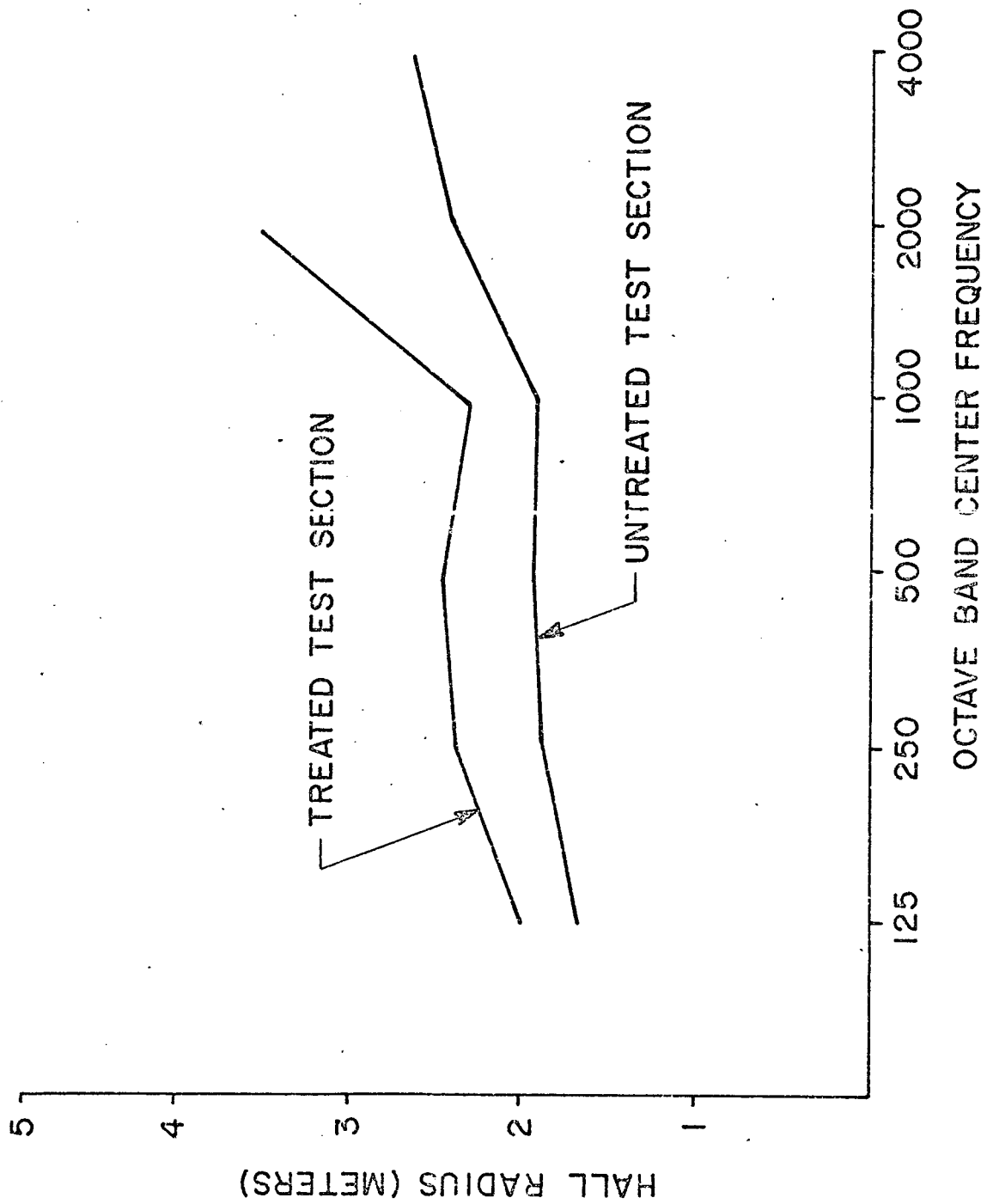


Figure 50. Predicted Improvement in Hall Radius with Treatment in the AMRDL 7-x10-Foot Wind Tunnel

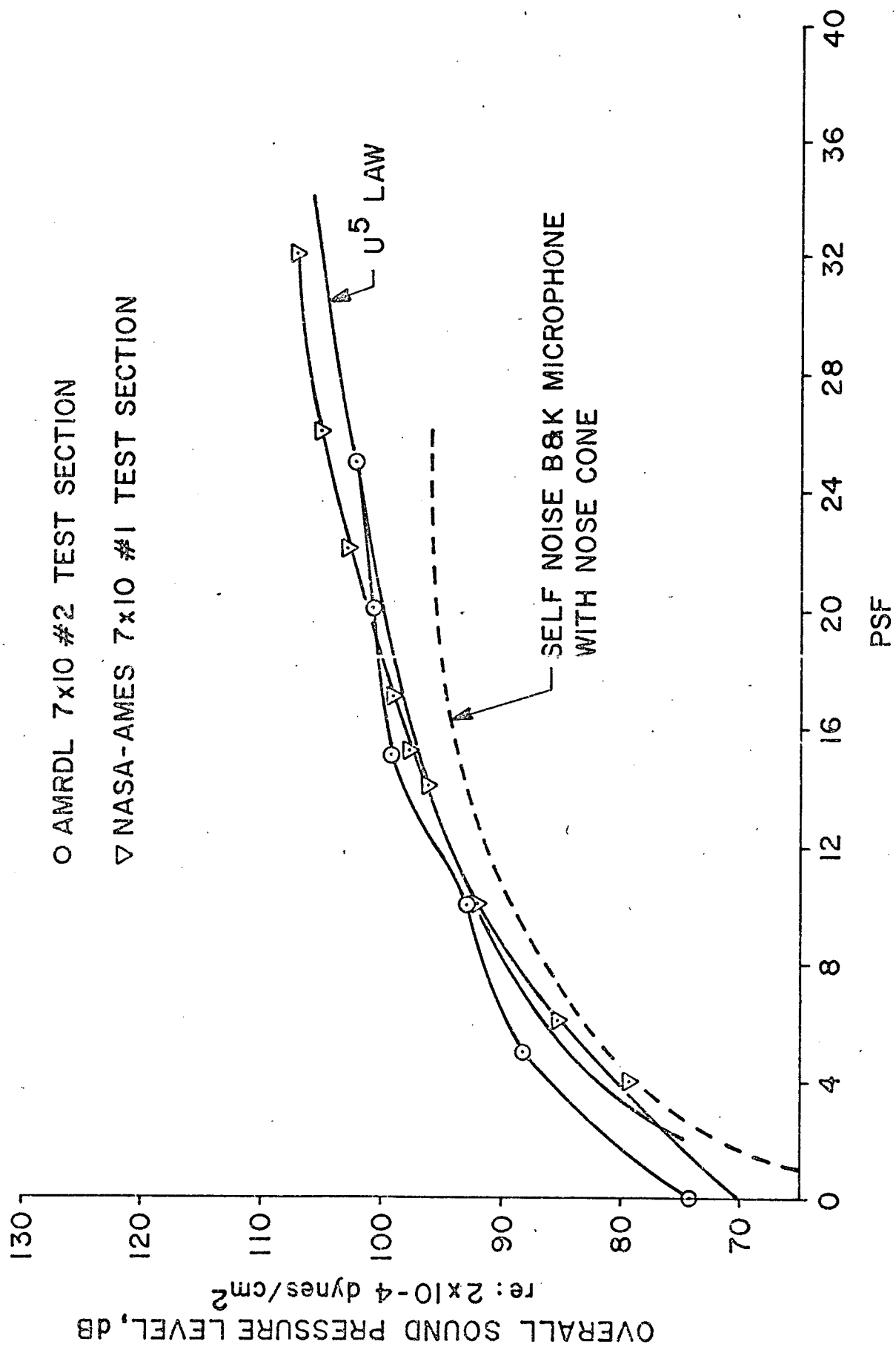


Figure 51. Background Noise Level in the AMRDL 7-x10-Foot Wind Tunnel

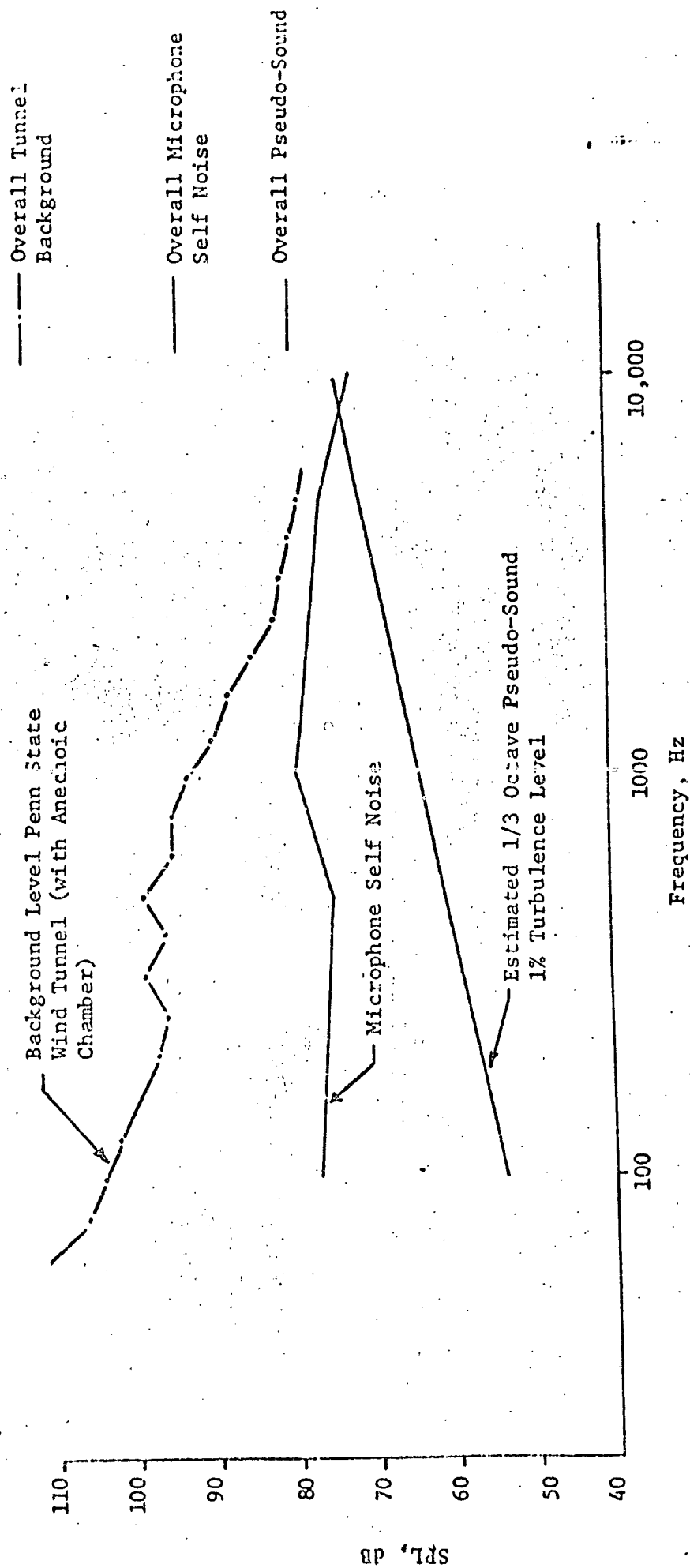


Figure 52. Typical Comparison between Tunnel Background Noise Level, Microphone Self-Noise and Turbulence Pseudo-Sound,  $U = 90$  mph

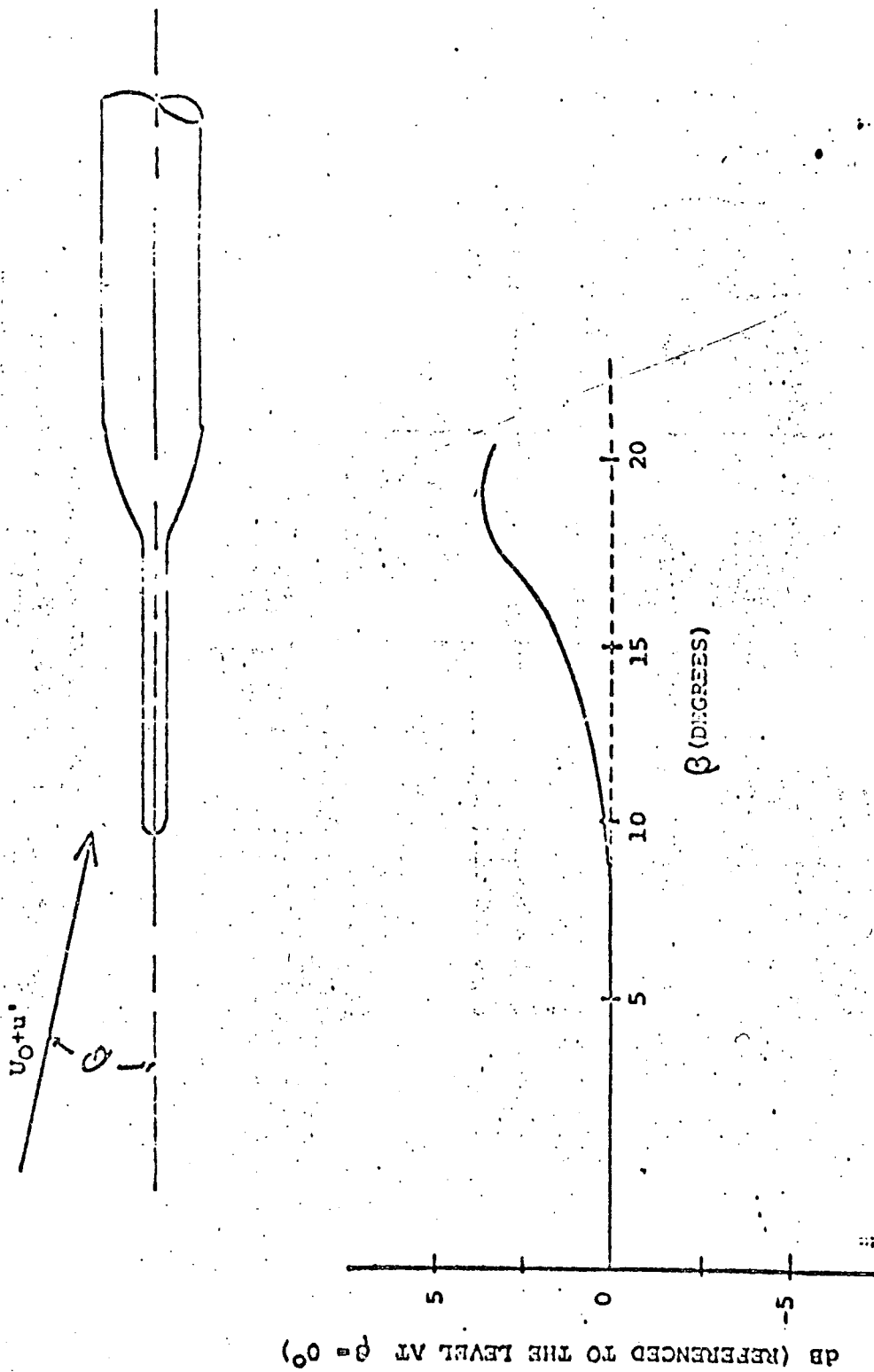


Figure 53. Influence of Angle of Attack on Microphone Probe  
(After Barefoot (24))

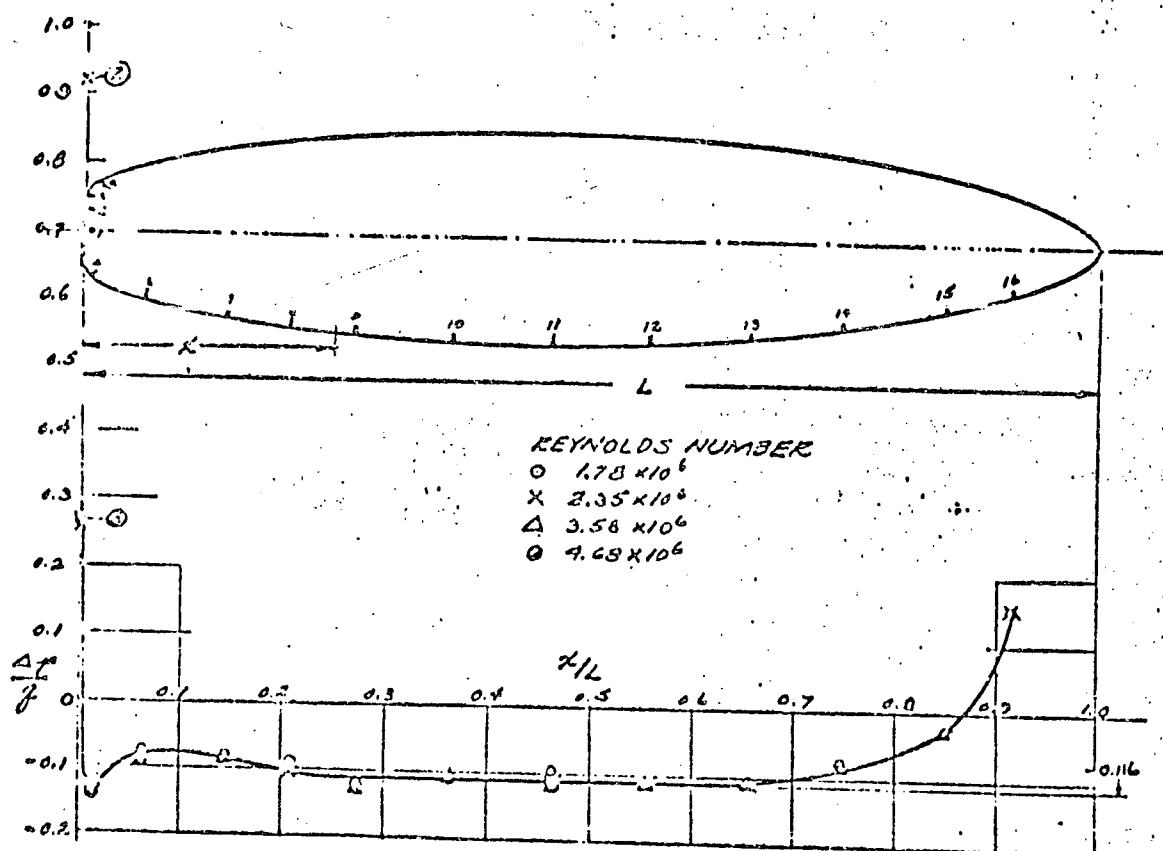
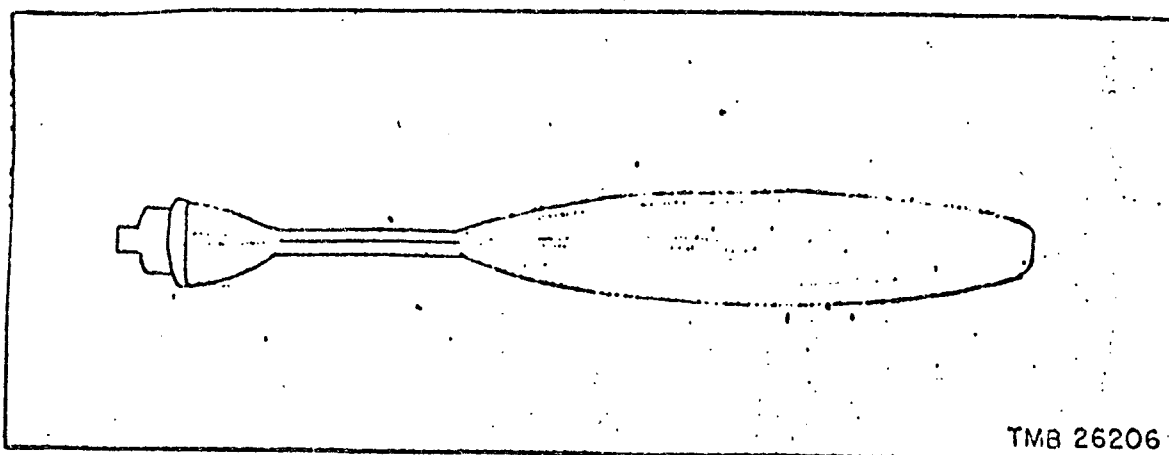
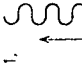
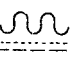
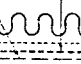
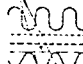

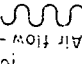
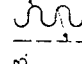
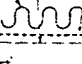


Figure 54. Example of Constant Pressure Body Suitable for Microphone Housing (After Eisenberg (28))

Materials	Maximum allowable velocity in straight runs	Materials	Maximum allowable velocity in straight runs
A. Ventilating ducts			
1.  Uncoated lining, see Note 1	25 ft/sec 8 m/sec	B. Large panels (e.g., test cell applications)  1.  2.  3.  4. 	75 ft/sec 25 m/sec
2.  Coated lining, see Note 2	30 ft/sec 10 m/sec		180 ft/sec 60 m/sec
3.  Blanket	75 ft/sec 25 m/sec		300 ft/sec 100 m/sec
4.  Perforated facing as in A3	125 ft/sec 40 m/sec		

Notes: 1. Examples of suitable materials: Johns-Manville, Microtex, Micro-bar, Micro-Coastic.

2. Examples of suitable materials: Johns-Manville, Microlite, Tent-Mat, Microtex; Gustin Bacon, Ultra-Liner; Owens-Corning, Fiberglas.

Figure 55. Protective Facings for Acoustical Linings Subjected to High Velocity Flow (After Beranek (18))

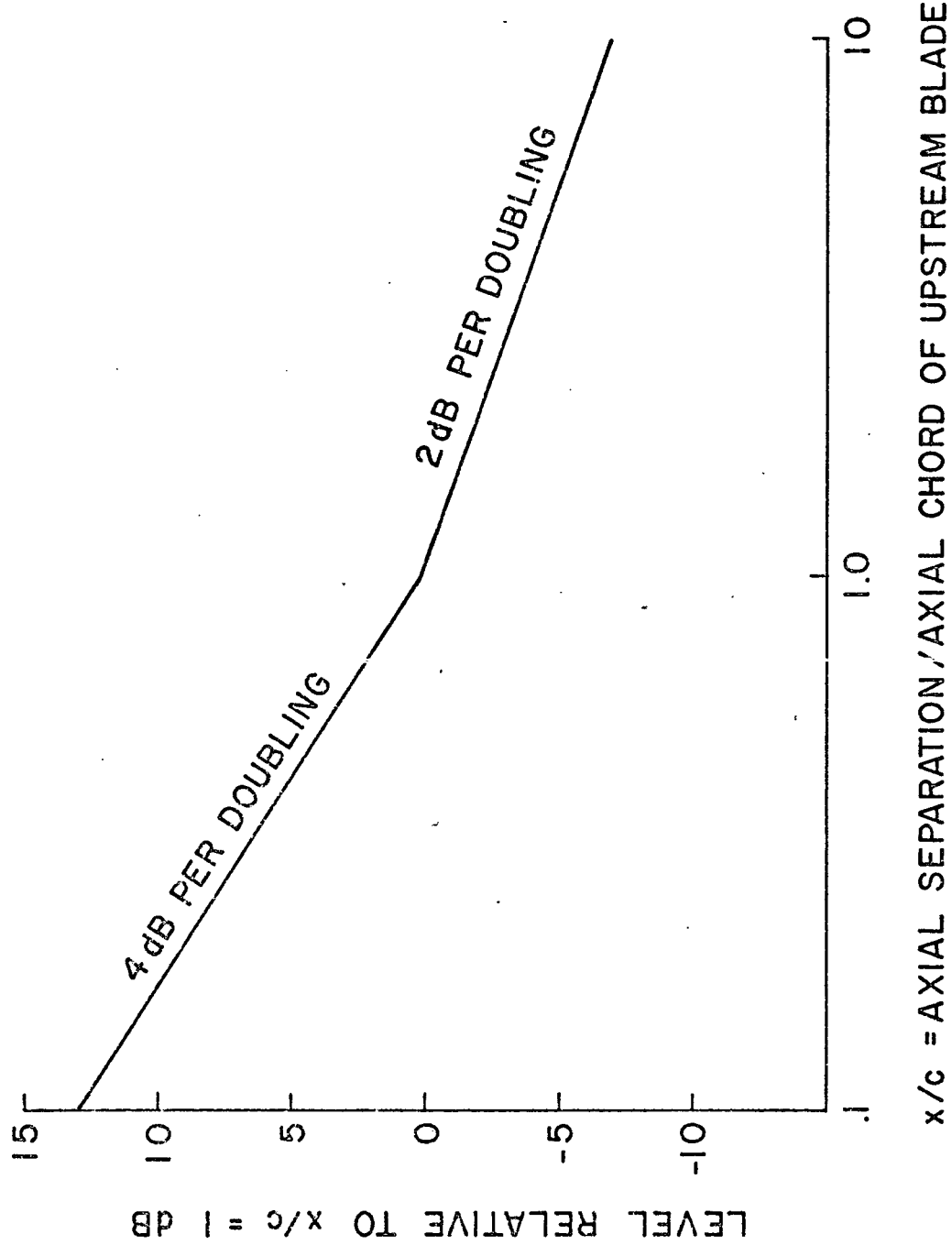


Figure 56. Effect of Axial Separation of Fan and Stator Blades

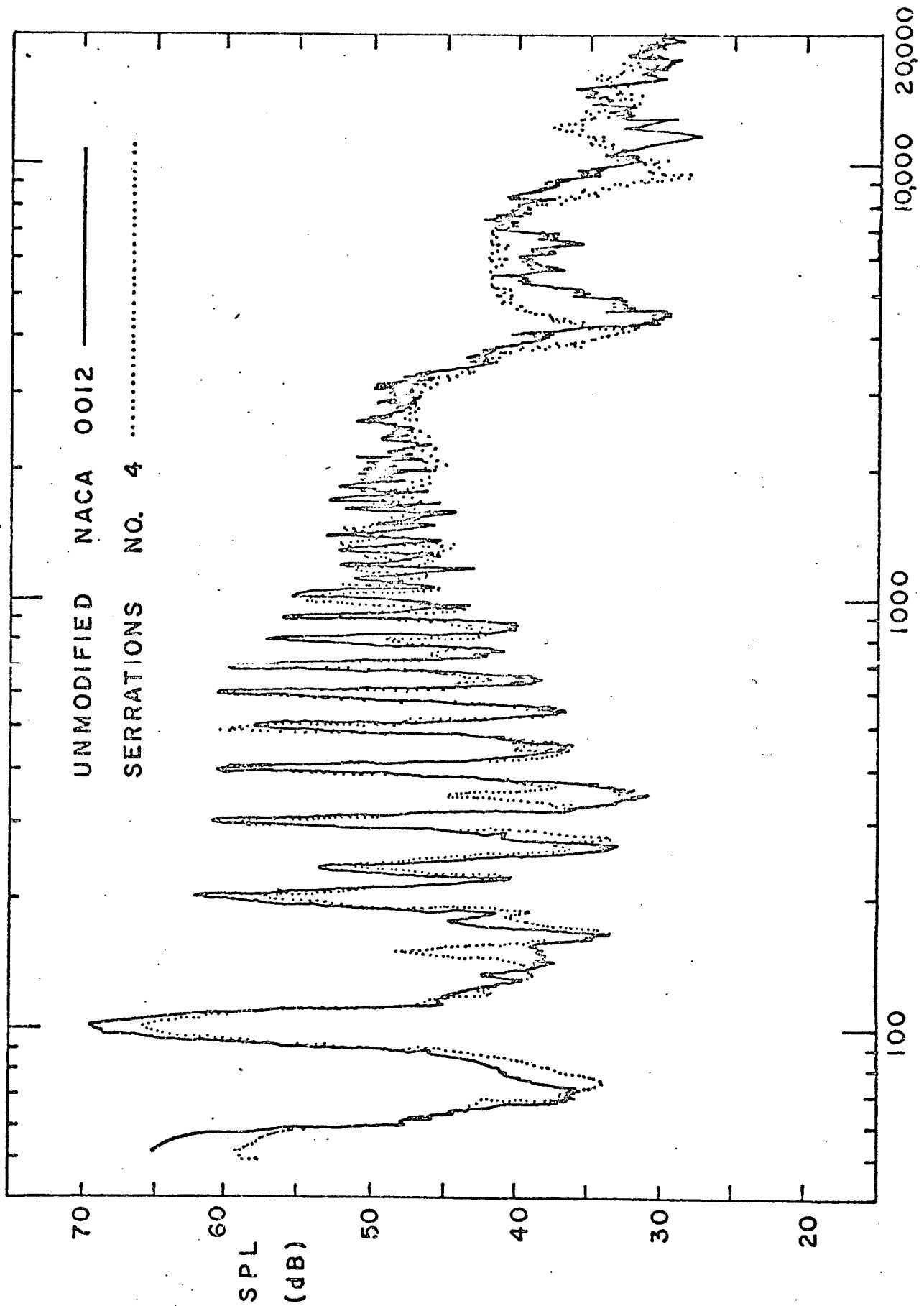


Figure 57. Far Field SPL Spectra of Model Rotor at 3000 rpm, 10° Pitch



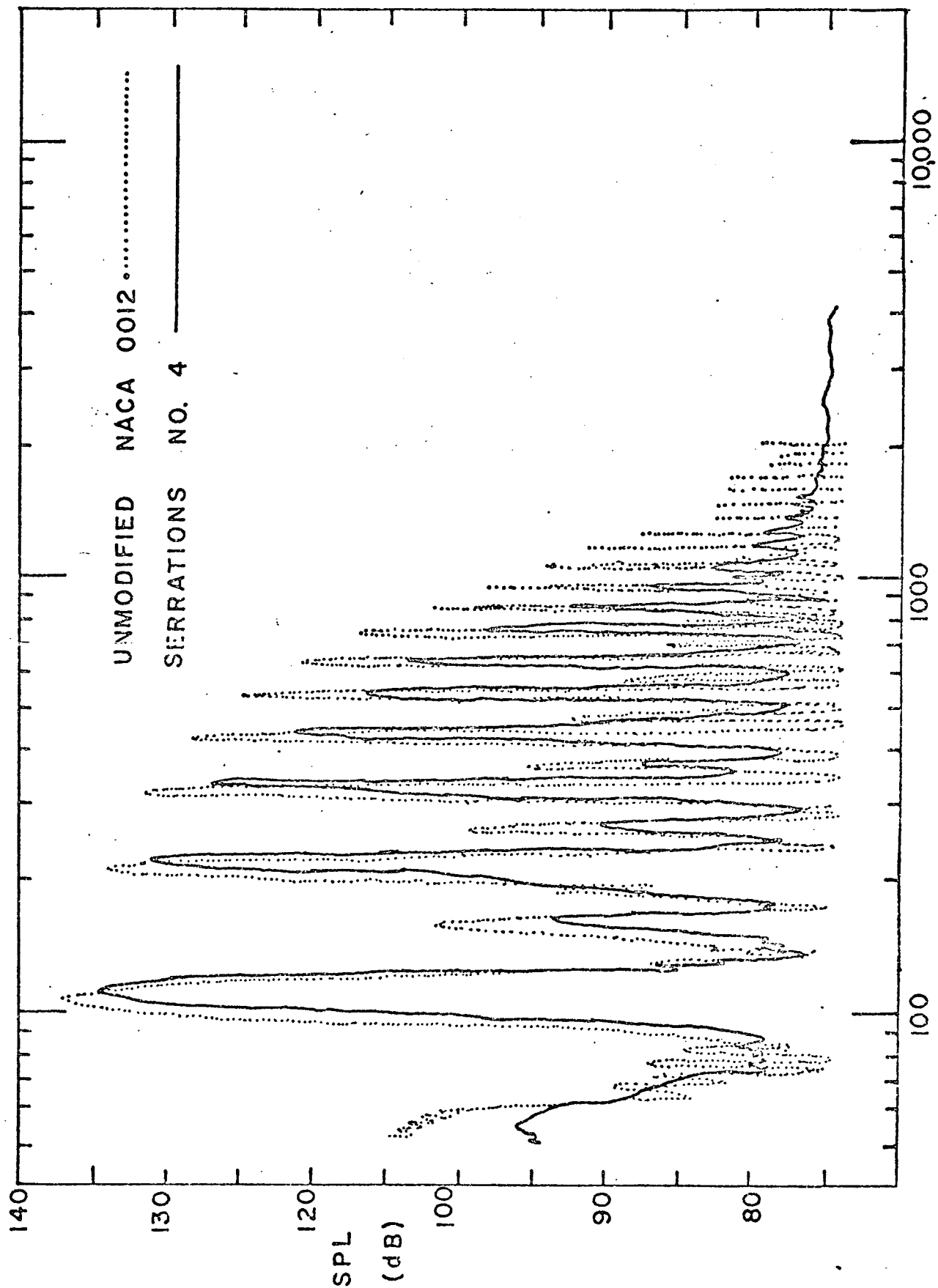


Figure 58. Near Field SPL Spectra of Model Rotor at 3000 rpm, 10° Pitch

# APPENDIX A. INVESTIGATION OF PANEL DAMPING ON REVERBERANT BUILDUP

During the course of this investigation the question of the effect of damping material on the outside of the tunnel was considered. The problem was to determine what happened to reflected energy, and if it could be decreased by using a viscoelastic material on the outside of the tunnel. This type of treatment would be easy to apply and would serve the additional purpose of raising the resonance frequency of the panels.

To investigate this question a single panel was considered as a series of spring-mass-damper systems, as shown in Figure A-1, where  $p_i$  is the incident pressure,  $p_t$  is the transmitted pressure, and  $p_r$  is the reflected pressure defined by,

$$p_i = A_1 e^{i(\omega t - k_1 x)} \quad (A-1)$$

$$p_r = B_1 e^{i(\omega t + k_1 x)} \quad (A-2)$$

$$p_t = A_2 e^{i(\omega t - k_2 x)} \quad (A-3)$$

The displacement of the wall is uniform and equal to  $\xi$  normal to its space,  $\dot{\xi}$  is the panel velocity, both positive in the positive  $x$  direction as shown in the figure. The constants are defined as,  $m$ , the mass per unit area,  $\bar{k}\xi$ , elastic force per unit area,  $b$ , damping constant. The damping constant is made up of two parts, the damping

inherent in a real spring, i.e., panel,  $\bar{k}\eta/\omega$ , and the added damping,  $b_a$ . Therefore,  $b = \bar{k}\eta/\omega + b_a$ . The differential equation to be solved is,

$$m \frac{d^2 \xi}{dt^2} + (2\rho a + b) \frac{d\xi}{dt} + \bar{k}\xi = 2A_1 e^{i\omega t} \quad (A-4)$$

The solution to this equation results in the particle displacement at  $x = 0$ ,

$$\xi_0 = \frac{2A_1}{(\bar{k} - \omega^2 m) + i\omega (2\rho a + b)} \quad (A-5)$$

The particle velocity at  $x = 0$  is obtained through differentiation of equation (A-5):

$$\dot{\xi}_0 = \frac{2A_1}{i(\omega m - \bar{k}/\omega) + (2\rho a + b)} \quad (A-6)$$

The transmitted pressure amplitude,  $A_2 = \rho a \dot{\xi}_0$ , is given by

$$A_2 = \frac{A_1}{1 + \frac{b + i(\omega m - \bar{k}/\omega)}{2\rho a}} \quad (A-7)$$

From continuity of velocity,

$$A_1 - B_1 = A_2 \quad (A-8)$$

Defining  $B_1/A_1$  as the fraction of reflected energy the result is,

$$\frac{B_1}{A_1} = 1 - \frac{A_2}{A_1} = 1 - \frac{1}{1 + \frac{b + i(\omega m - \bar{k}/\omega)}{2\rho a}} \quad (A-9)$$

E

In the undamped case the fraction of reflected energy is,

$$\frac{B_1}{A_1} = 1 - \frac{1}{1 + \frac{i(\omega m - \bar{k}/\omega)}{2\rho a}}$$

Therefore, the effect of adding damping to the outside of the tunnel would be to increase the fraction of energy reflected over the entire frequency range. The added damping apparently would be detrimental to the purpose at hand by causing a reverberant buildup.

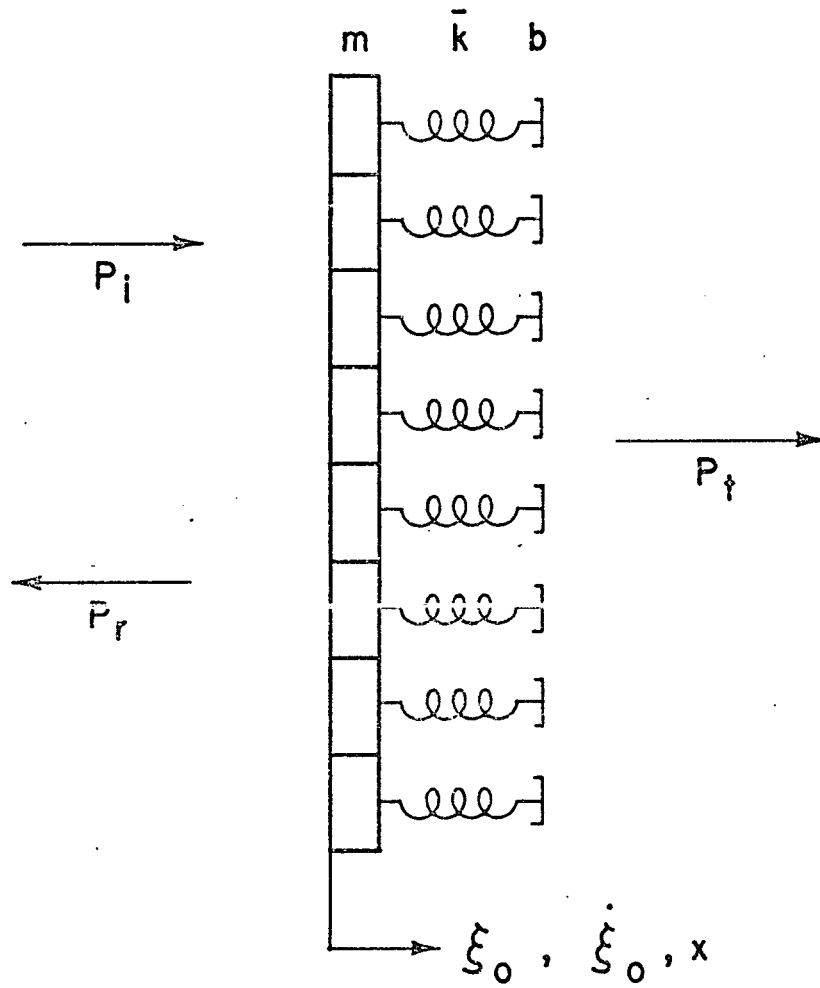


Figure A-1. Spring-Mass-Damper Model of a Panel

## APPENDIX B. DESIGN PROCEDURE

The design procedure described in Section III is given here in detail. Also shown are sample calculations from which the results in Figures 7 and 8 were obtained. Figure 7 also shows the duct with appropriate dimensions. This design procedure is taken from Beranek(14) Section 15.3.

Step 1 Choose the duct height  $h$ . Choose this as small as possible because attenuation increases rapidly with decreasing duct height. The choice of  $h$  also governs the bandwidth of the attenuation curve.

Sample  $h = 3.5 \text{ ft.}$

Step 2 Choose the frequency  $f_o$  where maximum attenuation is desired, and using  $h$  from step 1 calculate the frequency parameter  $\eta_o = 2h f_o / a_o$

Sample  $f_o = 400 \text{ hz}$

$$\eta_o = \frac{2 \cdot 3.5 \text{ ft.} \cdot 400 \text{ hz}}{1127 \text{ ft/sec}} = 2.49$$

Step 3 Calculate the depth  $d$  of the treatment

$d = 2.9 \times 10^3 / f_o \eta_o$  (inches). Find size of honeycomb cells

$$\delta < \lambda_o / 4$$

$$\text{Sample } d = \frac{2.9 \times 10^3}{(400)(2.49)} = 2.93 \text{ in.}$$

$$\delta < \frac{\lambda_o}{4} = \frac{1127}{400} \cdot \frac{1}{4} = .70 \text{ ft.}$$

Step 4 Find the thickness,  $t$ , of the porous layer,  $t < \lambda_o/10$ .

And calculate the flow resistance  $R_1 = 1.5 \times 10^4 \eta_o / t$  (mks rays/m,  $t$  in inches).

$$\text{Sample } t < \frac{\lambda_o}{10} = \frac{1127}{400} \cdot \frac{1}{10} = .27 \text{ ft.}$$

$$t < 3.38 \text{ in.}$$

$$R_1 = \frac{(1.5 \times 10^4) (2.49)}{3.38} = 1.1 \times 10^4 \text{ mks rays/m}$$

Step 5 Calculate normalized flow resistance  $R_f / \rho a_o = .92 \eta_o$ .

From these data a suitable material can be chosen. The values

$R_1$  and  $R_f$  are related by  $R_f = R_1 t$

$$\text{Sample } \frac{R_f}{\rho a_o} = .92 \eta_o = 2.29$$

Step 6 Set up a table with values of  $\eta$  across the top. Use  $\eta_o$  as one of these and a few higher and lower values.

Sample See Table B-1 for sample calculations of remaining steps.

Step 7 On the next line find the frequency,  $f$ , corresponding to the values of  $f = \eta a_o / 2h$ .

Step 8 Calculate normalized reactance of the lining for each frequency,  $X / \rho a_o = 2.23 \times 10^3 / fd$  ( $d$  in inches)

Step 9 From the values of  $\eta$  and  $X / \rho a_o$  find  $X / \eta \rho a_o$

Step 10 From the value  $R_f/\rho a_o$  (Step 5) and  $X/\rho a_o$  calculate

$$\frac{R_f}{X} = \frac{R_f/\rho a_o}{X/\rho a_o}$$

Step 11 From Figure B-1 and the values of  $R_f/X$  from Step 10 find  $|Z|/X$  and  $\phi$ . For each value of  $R_f/X$  enter the graph from the right-hand scale, project a horizontal line to the curve marked  $R_f/X$ . From the point drop a vertical line to the curve marked  $|Z|/X$ . From this point read the values of  $|Z|/X$  from the left hand scale and  $\phi$  from the lower horizontal scale.

Step 12 Find  $|Z|/\rho a_o \eta$  by multiplying values of  $|Z|/X$  by the corresponding value of  $X/\rho a_o \eta$ .

Step 13 For each pair of values  $|Z|/\rho a_o \eta$  and  $\phi$ , select the design curve of Figure B-2 with the corresponding value of  $\eta$ . For values  $\eta > 1$  use the  $\eta = 1$  curve.

Step 14 Determine  $D_h$ , the attenuation in dB per length of duct equal to the height by entering the proper chart with the values  $|Z|/\rho a_o \eta$  and  $\phi$  and interpolating among the contours.

Step 15 To get the total attenuation for a length of duct  $L$  multiplying  $D_h$  by  $L/h$ .

Sample  $L = 15.6$  ft.

$$L/h = 4.45$$



TABLE B-1

$\eta$	1.5	2.0	2.49	3.0	3.5
$f$	241	322	400	482	561
$x/\rho a_o$	3.18	2.38	1.92	1.59	1.37
$x/\eta \rho a_o$	2.12	1.19	.77	.53	.39
$R_f/x$	.72	.96	1.19	1.44	1.67
$ z /x$	1.25	1.4	1.5	1.8	2.1
$\phi$	-1.0	-.85	-.75	-.65	-.5
$ z /\rho a_o \eta$	2.65	1.67	1.16	.95	.82
$D_h$	1.7	5.0	7	3.5	2.7
$L/h \times D_h$	7.6	22.2	31.2	15.6	12.0

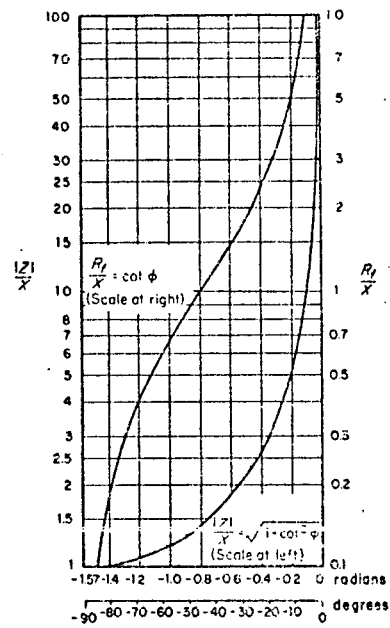


Figure B-1. Design Curve - copied from Beranek (20)

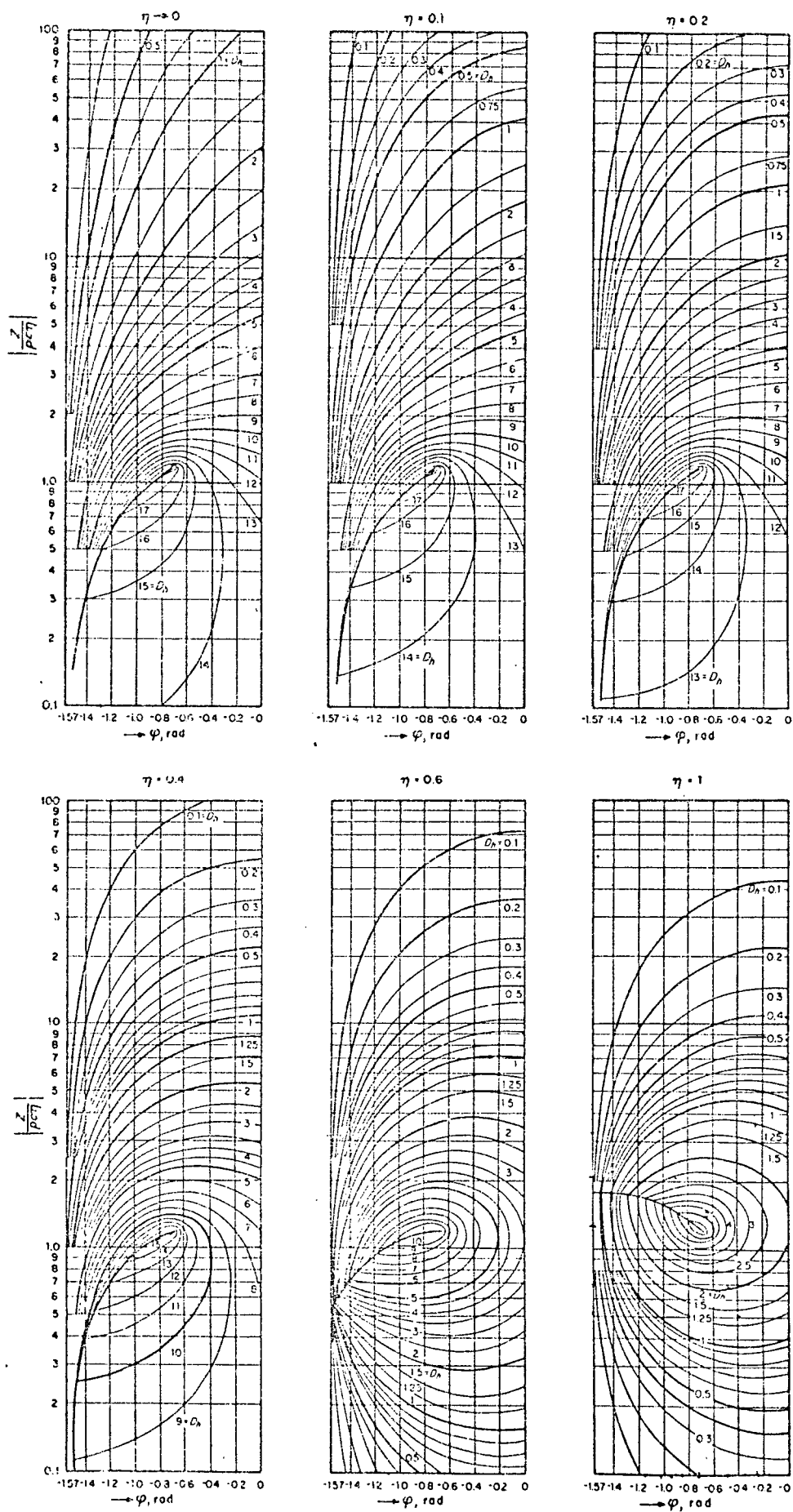


Figure B-2. Design Curve - copied from Beranek (20)

APPENDIX C

The following is a partial list of companies that manufacture standard acoustic treatments:

1. Eckel Industries, Inc.
2. Johns-Manville
3. Armstrong Cork Co.
4. Pittsburgh Corning Corp.
5. Sintered Specialties Div., Parker Pen Co.
6. U.S. Mineral Products Co.
7. Arno Adhesive Tapes, Inc.
8. PPG Industries, Fiber Glass Div.
9. Conwed Corp.
10. Troymills, Inc., Industrial Products Div.
11. Brokaw Cork Co., Inc.
12. Asbestospray Corp.
13. Ultra-Adhesives, Inc.
14. Markel Rubber Products Co., Inc.
15. Deccofelt Corp.
16. Flock Process Corp.
17. American Rubber & Plastics Corp.
18. The Aeroacoustic Corp.
19. Carey Electronics Engineering Co., Metal Wood Div.
20. Vibration Eliminator Co., Inc.
21. Dolphin Paint & Chemical Co.
22. Duracote Corp.
23. Brunswick Corp., Technical Products Div.
24. Celotex Corp.
25. Owens - Corning Co.